

12-2022

Risk-Factor Induced Changes In The Breast Microenvironment Facilitate Inflammatory Breast Cancer Progression And Lymphovascular Invasion

Wintana Balema

Wintana Balema

Follow this and additional works at: https://digitalcommons.library.tmc.edu/utgsbs_dissertations

 Part of the [Biology Commons](#), [Disease Modeling Commons](#), and the [Medical Cell Biology Commons](#)

Recommended Citation

Balema, Wintana and Balema, Wintana, "Risk-Factor Induced Changes In The Breast Microenvironment Facilitate Inflammatory Breast Cancer Progression And Lymphovascular Invasion" (2022). *Dissertations and Theses (Open Access)*. 1232.

https://digitalcommons.library.tmc.edu/utgsbs_dissertations/1232

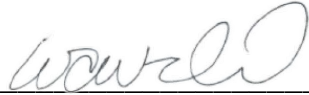
This Dissertation (PhD) is brought to you for free and open access by the MD Anderson UTHealth Houston Graduate School at DigitalCommons@TMC. It has been accepted for inclusion in Dissertations and Theses (Open Access) by an authorized administrator of DigitalCommons@TMC. For more information, please contact digcommons@library.tmc.edu.

RISK-FACTOR INDUCED CHANGES IN THE BREAST MICROENVIRONMENT FACILITATE
INFLAMMATORY BREAST CANCER PROGRESSION AND LYMPHOVASCULAR INVASION

By

Wintana Balema, BA

APPROVED:



Wendy Woodward, M.D., Ph.D.
Advisory Professor



Bisrat Debeb, DVM, Ph.D.



David Piwnica-Worms, M.D., Ph.D.



George Eisenhoffer, Ph.D.



Melissa Aldrich, Ph.D.

APPROVED:

Dean, The University of Texas

MD Anderson Cancer Center UTHealth Graduate School of Biomedical Sciences

**RISK-FACTOR INDUCED CHANGES IN THE BREAST MICROENVIRONMENT FACILITATE
INFLAMMATORY BREAST CANCER PROGRESSION AND LYMPHOINVASION**

A

DISSERTATION

Presented to the Faculty of

The University of Texas

MD Anderson Cancer Center UTHealth

Graduate School of Biomedical Sciences

in Partial Fulfillment

of the Requirements

for the Degree of

DOCTOR OF PHILOSOPHY

by

Wintana Balema, BA

Houston, Texas

December, 2022

Dedication

To my parents, who sacrificed and worked endlessly to provide me with incredible opportunities leading me to this point. I am so grateful for the upbringing you provided, encompassed by love and unwavering support. Thank you for instilling values, resilience, and a belief that I was capable of achieving all that I dreamt for.

Most importantly, my heart has been burdened for the past two years experiencing the inhumane, brutal genocidal war that has unjustly targeted and harmed the people of Tigray. To date, organizations like Amnesty International have reported on the atrocities impacting 6 million people in Tigray. These reports have accounted more than 500,000 Tigrayans have died in this conflict, including thousands brutally and unlawfully murdered. Ramped sexual violations and rape have been reported. Daily drone attacks and bombings have displaced over 2 million people from their homes. Starvation has been used as a weapon of war, with humanitarian aid blockades inflicting a man-made famine. Up to 80% of hospitals have been completely destroyed throughout the region leaving doctors pleading for medical supplies. Widespread electricity and telecom blackouts throughout the region have limited access to information and communication within and outside the region. With every passing day, the suffering only intensifies. I would be remised to write this section, without acknowledging the unjust and inhumane suffering. I refuse to allow this to be silently forgotten. My home, my land, my pride, my people. The resilience that flows in my veins, and beats in our hearts is what defines us, and prevails even in the darkest moments of our history. We chant, Tigray shall prevail.

ትግራይ ትሰዕር።

Tigray shall prevail.

Acknowledgements

Completing my PhD has been a long, challenging yet rewarding experience, which was made possible with the support of my mentors, lab colleagues, collaborators, friends and family.

First and foremost, I would like to thank both the Woodward and Debeb labs for always supporting me in this journey. Teaching me, challenging me, providing feedback on my writing and oral presentations, and being pillars of wisdom and encouragement along the way. I would like to thank Dr. Woodward for being an incredible mentor, words cannot express how much your mentorship, guidance, teaching, advice, support, advocacy and belief in me has molded my experience in this program and life. Your mentorship will always be cherished. Dr. Debeb, thank you for being an advisor, teacher, a supporter in my journey, your lessons on the importance of technical skills in basic science will never be forgotten. Thank you to the researchers and postdoctoral fellows in the Woodward and Debeb lab; Richard, Jessica, Emily and Ding who have helped me with my experiments, taught me technical skills and have contributed to my projects. I would also like to thank key collaborators that have helped shape my dissertation project; Dr. Eva Sevick and her lab, Dr. Natalie Fowlkes, and the Susan G. Komen Fellowship program. This fellowship allowed me to meet incredible researchers, passionate about breast cancer advocacy and reducing disparities among minority women, including Dr. Lorna McNeill, Dr. Kelly Hunt and Dr. Abenaa Brewster.

I would like to thank my family and friends, who have supported and encouraged me through this program, particularly during these difficult times back home. My family is a constant source of love, support and faith. To my friends, my sisters, who have been a source of love, support and community. To my fiancée, who is the kindest soul, and truly the most supportive, selfless and loving partner. I cannot express how grateful I am for your constant support, and unwavering belief in me. You've been there through it all. You've all been there for my successes, and many failures, and even my highlights and setbacks. Thank you for always being there, I love you all.

Thank you to all the people that have been a part of this journey, my committee, the graduate school, the cancer biology program, the Morgan Welch inflammatory breast cancer research program and clinic. I am eternally grateful for this opportunity, and journey, and for all the people that made it possible.

RISK-FACTOR INDUCED CHANGES IN THE BREAST MICROENVIRONMENT FACILITATE INFLAMMATORY BREAST CANCER PROGRESSION AND LYMPHOINVASION

Wintana Balema, BA

Advisory Professor: Wendy Woodward, M.D., Ph.D.

Inflammatory breast cancer (IBC) is a rapidly progressing, rare and highly lethal form of breast cancer. IBC is a clinical diagnosis, requiring >1/3 involvement on the affected breast and/or skin by erythema, and disease onset of < 6 months. The clinical symptoms of IBC vary in severity and presentation, these include redness, warmth, skin thickening and bruised or pink/purple discoloration appearance and skin changes such as peau d'orange. These skin symptoms are not attributed to inflammation, rather IBC is characterized by florid lymphovascular tumor emboli clogging dermal lymphatics. This leads to "classic" symptoms of breast swelling and skin edema or discoloration. To date, unique genomic drivers which differentiate IBC from non-IBC invasive breast cancers have not been identified highlighting a role for the microenvironment. Several epidemiological studies have unveiled subtype-specific risk factors associated with IBC that are known to alter the microenvironment. Obesity is an established risk factor for all subtypes of IBC. Never-breastfeeding increases risk for developing the most aggressive, triple-negative IBC. Further, never breastfeeding is associated with later clinical stage and worse outcomes. We worked to model these overlapping risk factors to understand microenvironment changes that may lead to the lymphatic change's indicative of IBC.

First, we investigated the association of a "classic" triad of clinical IBC signs with overall survival among patients to demonstrate the most overt clinical findings of lymphatic involvement were impacting prognosis. We evaluated a triad of IBC signs, including swollen involved breast, nipple change, and diffuse skin change, using breast medical photographs from patients enrolled on a prospective IBC registry. We reported that the ten-year OS was 29.7% among patients with the classic sign triad versus 57.2% for non-classic ($P < .0001$). We determined that a triad of classic IBC signs independently predicted OS in patients diagnosed with IBC suggesting the clinical outcome of diffuse lymphatic invasion by IBC is prognostic, and

potentially that targeting the mechanisms that promote lymphatic function and tumor invasion may improve outcomes.

Our prior work implied the changes in the breast that permit florid lymphatic involvement may even occur prior to tumor initiation. Noting a limitation of existing studies of breast cancer risk factors is the experimental isolation of risk factors, which fails to model the patient experience. Thus, we modeled synergistic effects of IBC risk factors, obesity and weaning timing, on *in vivo* lymphatic function pre- and post-tumor initiation, IBC tumor growth, and the mammary gland microenvironment. We hypothesized that weaning status (duration of breast feeding) and high fat diet (HFD) would synergize to induce pro-lymphatic changes in the microenvironment before tumor initiation and promote IBC tumor growth. We found that HFD increased lymphatic contractile activity prior to tumor initiation. This HFD-induced increase in lymphatic function correlated to increased SUM149 tumor growth and increased inflammatory cells in the mammary gland. Tumors increased lymphatic function to a similar extent. Increased CCL21+ cells, a ligand for lymphatic traffic homing, was correlated to pulsing. Thus, the relationship between lymphatic pulsing, tumor growth and CCR7-CCL21 related tumor trafficking warrant further investigation.

CCR7 is an immune cell receptor that mediates immune cell trafficking into lymphatics that can be expressed on tumor cells. We examined the expression of CCR7 in IBC and non-IBC cell lines, and IBC patient tumors to determine the prevalence of this receptor in IBC tumor cells. We found that CCR7 gene expression is increased in IBC versus non-IBC tumors, and was present across tumor subtypes in IBC cell lines and in both ER+ and ER- IBC patient tumors. Further, CCR7 was expressed on 23/24 IBC patient samples assessed by immunohistochemistry. This highlights the potential direction for developing novel therapies targeting CCR7, to improve therapeutic options and outcomes for IBC patients.

Table of Contents

TITLE PAGE	II
DEDICATION	III
ACKNOWLEDGEMENTS	IV
ABSTRACT	VI
LIST OF ILLUSTRATIONS	XI
LIST OF TABLES	XII
CHAPTER 1- INTRODUCTION	1
INFLAMMATORY BREAST CANCER	1
INCIDENCE AND EPIDEMIOLOGY	1
IBC PROGNOSIS.....	5
DIAGNOSTIC AMBIGUITY	6
IBC TREATMENT	6
LINKING RISK FACTORS TO BIOLOGY IN IBC; ALTERATIONS IN THE MICROENVIRONMENT	7
IBC IS A MODEL OF FLORID LVSI.....	11
LYMPHATIC FUNCTION IN THE NORMAL MAMMARY GLAND.....	11
THE MECHANISTIC ROLE OF CCR7 IN LYMPHATIC HOMING	13
CHAPTER 2-METHODS AND MATERIALS	15
CHAPTER 3 METHODOLOGY:	16
<i>Study Cohort</i>	16
<i>Statistical methods for patient analysis</i>	17
CHAPTER 4 METHODOLOGY:	18
<i>Animals</i>	18
<i>In vivo Near Infra-red Fluorescence (NIRF) lymphatic imaging</i>	18
<i>In vivo orthotopic cell lines</i>	19
<i>Multiplex IF</i>	19

<i>Leica Imagescope software Analysis for Quantification and Structural Analysis of Multiplex IF.....</i>	20
<i>Microarray statistics.</i>	20
CHAPTER 5 METHODOLOGY:	21
<i>Gene Array Data.</i>	21
<i>Tissue Microarray.</i>	21
<i>In vitro cell lines.</i>	21
<i>Western blot.....</i>	22
CHAPTER 3- INFLAMMATORY BREAST CANCER APPEARANCE AT PRESENTATION IS ASSOCIATED WITH OVERALL SURVIVAL:	23
ABSTRACT	24
INTRODUCTION	25
RESULTS.....	26
<i>Study participants</i>	27
<i>Demographic and clinical characteristics of our patient population</i>	27
DISCUSSION.....	40
CHAPTER 4- HIGH FAT DIET BUT NOT WEANING TIMING INCREASES PRE-TUMOR MAMMARY GLAND LYMPHATIC VESSEL PULSING AND SUBSEQUENT INFLAMMATORY BREAST CANCER TUMOR GROWTH IN A PRE-CLINICAL MODEL:	44
ABSTRACT	45
INTRODUCTION	47
RESULTS.....	49
<i>High fat diet significantly increased lymphatic pulsing in nulliparous and multiparous mice.....</i>	49
<i>High fat diet significantly increased IBC tumor growth in multiparous mice.</i>	53
<i>High fat diet induced increase in lymphatic function is independent of lymphatic vessel count in mammary gland.</i>	56
<i>Expression of mammary duct-infiltrating monocyte-derived species and lymphangiogenic PoEMs.....</i>	61
DISCUSSION.....	68

CHAPTER 5- CCR7 IS HIGHLY EXPRESSED IN INFLAMMATORY BREAST CANCER, AND BREAST

CANCER CELL LINES:..... 77

ABSTRACT 78

INTRODUCTION 80

RESULTS..... 82

DISCUSSION 88

CHAPTER 6- DISCUSSION:..... 94

DISCUSSION 95

BIBLIOGRAPHY101

List of Illustrations

Figure 1 Examples IBC patient photographs scored by clinical presentation	26
Figure 2: Kaplan-Meier curve of actuarial incidence of overall survival by presentation category.	36
Figure 3: HFD increases mammary lymphatic pulsing compared to LFD in nulliparous mice	50
Figure 4: HFD increases lymphatic pulsing from mammary gland draining lymphatics in multiparous mice similar to pulsing induced by tumor initiation.....	52
Figure 5: HFD promotes IBC tumor growth in scid/beige multiparous mice.....	54
Figure 6: Tissue microarray multiplex immunofluorescence effectively stained for 12 markers across two panels on mammary gland tissue and tumors.	57
Figure 7: HFD promotes lymphatic functionality independent of the number of lymphatic vessels	59
Figure 8: High fat diet and forced weaning synergistically significantly increased PDPN-positive macrophage ductal cells.....	62
Figure 9: High fat diet significantly increased mammary ductal immune cell inflammation	64
Supplemental Figure 1: Multiplex Immunofluorescence was conducted on IBC tumor sections from the multiparous mice	66
Figure 10: CCR7 and CCL21 are highly expressed in IBC patient samples	83
Figure 11: Demonstration of pathologist categorizing and scoring CCR7 expression in IBC patient tumors.....	86
Figure 12: In vitro analysis of CCR7 expression in IBC and non-IBC cell lines	87
Figure 13: A summary of overlapping “pre-tumor” signals in the normal breast and the IBC tumor microenvironment.....	98

List of Tables

Table 1 Comparative IBC clinical studies conducted globally.....	4
Table 2. Demographic and reproductive characteristics of the study population	28
Table 3. Tumor and clinical characteristics.....	30
Table 4. Self-reported breast features at time of presentation	32
Table 5. Comparison of epidemiologic, tumor and clinical characteristics by presentation appearance.....	34
Table 6A. Kaplan-Meier estimates analysis for categorical variables on overall survival outcome.	38
Table 6B. Univariate Cox regression analysis on overall survival and disease specific survival.....	39
Table 7. Multivariate Analysis of overall survival	39
Table 8. Correlation between lymphatic pusling and tumor growth and lymphangiogenesis	55
Table 9: Average number of lymphatic vessels in each mammary gland core quantified for each treatment group	58
Table 10: CCR7 Pathology results and ER status for all tumor samples.....	85
Supplemental Table 1: Summary of the top genes that were upregulated in the HFFW mice compared to LFNW (P<0.001).	92

Chapter 1- Introduction

Inflammatory Breast Cancer Overview-

Inflammatory breast cancer (IBC) is a rare and particularly aggressive variant of breast cancer. The name inflammatory breast cancer comes from the common inflamed appearance of the breast at the time of diagnosis rather than any distinguishing pathologic inflammatory infiltrate [1]. In fact, AJCC defines IBC, staged T4d, as a clinical diagnosis characterized by diffuse erythema and edema involving at least one-third of the skin of the affected breast. (AJCC) [2]. Significant variation at presentation leads to ambiguity and misdiagnosis, yet numerous efforts to define a molecular signature, driver, or diagnostic that accurately captures IBC have yet to be successful [3]. Diagnosis-defining characteristics such as the skin changes, peau d'orange, and erythema are attributed to diffusely distributed tumor clusters migrating and clogging both the breast and dermal lymphatics in the breast [4], [5]. Pathologically, individual IBC tumor cells are indistinguishable from similarly aggressive non-IBC tumor cells [6]. This and the absence of clear clinical drivers to date leads to the hypothesis that the stroma facilitates IBC progression and drives the features of emboli-based growth and spread and lymphatic invasion of the breast and breast skin lymphatics [7]. Understanding the predilection for the lymphatics of this disease is key to unraveling the mechanisms of progression and metastasis.

Incidence and Epidemiology

Inflammatory breast cancer is a rare, but highly aggressive subtype of breast cancer that contributes significantly to breast cancer related-mortality [8]. IBC accounts for only 2%–4% of all breast cancer cases [9]; however, the disease is responsible for 10% of breast cancer-related deaths in the US [10]. A recent study examining the Surveillance, Epidemiology, and End Results (SEER) data reported IBC survival from 1973-2015. The incidence of IBC during this period was 2.76 cases per 100,000 people [11], however the reported incidence of IBC has changed over time with the introduction of the AJCC “T4d” staging criteria and increased global collaborative staging guidelines. The overall age-adjusted incidence of IBC for white, black and other races are 2.63, 4.52 and 1.84 cases per 100,000 people, respectively, ($p < 0.00001$) [11]. Thus, black women have a significantly higher incidence of IBC compared to white women.

Historically, due to its low incidence, IBC has not been extensively studied in large prospective cohorts. The subjectivity in diagnosis makes it difficult to ensure the population being reported is correctly diagnosed. There have been comparative IBC clinical studies conducted globally (Table 1). The largest study is a retrospective nested case-control analysis from the Breast Cancer Surveillance Consortium Database, including 617 IBC cases [12]. This dataset expansively included locally advanced non-IBC involving the skin and chest wall (LABC), breast cancer not involving chest wall or skin (BC), and healthy controls. High body mass index (BMI) increased IBC risk irrespective of menopausal status and estrogen receptor (ER) expression; younger age at first birth was associated with higher risk of ER-negative IBC [12]. In a separate single institution case-control study at MD Anderson, including 224 women with IBC from a prospectively collected IRB-approved IBC registry, and 396 cancer-free women, identified subtype specific-IBC risk factors [13]. Women aged <26 years at the time of their first pregnancy were at a higher risk for triple-negative IBC, and a history of breast-feeding was associated with a reduced risk for triple-negative IBC [13]. BMI ≥ 25 kg/m² significantly increased risk for all IBC subtypes [13], [14]. Additionally, a history of smoking was associated with a higher risk of luminal IBC. Thus, in two large studies comparing IBC cases to healthy controls, the ideal at-risk group, differ by tumor subtype, however BMI and reproductive factors (young age of first pregnancy) are common across most subtypes [13], [15].

A subsequent study conducted from the IRB-approved prospective IBC registry database (2006-2013) at MD Anderson Cancer Center, expanded the analysis of IBC patients (N = 248) and identified significant differences in risk factors by race [16]. The racial distribution of the IBC patients included white (77.8%), Black (9.5%), Hispanic (10.5%) and Asian/Asian Pacific (2.4%) women. While White and Hispanic patients were mostly diagnosed at stage III (64% and 73%), African American patients were significantly over-represented with stage IV diagnosis (48% vs 36%, 25% for Whites and Hispanics, respectively) [16]. Despite representing a small proportion of this patient cohort, African American women had the highest frequency of the most aggressive subtype, triple-negative IBC (43.5%, compared to Hispanics (34.6%) and Whites (22.3%)) [16]. Among black women, shorter periods between menarche and age at first birth, in combination with a lack of breastfeeding increased IBC risk [16]. Interestingly, examining reproductive factors in IBC cases compared to non-IBC cancer patient controls in Tunisia, Mejri et al found an extended

duration of breast feeding (> 12 months), BMI, and oral contraceptive use were associated with IBC, however breast-feeding duration was not associated with TN-IBC [17]. In a broader study across North Africa, molecular and presentation differences among IBC patients in Tunisia, Egypt, and Morocco revealed Egyptian patients having the most classic IBC clinical symptoms [18].

Considering the association of risk factors with cancer outcomes, a multivariate Cox proportional hazard analysis from the prospective dataset from MDACC [16], women of African American or Hispanic decent, lacking a history of breastfeeding were associated with a higher clinical stage ($P=0.0019$) and TNBC subtype ($P= 0.0023$) at diagnosis, and were associated shorter survival ($HR=3.023;95\% CI: 3.023,1.504$, $HR=0.232; 95\% CI: 0.232,0.091$, respectively) [16]. Similarly, in a separate study at MD Anderson, which assessed IBC patient outcomes in relation to their breastfeeding status [19], parous women with IBC that did not breast feed had worse rates of distant metastasis ($P=0.008$), relapse-free survival ($P=0.006$) and overall survival ($P=0.04$) compared to their breastfeeding counterparts resulting in an overall worse prognosis [19].

Table 1 Comparative IBC clinical studies conducted globally.

	Study population	Country	Main findings
Soliman A et al. 2011	Egypt (48 IBC vs. 64 non-IBC), Tunisia (24 IBC vs. 40 non-IBC) and Morocco (42 IBC vs. 41 non-IBC).	Tunisia, Egypt and Morocco	Egyptian patients had increased IBC symptoms compared to other IBC patients, including highest erythema, edema, peau d'orange and metastasis among the three groups.
Schairer C et al. 2013	617 IBC vs. 7600 non-inflammatory invasive BC (BC), 1151 Locally advanced, invasive BC (LABCs) patients.	Egypt and Tunisia	IBC risk factors: High BMI, increased IBC risk irrespective of menopausal status and estrogen receptor (ER) expression; younger age at first birth was associated with higher risk of ER-negative IBC
Atkinson R et al. 2016	224 IBC vs. 396 cancer-free women	MD Anderson Cancer Center (US).	Obesity is a risk factor for all subtypes. Subtype specific-modifiable risk factors include age at first pregnancy (≥ 26), breast-feeding status and smoking.
Fouad T et al. 2018	248 IBC only.	MD Anderson Cancer Center (US).	Risk factors varied by race. Black women had higher frequency of stage IV diagnosis, triple-negative IBC diagnosis, and had shorter periods between menarche and age at first birth, in combination with a lack of breastfeeding increased IBC risk, compared to white and Hispanic women.
Mejri N et al. 2020	160 IBC vs. 580 non-IBC	Tunisia.	An extended duration of breast feeding (> 12 months), BMI, and oral contraceptive use were associated with IBC, however breast-feeding duration was not associated with TN-IBC

Together these studies emphasize the impact of BMI, and demonstrate variable effect in reproductive factors, while commonly identifying aspects of pregnancy timing and lactation in IBC risk. Pregnancy and breastfeeding alter the breast microenvironment, potentially providing a conducive microenvironment for

the progression and invasive nature of IBC in the breast. The specific mechanisms that may drive this and the intersection with obesity remain understudied.

IBC Prognosis

A comparative study with IBC and non-IBC patients reported the median overall survival (OS) duration is 4.8 versus 13.4 years for stage III disease, and 2.27 years vs 3.4 years with stage IV tumors, respectively [20]. Breast cancer treatment is guided by the expression of three tumor receptors, the estrogen receptor (ER), progesterone receptor (PR) and the gene product of *HER2-neu*, (HER2) [21], [22]. In the general population, ER/PR-positive breast cancer represents ~ 75% of all breast cancers, and is particularly prevalent among post-menopausal women [23]. Patients considered negative for all three receptors are considered to have “triple negative” breast cancers which are associated with worse outcomes due to a lack of systemic therapeutic options. The subtypes of a cohort of IBC patients were luminal A (HR+/HER2-) (34.6%), luminal B (HR+/HER2+) (17.9%), HR-/HER2 + (24.4 %), and triple negative-IBC (20.5 %) [24]. Thus, the more aggressive HER2 and triple negative subtypes make up over a third of IBC.

Studies have estimated 75% of IBC cases exhibit signs of the dermal-lymphatic invasion, characterized by tumor emboli invading the dermal lymphatic vessels attributing to rapid lymph node and distant metastasis [25], [26]. Lymphovascular space invasion (LVSI) is defined as the presence of viable tumor cells in endothelial-lined channels, outside the bulk for the invasive tumor mass [27]. LVSI is classified as the beginning of lymphogenous and hematogenous metastases, hallmarked by the invasion of tumor cells into lymphatic and/or blood vessels [27]. Clinical studies have reported that lymphovascular invasion correlates with lymph node metastases and poor breast cancer prognosis [28], [29]. A recent meta-analysis based on retrospective data showed that early-stage breast cancer patients that undergo breast-conserving surgery with LVI experienced worse overall survival, distant metastasis and local recurrence compared to patients without LVI [30]. Thus, clinical presentation and overall outcome in IBC patients is attributed to the lymphotactic-nature of IBC; as such the mechanisms which drive this phenomenon need to be further understood and identified.

Diagnostic Ambiguity

Given the diagnosis of IBC is clinical and therefore subjective, diagnostic ambiguity can occur in IBC cases that present with borderline features, or overt skin change that is not readily apparent as erythema [15]. IBC is an aggressive disease, with urgent demands for early detection and diagnosis. Patients lack the presence of a palpable lump on the breast, hindering detection [31]. Ultrasounds are often more reliable and effective than mammograms. Ultrasounds provide effective imaging for detection and diagnosis, without breast compression or ionizing radiation, unlike mammograms [32], [33]. At MD Anderson, breast examinations for IBC encompass three assessments; including skin thickening of the affected breast (skin thickness greater than 3mm), detection of breast lesions and regional lymph node involvement [32].

The international IBC diagnosis consensus guidelines determined that minimal diagnostic criteria include rapid onset of erythema, edema, peau d'orange, and/ or breast warmth [34], [3]. IBC is characterized with rapidly developing skin symptoms, rather than a mass detected by palpation or mammography [3]. Most patients with IBC present with axillary lymph node involvement at the time of diagnosis, and 30% present with distant metastasis [35]. For some women, skin discoloration from baseline is darkening or purplish rather than red/erythema, for others skin edema on the breast could be subtle and observed upon further examination [36]. Examining the association between outcome and clinical findings regarding breast appearance, we demonstrated that a more classic clinical IBC presentation which is classified by swollen involved breast, diffuse skin change (not limited to erythema) and nipple change was associated with later disease staging and worse overall survival (chapter 2). Considering the potential relationship between LVSI and this classic –appearing IBC, we focused further studies on the drivers of lymphatic vessels and function both in the pre-cancer mammary gland and within tumors.

IBC treatment

IBC treatment of non-metastatic disease begins with neoadjuvant chemotherapy based on tumor markers called receptors, that reflect to a certain degree the biologic classification of the tumor and in doing do serve as biomarkers for therapy [37], [34]. Breast cancers are highly heterogeneous. Extensive comprehensive microarray-based gene expression profiling identified intrinsic molecular subtypes of

breast cancers classified as luminal A, luminal B, HER2+, normal-like and basal-like, more recently claudin-low [38]. Histopathologically, the genomic subtypes are related to receptor-based characterization subgroups: Hormone receptor (HR)-positive (defined as estrogen receptor-positive, and/or progesterone receptor-positive), HER2+ (Human Epidermal Growth Factor Receptor 2), and triple negative breast cancer (TNBC) [39]. Further studies have identified multiple subtypes within TNBC [39]. All currently identified molecular subtypes identified in non-IBC have been identified in IBC, however the proportions of these subtypes differ as TNBC is the most common subtype in IBC accounting for up to 30% of the IBC cases and HR-positive is the most common in non-IBC accounting for up to 80% of non-IBC cases [40]. Triple negative patients receive chemotherapy with pembrolizumab based on the Keynote 522 regimen [41], HER2-positive patients receive dual her2 targeted agents with chemotherapy [42] and ER+ patients are offered neoadjuvant chemotherapy followed by weekly taxol [43]. After neoadjuvant chemotherapy, a modified radical mastectomy is recommended, and pathologic review will quantify the efficacy of chemotherapy by reporting the size and density of remaining disease in the breast and number of resected lymph nodes with tumor present. No tumor in the breast or nodes is defined as a pathologic complete response (PCR). Outcomes after PCR are improved compared to no-PCR but remain lower than PCR in non-IBC patients [44], [45]. Post-mastectomy radiation to the chest wall and undissected regional lymph nodes is offered after surgery, often tailored to the residual disease and targeting any regional lymph nodes that were not resected, such as those in the internal mammary chain or supraclavicular fossa [46], [47]. Adjuvant targeted therapy is offered to patients with residual disease based on the receptor status, TDM1 (contains trastuzumab) for HER2+ patients, ongoing pembro for TNBC, and CDK 4/6 inhibitors and anti-hormonal therapy for ER+ patients. In addition, BRCA mutation carriers may be offered adjuvant olaparib [48]. In cases of hormone receptor positive IBC, estrogen blocking hormonal therapy is continued for 5-10 years as part of the treatment regimen. Thus, given the poor outcomes expected of this aggressive disease IBC patients are treated with maximal tri-modality therapy.

Linking risk factors to biology in IBC; alterations in the microenvironment

Considering the risk factors of IBC described above, several identified risk factors are known to alter the stroma of the breast and the biology of these changes may provide clues to the pathogenesis of IBC in the breast. Studies have not shown unique genomic drivers that can be attributed to this aggressive disease even after balancing for subtype differences in IBC [38], [49]. In fact, a 79 gene signature defining IBC-like patients is present in ~25% of patients in the TCGA, clearly a much larger proportion than present as IBC patients, and includes genes largely predicted to be present in stroma [49]. This implicates the stroma in the progression and characteristics of IBC.

During pregnancy in preparation for lactation, the breast remodels itself by extensive proliferation of mammary epithelium and further differentiation during lactation [50]. Subsequently, during the lactation to involution cycle the majority of the epithelium undergoes programmed cell death [51].

As previously described, IBC epidemiological studies have established that a lack of breastfeeding is associated with IBC. During pregnancy, the alveolar epithelium expands and increases in size in response to elevated estrogen levels, the ductal cells undergo proliferation and elongation, and adipose tissue proliferate. This leads to the stimulation of prolactin, inducing lactation in alveolar cells of lobules in response to estrogen [52]. After weaning, forced or natural, involution occurs. Involution is a multistep process that occurs to revert the breast to the pre-pregnancy state [50]. Involution occurs in two stages, the first termed the reversible stage which spans the initial 48 hours and is characterized by milk stasis, and the initiation of epithelial cell death. The second phase is termed the irreversible phase, where the expanded breast epithelium undergoes apoptosis, stromal remodeling occurs with immune cell infiltration facilitating the remodeling of the breast to its pregnant state [50], [53], [54]. Further, the regression of mammary gland epithelium, and tissue remodeling which include ECM remodeling, increased lymphatic vessel density (LVD) and immune filtration [55], [56]. Clinical studies have indicated that new mothers diagnosed with breast cancer have a higher metastatic potential, and thus a worse prognosis [57]. The process of mammary gland involution which includes the physiologic gland regression, high macrophage populations, fibrillar collagen deposition and epithelial apoptotic signaling contributing to a tumor-promotional mammary microenvironment, utilizing aspects of wound-healing and inflammation programs [58].

Prior to pregnancy the mammary-epithelium is embedded in a mesenchymal-derived fat pad, during pregnancy the epithelium undergoes an extensive proliferation and differentiation in preparation for lactation [59]. Following weaning, the mammary gland resorbs the elaborate milk-producing lobuloalveoli and returns to its rudimentary pre-pregnant state. The remodeling of the lactating gland requires the removal of secretory alveolar cells, extensive remodeling of extracellular matrix molecules, and the gland returns to the mesenchymally-derived adipocytes populations and fibroblasts [58],[60]. The microenvironment during involution demonstrates similarities in wound-healing and tumor promoting characteristics [61], [62]. In particular, during the process of involution there is an upregulation of collagen genes such as collagen I, III and IV. Collagen I is associated with predicting metastasis in solid tumors, and collagen III are expressed at elevated levels at sites of active tumor invasion and tumor promotion [58]. Our lab hypothesized that if not breast feeding was preventing normal or complete involution in some patients to contribute to lymphatics in the pre-IBC breast, involution-related signals would be present in the normal tissues of women with IBC. Bambhroliya and colleagues evaluated time point based gene signatures from abrupt post-lactational involution in post-natal mice in normal breast and normal breast tissue remote from IBC tumor [63]. This demonstrated one of the murine post-lactational gene signatures, genes over-expressed at 12 hours that should diminish by 24 hours were enriched in IBC versus non-IBC [63]. The top three over-expressed genes in IBC were Involucrin (*IVL*), Cluster of Differentiation 79B (*CD79B*), and Leptin (*LEP*). These hypothesis-generating data intriguingly demonstrate gene expression related to this temporal biologic process of involution in the normal breast long after pregnancy [63].

Additionally, during lactation there are significant changes to the adipocytes and stromal remodeling, these features are recognized for nutritional and metabolic sources for expanding epithelium and for milk production [64],[65]. A pregnancy-associated breast cancer (PABCs) study, identified local and systemic factors promoting breast cancer when studying nulliparous glands, pregnant mice with glands isolated 10 days after vaginal plugs were present, and involuting and full regression groups, with involuting mammary glands removed 3 days or 21 days after pup removal, respectively [66]. Using 4T1-12B carcinoma cells to study the effects of the mammary glands at these major stages of post-natal development, they found that 4T1-12B tumors grew the largest in the involuting mammary glands relative to the nulliparous. In addition,

the tumors harvested from the pregnant and lactating mice were 3.5 fold larger than their nulliparous counterparts [66]. This suggests that pregnancy and lactation contribute significantly to tumor growth in relation to involution. The effects here are two fold, one being the hormonal effects as there are higher levels of estrogen and progesterone during pregnancy, and elevated levels of prolactin which is a potent mitogen of breast cancer cells which are also influential. Alternatively, mammary adipose stromal cells (ASCs) present during lactation were the biggest affecters of breast tumorigenesis and were thus considered to increase the aggressiveness of the tumors [66]. Lactating ASCs also expressed elevated levels of inflammatory cytokines which promote growth. Additionally, they also established that *crabp1*, is expressed in lactating ASCs which inhibits lipids from undergoing adipogenesis [66]. Most studies understandably seek to only examine one variable; however, this is a gap in our understanding of the synergy of risk factors in the breast stroma.

Generally, several characteristics are shared between an involuting mammary gland and the breast tumor microenvironment, including expression of tumor-promotional collagen, upregulation of matrix metalloproteinases, infiltration of M2 macrophages, and remodeling of blood and lymphatic vasculature [63], [67]. In a global collaborative analyses across institutions, a study demonstrated both epidemiological evidence and mechanistic evidence linking longer breastfeeding periods with a reduced risk for breast cancer. Basree and colleagues modeled two mammary gland involutions, gradual involution and abrupt involution, and found that abrupt involution following pregnancy resulted in a denser stroma with altered collagen, higher inflammation and proliferation, and reported a higher risk of developing breast cancer [68]. In mice, it has been established that the mammary epithelium is tightly associated with the surrounding lymphatics, as the lymphatics undergo simultaneous expansion and regression with the epithelium, during pregnancy, lactation and involution [69]. In healthy women, Jindal et al. have demonstrated that following pregnancy, the breast has increased lymphatic density and inflammatory infiltration that persist for years [70]. Taken together, this highlights the overlap between the lymphotactic nature of IBC, and the risk-factor induced signals in the breast eliciting a conducive tumor microenvironment.

IBC is a model of florid LVSI

Consistent with the hypothesis that pre-cancer lymphatics are integral to IBC phenotype, the clinical characteristics of IBC, erythema and swelling, are attributed to ectatic and dilated dermal lymphatics clogged by malignant cells in extensive lymphangiogenesis [71],[72]. In a comprehensive comparative study between IBC and non-IBC conducted by Van der Auwera and colleagues, peritumoral lymph vessels in tumor specimens of patients with IBC had higher proliferating lymphatic endothelial cells compared to non-IBC tumors [71]. IBC is highly lymphotactic, as dilated dermal lymph vessels clogged by tumor emboli serve as pathologic hallmarks histologically [71].

Lymphatic function in the normal mammary gland

The lymphatic system is made up of an extensive network of lymphatic vessels, beginning with the initial lymphatic capillaries that serve an absorptive role, collecting vessels which transport lymph, and the lymph node which mediates immune responses [73], [74]. The lymphatic system has several roles including removal of excess fluids from interstitial tissue, transporting macromolecules, the absorption of fat in the form of chyle, trafficking and surveilling immune cells and maintaining overall homeostasis [75], [76]. However, unlike the cardiovascular circulatory system, the lymphatic system does not have a central pumping system and hence relies on the systematic mechanics of the lymphangion to ensure the flow of lymph fluid [77]. The process of lymphatic pumping requires a combination of extrinsic (passive) and intrinsic (active) forces to propel lymph fluid [78], [79]. The process of lymph propulsion relies on robust contractions of lymphatic muscle cells which are initiated by action potentials, these contraction waves must be synchronized along the lymphangion with competent valves that minimize fluid backflow [77]. During tumor invasion, the tumors drain into lymphatic vessels resulting in lymphangiogenesis, marked by the dilation of lymphatic vessels, the increase lymph transport, and ultimately the expansion of these lymphatic vessels. This lymphatic expansion is caused by the elevated expression of VEGFC by the tumor-associated leukocytes such as macrophages and even by the tumors [80].

Studies on the intersection of the microenvironment and lymphatics have been largely focused on static assessment of lymphatics in post-mortem tissue sections. This leaves the relevance of the function of the

vessels under-studied. There have been studies that have used *in vivo* near infra-red fluorescence (NIRF) imaging that have sought to identify changes in lymphatic vasculature, drainage and architecture attributed to several pathologies [81], [82], [83]). The main hallmark of IBC is the dermal lymphatic invasion by tumor emboli, which cause the obstruction of lymphatic drainage which is attributed for the clinical presentation features such as the peau d'orange, breast enlargement and diffuse erythema and edema [1],[84]. Although there have been studies that have described the pathological characteristic of IBC drainage into the dermal lymphatics, there have not been imaging studies that have illustrated this. This study conducted by the Sevick research group, used non-invasive and longitudinal novel near infrared fluorescence (NIRF) imaging to study the impact of IBC tumors on the lymphatic drainage patterns and architecture [85], [86]. These NIRF-imaging captured fluorescence images of well-defined lymphatic vessels following intradermal injections of indocyanine green (IcG), lymphatic vessel architecture and drainage prior to tumor inoculation [87]. Subsequently, after 11 weeks mice were subcutaneously or orthotopically inoculated with human triple-negative IBC tumor cells stably transfected with infrared fluorescence (iRFP) gene reporter (SUM149-iRFP). They imaged these mice longitudinally to determine tumor impact on the lymphatic vasculature. The longitudinal NIRF imaging showed the IBC tumor growth obstruction of normal lymphatic drainage patterns, as well as an increase in dilated fluorescent lymphatic vessels around the tumor periphery, hallmark characteristics of lymphangiogenesis [87]. This functional, longitudinal NIRF lymphatic imaging study was a novel approach to visualizing and demonstrating the lymphovascular invasion, lymphatic drainage obstruction and metastasis caused by IBC tumors using mice models [87]. In other cancers, antiangiogenesis agents, specifically targeting the vascular endothelial cell growth factor (VEGF) have been incorporated into treatment regimens [88]. In 2011, despite growing interest of using anti-VEGF-A, bevacizumab, in breast cancer, the FDA revoked approval for the use of bevacizumab in combination with neoadjuvant paclitaxel for metastatic BC patients due to drug safety and efficacy concerns [89]. Since then, clinical trials have sought to assess the appropriate dosage and use of bevacizumab with chemotherapy in metastatic HER2-negative BC, and even brain metastasis studies in BC, however the concerns bevacizumab adding toxicity to chemotherapy have not been resolved [90], [91]. Further, the identifying the mechanism of lymphovascular invasion in IBC is critical, and thus we sought to study the

role of the CCR7/CCL21 axis, an establish lymphatic homing pathway, to better understand IBC and IBC-related lymphangiogenesis.

The mechanistic role of CCR7 in lymphatic homing

C-C chemokine receptor 7 (CCR7) is a G-protein coupled receptor, part of a larger chemokine family which has been established as key regulator of leukocyte trafficking and contribute to immunity and tolerance [92]. The recruitment of immune cells to tumor sites is regulated by the actions of chemokines and their respective receptors. The binding of these ligands induces a conformational change of the receptor [93]. CCR7 is involved in lymph-node homing of naïve and regulatory T cells *via* high endothelial venules, and the inflammation-induced migration of dendritic cells to the lymph nodes. CCR7 is expressed by dendritic cells and B cell subpopulations. CCR7 has two ligands, including CC-chemokine ligand 19 (CCL19) and CC-chemokine ligand 21 (CCL21) [94]. These high endothelial venules are CCL21 positive, during an inflammation-induced homing of CCR7-expressing immune cells, to the CCL21-expressing afferent lymphatic vessels which connect to a lymph node across a chemotactic gradient [95]. A study on metastatic melanoma demonstrated that the recruitment and homing of CCR7 (+) metastatic melanoma cells to tumor draining CCL21-positive lymph nodes [93], mimicking CCR7-expressing immune cells resulting in the chemotactic spread and migration of these melanoma cells toward lymph nodes [93]. In breast cancer, studies have demonstrated the prognostic and therapeutic potential of CCR7 [96]. Metastatic triple-negative breast cancer studies note that CCR7 is highly expressed in TNBC cell lines, and promotes the invasiveness and metastasis of triple-negative breast cancer [97]. An *in vivo* breast cancer model demonstrated, that the CCL21/CCR7 chemokine axis promoted tumor-induced lymphangiogenesis [98]. Additionally, CCR7 mRNA tissue expression in human breast cancer positively correlated to lymphatic markers, LYVE-1, prox-1 and VEGF-C [98]. A separate study conducted at MDA using immunohistochemistry staining of IBC patient tissue, showed that 20% of the IBC tumors were CCR7 positive [99], which is equivalent to the frequency of HER2+ IBC disease [11], [24]. Taken, together this suggests a potential chemotactic metastasis model for IBC into the lymphatics, and warrants further study to explore prognostic and therapeutic options.

Herein, we have undertaken a series of studies to understand the role of lymphatic function and mechanisms of lymphatic function in IBC. We examine the visible clinical symptoms of presumed fulminant clogged lymphatics clinically, and demonstrate they correlate to outcomes. We examine the synergy of multiple risk factors on lymphatic pulsing to further our understanding of how pretumor changes in the breast facilitate IBC progression and lymphovascular invasion. And lastly, we assess CCL21/CCR7 signaling in IBC and pre-clinical studies, and report that tumor size was significantly associated with lymphatic pulsing.

Chapter 2-Methods and Materials

Chapter 3 Methodology:

Study Cohort.

Since 2007, all patients evaluated and diagnosed with IBC using international consensus guidelines for IBC [3] and seen at the MD Anderson Cancer Center Morgan Welch IBC Clinic have been offered participation in an IRB approved prospective registry [4]. The international IBC diagnosis consensus guidelines note diagnostic minimal criteria include rapid onset of erythema, edema, peau d'orange and/or breast warmth. Thus, patients were diagnosed with IBC who have obvious skin changes over at least 1/3 of the breast without erythema. For some women, skin discoloration from baseline is darkening or purplish rather than red/erythema. For some women skin edema > 1/3 of the breast (either frank peau d'orange skin change or more subtle edema only visible on close inspection) may be evident without any redness or discoloration (**Fig 1**). Examination of the registry database specifically demonstrates erythema is less common among African American women [16]. Participation in the registry included completing an interviewer-administered questionnaire to collect risk factor information such as demographics, lifestyle, reproductive and family history. All patients underwent multi-disciplinary evaluations, that included assessment by a breast medical oncologist, breast surgeon, breast radiation oncologist, and breast radiologist. Routine imaging included bilateral mammogram, bilateral ultrasound, and staging (CT chest abdomen and pelvis with bone scan or PET/CT) [100], [101], [102], [103], [104]. MD Anderson breast pathologists reviewed patient biopsies and specimens, and recommendations from the American Society for Clinical Oncology and College of American Pathologists were used to determine the 1% nuclear expression cutoff for estrogen receptor (ER) and progesterone receptor (PR) expression [105].

For this analysis, we reviewed pre-treatment medical photographs and charts of patients from the IBC registry. Breast medical photographs at time of diagnosis are an essential component of disease evaluation, since the images serve to inform and guide radiation treatments and assessment of treatment response. All the available breast medical photographs were reviewed by two independent non-IBC experts, a non-oncological physician and a graduate student. Scoring discrepancies were resolved by a high-volume IBC clinician. Photographs with evident ipsilateral breast swelling, diffuse skin change (not limited to erythema but in all cases encompassing all or nearly all of the breast), and nipple change (all

compared to the uninvolved side), were scored as positive for the triad of signs deemed classic (**Fig 1B**). Those without all three signs were scored as non-classic and ambiguous or difficult to assign cases were scored as a third group (**Fig 1A**). This group included patients with two overt signs but not the third, such as evident diffuse skin change but retraction of the breast rather than swelling, or borderline calls for any one sign.

Statistical methods for patient analysis.

Descriptive statistics including mean, standard deviation, median and range for continuous variables and tabulation for categorical variables were used to present patient demographic and clinical/pathological characteristics. To compare differences between or among the patient groups, Chi-squared test or Fisher's exact test was used for categorical variables and Wilcoxon rank sum test or Kruskal-Wallis test for continuous measures. IBC diagnosis dates were used to measure overall survival times. The Kaplan-Meier method was used to estimate overall survival distributions, and the log-rank test to assess differences in overall survival between or among patient groups. Univariate and multi-variate Cox regression models were used to evaluate presentation and the effect of other important covariates on overall survival. All computations are carried out in SAS 9.4 (SAS Institute Inc., Cary, NC, USA) and Splus 8.2 (TIBCO Software Inc, Palo Alto, CA).

Chapter 4 Methodology:

Animals.

All animal experiments were performed in accordance with guidelines of the institutional animal regulations and American Association for Laboratory Animal Science guidelines. Balb/c SCID/Beige mice purchased from The Jackson Laboratory (Bar Harbor, ME) and maintained in a pathogen-free mouse facility.

For Experiment 1 (nulliparous animals). 10 female mice were started on high fat diet (HFD) (60 Kcal%, N=5) (Research Diets, Inc) or a low fat diet (LFD) (10 Kcal%, N=5) when pups were 3 weeks old.

For Experiment 2 (multi-parous animals). Prior to pregnancy at 3 weeks of age, 20 animals were divided into two groups fed a high fat (60 Kcal%, N=10) (Research Diets, Inc) or a low fat diet (10 Kcal%, N=10). These mice were bred and impregnated twice in succession, and each diet group was further randomized in weaning groups: nurse weaned (NW) versus forced weaned (FW) (10 mice each respectively, 5 per diet + weaning group).

***In vivo* Near Infra-red Fluorescence (NIRF) lymphatic imaging.**

Mice were transferred from MD Anderson to UTHS for imaging and maintained there through sacrifice. At each imaging session, depilatory cream (Nair; Church & Dwight Co., Inc) was used to remove hair from the skin over the #4 mammary glands. Mice were then anesthetized with isoflurane (2% oxygen), placed on a warming pad (37°C), and images obtained as follows. A volume of 10- μ L of Indocyanine Green (IcG) (Akron, Inc.) was intradermally injected, around the areolar into the left ventral #4 mammary fat pad. Fluorescence images were acquired immediately and continuously over 8 minutes using an electron-multiplying charge-coupled device (EMCCD) camera (PhotonMax 512B, Princeton Instruments, Tucson, AZ). Image acquisition was accomplished by V++ software (Digital Optics, Auckland, New Zealand). Matlab (The MathWorks Inc., Natick, MA) and ImageJ (National Institutes of Health, Washington, DC) based analyses were performed to analyze and quantify lymphatic contractile activity at a defined region of interest (ROI) on each fluorescent vessel.

***In vivo* orthotopic cell lines.**

The triple negative parental IBC SUM149 cell line (MD Anderson Cancer center, Houston, TX) was passaged and cultured in Ham's F-12 media supplemented with 10% FBS (GIBCO, Thermo Fisher, Carlsbad, CA, USA), 1 $\mu\text{g}\cdot\text{mL}^{-1}$ hydrocortisone (#H0888, Sigma-Aldrich, St. Louis, MO, USA), 5 $\mu\text{g}\cdot\text{mL}^{-1}$ insulin (#12585014; Thermo Fisher), and 1% penicillin and streptomycin (#15140122; Invitrogen, Carlsbad, CA, USA). All cell lines were kept at 37 °C in a humidified incubator with 5% CO₂. Tumor initiation involved orthotopic inoculation of 1.0×10^6 cells above the areola into the fat pad of mammary gland #4 at 14 months after initiation of the diet.

Multiplex IF.

FFPE (formalin fixed paraffin-embedded) blocks of tumor and mammary gland were submitted for tissue microarray construction, multiplex panel optimization and testing. A pathologist (NF) reviewed H&Es for each FFPE sections, and identified ROIs in the mammary gland that would capture tissue heterogeneity. Subsequently, core punch biopsies were performed on the FFPE blocks to obtain cylindrical cores that are transferred to the recipient block, and further to cut the tissue using a microtome to 4 μm thick sections. Each mammary gland section had two replicates from intentionally distinct tissue regions when applicable. All sections were subjected to chromogenic immunohistochemistry staining was performed to validate and optimize targets using the Leica Bond RX autostainer with an incubation time of 60 minutes at 1:15,000 after 20 minutes of heat-induced antigen retrieval at pH 6.0. Each panel had 6 antibody targets. The Leica bond autostainer is manufactured for a capacity of 6 targets per panel. Antibody target stains were grouped in two panels: Panel A targets were CD31 (ABCAM, cat #28364), IBA-1 (ABCAM, cat #178847), alpha-smooth muscle actin (SMA) (ABCAM, cat #5694), podoplanin (Invitrogen, cat #29742), vimentin (Cell Signaling, cat #5741), and CK19 (ABCAM, cat #52625). Panel B targets were CD163 (ABCAM, cat #182422), CD11b (ABCAM, cat #133357), CCR7 (Invitrogen, cat #MA5-31992), CD11c (Cell Signaling, cat #97585), CCL21 (Invitrogen, cat #114959), and CK19 (ABCAM, cat #52625). Immunohistochemically stained samples were scanned using the Aperio AT2 (Leica Biosystems, Wetzlar, Germany). Multiplex, immunofluorescence (MIF) staining was performed using Akoya biosciences 7-color opal kit (Akoya

Biosciences, Marlborough, MA) on a Leica Bond Rx autostainer. The stained mIF slides were subsequently scanned with a Leica Versa 8 (Leica Biosystems, Wetzlar, Germany). Images captured using Leica Imagescope software.

Leica Imagescope software Analysis for Quantification and Structural Analysis of Multiplex IF.

Entire plates with cores containing mice mammary gland tissue and tumor sections were stained for the respective Panel A and B markers using Multiplex IF, and scanned into the Leica Imagescope software. The IF quantification was done using the image analysis tool, the cellular IF algorithm was selected and modified for each plate. Four different algorithms were modified for each panel and tissue type. The tissue cores were annotated and labeled based on the tissue section and mouse ID. Algorithms were uniquely created to detect the number of positive cells for each marker in the mammary glands and tumor sections for each panel. First, the cellular IF algorithm was tuned to segment cellular nuclei to ensure accurate identification and quantification of 4',6-diamidino-2-phenylindole (DAPI) -stained nuclei. Next, the algorithm was tuned for positive fluorescence intensity to quantify the tissue expression of each marker while minimizing non-specific background staining or autofluorescence. Once the autotuning was completed for the individual markers, the cellular co-expression of selected markers was included in the algorithm quantification. To evaluate the lymphatic vessel and mammary duct cellular environment, each vessel and duct was individually annotated in the mammary gland cores for structural and functional analysis with these algorithms.

Microarray statistics.

Due to heterogeneity in tumors based on H & E and review of vimentin staining, both replicates from each tumor were included in analyses without averaging. GraphPad Prism was used to plot graphs and perform t-test and one-way ANOVA analyses, assuming independent samples. P-values < 0.05 were considered significant. Pearson's correlations were performed in SPSS (version 23). The Kaplan Meier survival curves and log rank statistic were performed to assess tumor free survival, using GraphPad Prism.

Chapter 5 Methodology:

Gene Array Data.

CCR7 and *CCL21* expression in inflammatory breast cancer (IBC) samples as analyzed using the IBC Consortium dataset [49]. Tumor samples were stratified as CCR7-high when expression in tumor was greater than or equal to the median, otherwise, the sample was classified as CCR7- low in the normal breast samples. Mann-Whitney tests were used when two groups were compared, and one-way analysis of variance was used for multiple experimental groups. Black lines in each group indicate median \pm SD, and p values of <0.05 were considered significant. Spearman rank correlation coefficient was used to measure the strength of the association between *CCR7*, and its ligand *CCL21* with lymphatic marker, *LYVE-1*. A P value of < 0.05 was considered significant. GRAPHPAD software (GraphPad Prism 8, La Jolla, CA, USA) was used.

Tissue Microarray.

Immunohistochemistry (IHC) staining for CCR7 was conducted on breast tissue biopsies from post-chemotherapy mastectomy specimens of 36 IBC patients, each with three replicates was subjected to immunohistochemical staining for CCR7 (Invitrogen, catalog number MA5-31992) performed using a Leica Bond RX autostainer with an incubation time of 60 minutes at 1:15,000 after 20 minutes of heat-induced antigen retrieval at pH 6.0. In 15 cases there were no tumor cells observed in the cores. Entire plates with cores of 39 primary breast tissue biopsies from IBC patients underwent immunohistochemistry staining were scanned by Aperioscope for visual analysis. Staining was scored by an expert breast pathologist for intensity and percent tumor stained. Staining patterns were scored. Descriptive statistics were examined for representation by receptor subtype.

***In vitro* cell lines.**

SUM 149, SUM159 and SUM190 (Asterand, Detroit), MDA-231 (ATCC, Manassas), MDA-IBC3 and KPL4 (MD Anderson, Houston):

The following cell lines were passaged and cultured in Ham's F-12 media (Corning 10-080-CV) supplemented with 10% FBS (GIBCO, 16000-044 Thermo Fisher, Carlsbad, CA, USA), $1 \mu\text{g}\cdot\text{mL}^{-1}$

hydrocortisone (#H6909, Sigma-Aldrich, St. Louis, MO, USA), 5 $\mu\text{g}\cdot\text{mL}^{-1}$ insulin (#12585014; Thermo Fisher), and 1% Antibiotic/Antimycotic (Gibco 15240-062, Carlsbad, CA, USA). All cell lines were kept at 37 °C in a humidified incubator with 5% CO₂.

Western blot.

Protein lysates from IBC and non-IBC cell lines SUM 149, 159 and SUM190, MDA-231, MDA-IBC3, KPL4 were subjected to immunoblotting using anti CCR7 (Invitrogen, catalog number MA5-31992). Cells were lysed in RIPA buffer (Sigma) supplemented with 10 μLmL^{-1} phosphatase and 10 μLmL^{-1} protease inhibitor cocktail. SDS/PAGE and immunoblotting were carried out. The following primary antibodies were used: CCR7 (Invitrogen, catalog number MA5-31992) GAPDH (Cell signaling, 5174 1: 5000), and samples were incubated overnight at 4°C. Secondary antibodies (Cell signaling, 70745 1: 5000), were incubated with the samples for 2 hours at room temperature. Immunoreactivity was visualized with Super signal west pico plus chemiluminescent Substrate #34577 (Thermofisher, Waltham, MA USA) using ImageQuant LAS4000 (GE Health-care, Chicago, IL, USA).

Chapter 3: Inflammatory breast cancer appearance at presentation is associated with overall survival.

This chapter is based upon “Balema, W., Liu, D., Shen, Y., El-Zein, R., Debeb, B. G., Kai, M., Overmoyer, B., Miller, K. D., Le-Petross, H. T., Ueno, N. T., & Woodward, W. A. (2021). Inflammatory breast cancer appearance at presentation is associated with overall survival. *Cancer medicine*, 10(18), 6261–6272. <https://doi.org/10.1002/cam4.4170>”.

ABSTRACT

Background: Inflammatory breast cancer (IBC) is a clinical diagnosis. Here, we examined the association of a “classic” triad of clinical signs, swollen involved breast, nipple change, and diffuse skin change, with overall survival (OS).

Method: Breast medical photographs from patients enrolled on a prospective IBC registry were scored by two independent reviewers as classic (triad above), not classic, and difficult to assign. Chi-squared test, Fisher’s exact test and Wilcoxon rank sum test were used to assess differences between patient groups. Kaplan Meier estimates and the log-rank test and Cox proportional hazard regression were used to assess overall survival.

Results: We analyzed 245 IBC patients with median age 54 (range 26-81), M0 vs. M1 status (157 and 88 patients, respectively). The classic triad was significantly associated with smoking, post-menopausal status, and metastatic disease at presentation ($P = 0.002, 0.013, \text{ and } 0.035$, respectively). 10-year actuarial OS for not classic and difficult to assign were not significantly different and were grouped for further analyses. Ten-year OS was 29.7% among patients with the classic sign triad versus 57.2% for non-classic ($P < .0001$). The multivariate Cox regression model adjusting for clinical staging ($P < .0001$) and TNBC status ($< .0001$) demonstrated classic presentation score significantly associated with poorer OS time (HR 2.6, 95% CI 1.7-3.9, $p < .0001$).

Conclusions: A triad of classic IBC signs independently predicted OS in patients diagnosed with IBC. Further work is warranted to understand the biology related to clinical signs and further extend the understanding of physical examine findings in IBC.

INTRODUCTION

Inflammatory Breast Cancer (IBC) is a rare and particularly aggressive variant of breast cancer. IBC accounts for only 2-4% of all breast cancer cases, however, the disease is responsible for 10% of breast cancer-related deaths in the US [10]. In a comparative study with non-inflammatory locally advanced breast cancer (LABC) patients, women diagnosed with IBC had a significantly poorer survival time (2.9 years versus 6.4 years) over 10 years [14]. IBC is a clinical diagnosis, requiring >1/3 involvement on the affected breast and/or skin by erythema, and disease onset of < 6 months [1], [34]. Diagnostic ambiguity can occur in cases that present with borderline features, or overt skin change that is not readily apparent as erythema. To date no study has examined the association between outcome and clinical findings regarding breast appearance.

It is increasingly recognized that not all skin change is overtly erythematous in IBC [16]. Marked swelling of the involved breast is often noted at the time of diagnosis and nipple changes (flattening or inversion) are a common finding among IBC cases [4], [34], [106]. While it has been well-demonstrated that frank peau d'orange and other skin changes are prognostic for worse outcome in all patients, very little is known about the prognostic effect of variations in skin change on IBC presentation [31], [107], [108]. For over ten years in a dedicated IBC multi-disciplinary clinic, we increasingly associate the clinical signs triad of diffuse skin change (not solely limited to erythema), obvious swelling of the involved breast and nipple change, with an unambiguous diagnosis of IBC if the onset of the disease is rapid occurring in less than 6 months. Here we sought to review pre-treatment medical photographs from IBC patients, to determine whether this triad of breast signs was associated with poorer outcome than cases that met diagnostic criteria.

RESULTS

Figure 1. Examples IBC patient photographs scored by clinical presentation



Figure 1. Examples IBC patient photographs scored by clinical presentation (A). Representative photo scored as non-classic as breast shows diffuse erythema of a fairly symmetrical possibly slightly retracted left breast (B). Representative classic patient demonstrating significant swelling of the affected right breast, flattened nipple, and diffuse change in skin tone.

Study participants

From 2007 to 2020, a total of 701 patients were enrolled in the prospective IBC registry of which 423 (60.3%) were enrolled prior to beginning any therapy. Medical photographs were available on 250 patients (59%). Images were scored for presentation (classic N =60, not classic N =130 or difficult to assign N =52). Five patients lacking outcomes or without a contralateral breast or photograph of the contralateral breast for comparison to assess the scoring were excluded leaving 245 patients in this analysis.

Demographic and clinical characteristics of our patient population

Table 2, describes the demographic and reproductive factors of the study participants. The mean age at diagnosis was 54 years (range, 26-81). The average BMI at diagnosis was 30.9 (14.9-76.9). BMI patient distribution was normal (14.7%), overweight (23.3%), obese I (BMI 30-34.9) (27.3%), obese II (BMI 35-39.9) (10.2%), obese III (BMI>40) (5.3%). The race/ethnicity distribution was White (80.4%), Black (7.3%), Hispanic (6.9%), Asian pacific (3.3%), Native American (0.4%) and other (0.8%).

Two hundred and ten patients (85.7%) reported having been ever pregnant with mean age of 23.4 years (14-37 years) at first pregnancy. One hundred and twelve (59.6%) parous women reported a history of breastfeeding. Based on a subset (N = 27) of patients that responded to a set of questions regarding breastfeeding history that were introduced more recently to the questionnaire, two patients breastfed for <1 month (7.4%), four for 1-3 months (14.8%), four for >3-<6 months (14.8%), 17 for >6 months (63%). The majority of the patients were post-menopausal (67.5% vs. 32.5%). Never smokers accounted for 57.8% of the patients, while 33.3% were former smokers and 8.8% were current smokers.

Table 2. Demographic and reproductive characteristics of the study population.

Demographic and Reproductive Characteristics	Value (n=245)
Age at Diagnosis, Mean (Range)	54.25 years (26-81 years)
Age at menarche, Mean (Range)	12.5 years (8-16 years)
Age at first pregnancy, Mean (Range)	23.4 years (14-37 years)
Ever Pregnant, No. (%)	
No	24 (9.8%)
Yes	210 (85.7%)
Gravida, Mean (Range)	2.51 (0-10)
Number of miscarriage, Mean (Range)	0.47 (0-4)
Number of children, Mean (Range)	2.12 (0-6)
Body Mass Index at Diagnosis, Mean (Range)	30.91 (14.87-76.95)
Race/Ethnicity, No. (%)	
White	197 (80.4%)
Black	18 (7.3%)
Hispanic	17 (6.9%)
Asian Pacific	8 (3.3%)
Native American	1 (0.4%)
Other	2 (0.8%)
Breastfeeding history, No. (%)	
Yes	112 (45.7%)
No	76 (31%)
Breastfeeding Duration (months), No. (%)	
<1 month	2 (0.8%)
1 ≤3 months	4 (1.6%)
>3 ≤6 months	4 (1.6%)
>6 months	17 (6.9%)
Menopausal Status, No. (%)	
Pre-menopausal	66 (26.9%)
Post-menopausal	179 (73.1%)
Smoking history, No. (%)	
Current	18 (7.3%)

Former	68 (27.8%)
Never	118 (48.2%)
Alcohol Consumption, No. (%)	
No	48 (19.6)
Yes	146 (59.6)

¹ Patients that breastfed for 3 months were included in the 1 ≤3 months category, patients that breastfed more than 3 months and up to 6 months were included in the >3 ≤6 month breastfeeding time range.

² Percentages do not add up to 100% due to missing patient values.

Table 3, shows the tumor and clinical characteristics, the distribution of clinical stage across the cohort were IIIB (32%), IIIC (32%) and stage IV (36%). The hormone receptor (HR)-positive subtype surrogate (positive for estrogen receptor [ER] and/or progesterone receptor [PR] and negative for HER2) was present in (73/245=29.8%), while HER2-positive ER/PR- and triple negative (TNBC) were present in (95/245=38.8%) and (68/245=27.8%) of patients, respectively. Among M0 patients 93% received neoadjuvant and 26.1% received adjuvant chemotherapy. Further, 82.5% of M0 received documented adjuvant radiation therapy. The median follow-up period was 6 years. At the time of current analysis, 141 (57.6%) patients were alive, 36% among the de novo metastatic cohort.

Table 3. Tumor and clinical characteristics

Clinical Characteristics	Value (N=245)
Clinical Stage, No. (%)	
IIIB	78 (31.8%)
IIIC	78 (31.8%)
IV	88 (36.1%)
Subtype, No. (%)	
ER/PR+, HER2-	73 (29.8%)
HER2+	95 (38.8%)
Triple-Negative	68 (27.8%)
Lymphatic Invasion, No. (%)	
Negative	101 (41.2%)
Positive	101 (41.2%)
Vascular Invasion, No. (%)	
Negative	102 (41.6%)
Positive	100 (40.8%)
Neoadjuvant Chemotherapy, No. (%)	
No	93 (38%)
Yes	151 (61.6%)
Adjuvant Chemotherapy, No. (%)	
No	202 (82.4%)
Yes	42 (17.1%)
Pathologic Complete Response (Pcr), No. (%)	
No	221 (90.2%)
Yes	21 (8.6%)
Unknown	3 (1.2%)

³Percentages do not add up to 100% due to missing patient values.

Table 4, describes the self-reported breast features at time of presentation. Breast swelling, redness and edema were reported by 48.6%, 69.8% and 53.9% of patients, respectively. Additionally, 35.1% of patients reported experiencing skin change, such as warmth (38.4%), nipple inversion (29%) and skin thickening (29%). With regards to the time lag between initial symptoms and clinical diagnosis of IBC, 33.5% (N = 90) of patients reported an onset of less than 90 days.

Table 4. Self-reported breast features at time of presentation.

Characteristics	Value (n=245)
Lump, No. (%)	
No	134 (54.7%)
Yes	99 (40.4%)
Peau d'orange, No. (%)	
No	90 (36.7%)
Yes	14 (5.7%)
Unknown	104 (42.4%)
Skin Change, No. (%)	
No	150 (61.2%)
Yes	86 (35.1%)
Nipple Discharge, No. (%)	
No	219 (89.4%)
Yes	16 (6.5%)
Swelling, No. (%)	
No	117 (47.8%)
Yes	119 (48.6%)
Redness, No. (%)	
No	67 (27.3%)
Yes	171 (69.8%)
Edema, No. (%)	
No	104 (42.4%)
Yes	132 (53.9%)
Warmth, No. (%)	
No	141 (57.6%)
Yes	94 (38.4%)
Nipple Inversion, No. (%)	
No	165 (67.3%)
Yes	71 (29%)
Skin Thickening, No. (%)	
No	121 (49.4%)
Yes	60 (24.5%)
Pain, No. (%)	
No	178 (72.7%)
Yes	57 (23.3%)
Days Initial Symptoms appear, No. (%)	
0-90 days	82 (33.5%)
91-180 days	6 (2.4%)
>180 days	2 (0.8%)
Unknown	155 (63.3%)

⁴Percentages do not add up to 100% due to missing patient values.

Patient photographs were reviewed and classified into three groups with 60 (24.8%) classic showing all triad signs, 130 (53.7%) non-classic and 52 (21.5%) ambiguous. The classic presentation was significantly associated with ever smoking (57.7% classic vs. 30.1% non-classic, $P = 0.002$), post-menopausal status (78% of classic vs 58.7% non-classic patients, $P = 0.013$), and metastatic disease at presentation (50% of classic vs 33.1% of non-classic patients, $P = 0.035$) (**Table 5**).

Table 5. Comparison of epidemiologic, tumor and clinical characteristics by presentation appearance (non-classic, in between and classic presentation were individually scored as 1, 2 and 3, respectively).

Covariate	Presentation	Categories					P-value
		Black	Other	White			
Race	1	6(4.7%)	17(13.2%)	106 (82.2%)			0.4797
	2	5 (9.8%)	6 (11.8%)	40 (78.4%)			
	3	6 (10%)	5 (8.3%)	49 (81.7%)			
BMI	1	19(19.2%)	31(31.3%)	35(35.4%)	9(9.1%)	5(5.1%)	0.7668
	2	9(20%)	9(20%)	15(33.3%)	8(17.8%)	4(8.9%)	
	3	8(15.1%)	17(32.1%)	17(32.1%)	7(13.2%)	4(7.5%)	
Smoking Status		Current	Former	Never			0.0021
	1	6(5.8%)	25(24.3%)	72(69.9%)			
	2	2(4.3%)	21(45.7%)	23(50%)			
Alcohol consumption		No	Yes				0.9133
	1	25(25%)	75(75%)				
	2	10(22.7%)	34(77.3%)				
ER/PR+		NEG	POS				0.8928
	1	60(46.2%)	70(53.8%)				
	2	26(50%)	26(50%)				
TNBC		Non-TNBC	TNBC				0.959
	1	93(71.5%)	37(28.5%)				
	2	37(71.2%)	15(28.8%)				
Menopausal Status		POST	PRE				0.0129
	1	61(58.7%)	43(41.3%)				
	2	36(78.3%)	10(21.7%)				
Clinical N stage		N0/N1	N2/N3				0.5578
	1	54(41.5%)	76(58.5%)				
	2	20(38.5%)	32(61.5%)				
Clinical Stage		III	IV				0.0351
	1	87(66.9%)	43(33.1%)				

	2	37(71.2%)	15(28.8%)	
	3	30(50%)	30(50%)	
Lymphatic Invasion		NEG	POS	
	1	56(50.9%)	54(49.1%)	0.3726
	2	23(56.1%)	18(43.9%)	
	3	20(41.7%)	28(58.3%)	
Neoadjuvant Chemotherapy		No	Yes	
	1	41(31.8%)	88(68.2%)	0.0323
	2	20(38.5%)	32(61.5%)	
	3	31(51.7%)	29(48.3%)	

⁵Percentages do not add up to 100% due to missing patient values.

⁶BMI classification normal (1), overweight (2), obese I (3), obese II (4), and obese III (5).

Figure 2: Kaplan-Meier curve of actuarial incidence of overall survival by presentation category.

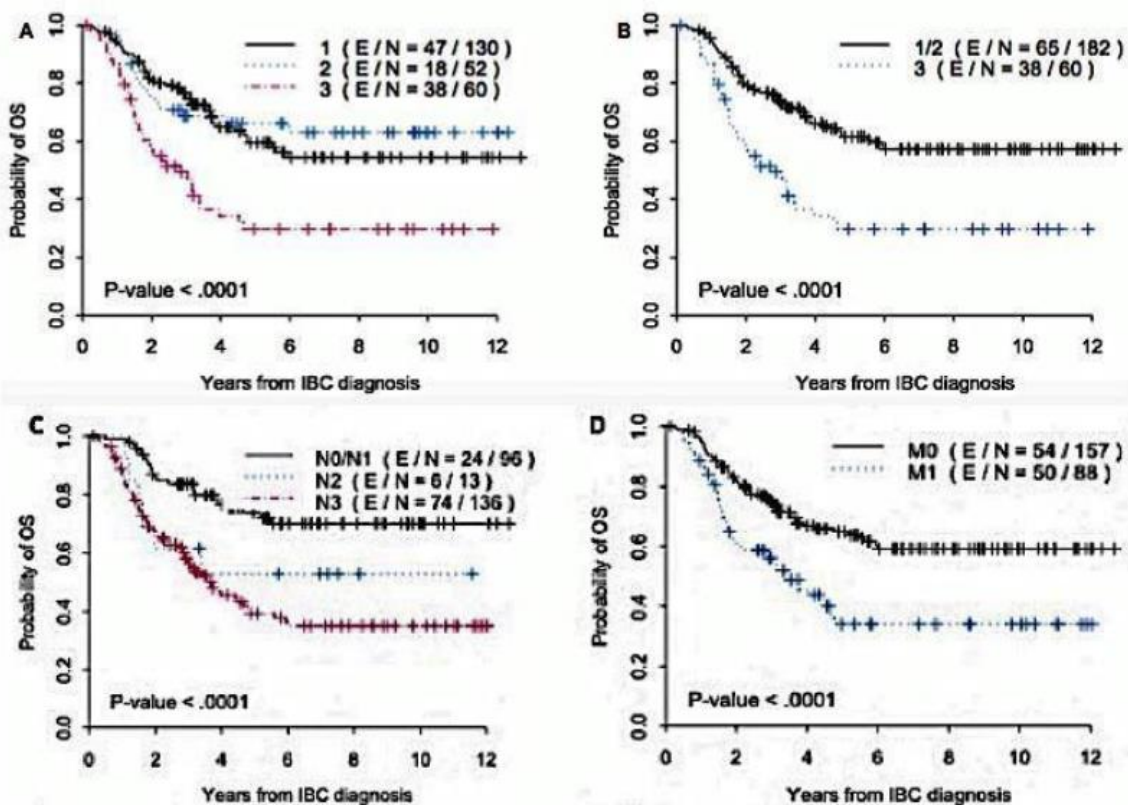


Figure 2. Kaplan-Meier curve of actuarial incidence of overall survival by presentation category. (classic= 3, ambiguous=2 and non-classic =1) (A,B), and clinical N and M stage (C,D). Number of IBC patients surviving at 10 OS indicated on respective graphs. (E) representing the number of patients that experienced an event from the (N) total patients in that specific group. Log-rank test was used to obtain p-values.

Univariate analysis of OS, showed that the non-classic and ambiguous groups were not significantly different from each other (**Fig 2A**) and were therefore grouped together for further analyses. Ten-year actuarial overall survival for the classic group was 29.7 vs. 57.2% for all others (**Fig 2B** P =0.001). The 10-year actuarial OS for clinical N stage was 70.1% vs. 37.2% for N0/N1 versus N2/N3 (**Fig 2C** P<0.0001), 59.2% for stage III and 34% for Stage IV (**Fig 2D** P=0.0001) **Table 6A**. The multivariate Cox regression model demonstrated classic presentation score was independently associated with poorer OS time (HR 2.6, CI 1.7-3.9, p<.0001) after adjusting for clinical staging (IIIC/IV vs. III/IIIB, HR 2.9, CI 1.7-4.9, P<.0001) and TNBC status (TNBC vs non-TNBC, HR 3.5, CI 2.3-5.2, P<.0001) **Table 7**.

Table 6A. Kaplan-Meier estimates analysis 1 **Table 6A. Kaplan-Meier estimates analysis for categorical variables on overall survival outcome, 95% CI provided for each 2, 5 and 10-year OS probability estimate, respectively. Log-rank test was used to obtain p-values.**

Covariate	Categories	Year	OS	95% CI		P-Value
Race	Black	2	0.59	0.327	0.78	0.083
		5	0.324	0.115	0.555	
		10	0.324	0.115	0.555	
	Other	2	0.668	0.457	0.812	
		5	0.565	0.346	0.736	
		10	0.565	0.346	0.736	
	White	2	0.777	0.711	0.829	
		5	0.566	0.486	0.639	
		10	0.52	0.437	0.597	
Breastfeeding	No	2	0.645	0.526	0.741	0.0081
		5	0.441	0.321	0.554	
		10	0.423	0.304	0.537	
	Yes	2	0.841	0.757	0.898	
		5	0.625	0.511	0.719	
		10	0.588	0.469	0.688	
Clinical N stage	N0/N1	2	0.86	0.771	0.916	<.0001
		5	0.738	0.627	0.821	
		10	0.701	0.583	0.792	
	N2/N3	2	0.669	0.586	0.739	
		5	0.409	0.319	0.496	
		10	0.372	0.283	0.462	
Clinical M Stage	M0	2	0.817	0.746	0.87	0.0001
		5	0.649	0.562	0.724	
		10	0.592	0.498	0.674	
	M1	2	0.612	0.499	0.706	
		5	0.34	0.229	0.456	
		10	0.34	0.229	0.456	
Clinical Stage	III	2	0.817	0.746	0.87	0.0001
		5	0.649	0.562	0.724	
		10	0.592	0.498	0.674	
	IV	2	0.612	0.499	0.706	
		5	0.34	0.229	0.456	
		10	0.34	0.229	0.456	

Table 6B. Univariate Cox regression analysis on overall survival and disease specific survival (non-classic, in between and classic presentation were individually scored 1, 2 and 3, respectively). Log-rank test was used to obtain p-values.

Covariates	Hazard Ratio	HR lower CL	HR upper CL	p-Value
Age	1.01	0.99	1.03	0.23
BMI	0.99	0.97	1.03	0.96
Age at Menarche	0.89	0.79	1.02	0.10
Gravida	1.04	0.90	1.20	0.59
Age at 1st Pregnancy	0.97	0.93	1.02	0.22
Number of Children	1.08	0.91	1.27	0.37
Number of Miscarriages	0.98	0.72	1.31	0.87
Time between pregnancies	0.95	0.81	1.11	0.52
Average weight gain during pregnancy	1.02	0.98	1.06	0.38
Breast feeding duration (months)	0.99	0.97	1.02	0.63
Birth control usage (years)	0.99	0.95	1.03	0.56

Table 7. Multivariate Analysis of overall survival.

Parameter	Category	Hazard Ratio	95% Hazard Ratio Confidence		p-value
Presentation Scoring	Classic vs. Other	2.58	1.72	3.88	<.0001
Clinical Stage	IIIC/IV vs III/IIIB	2.92	1.73	4.93	<.0001
TNBC	TNBC vs non- TNBC	3.49	2.34	5.21	<.0001

⁷Multivariate Cox Regression Model (including Clinical Stage in the model, N=244)

DISCUSSION

The clinical diagnosis for IBC remains subjective and is often ambiguous [109]. AJCC defines IBC, staged T4D as a clinical diagnosis characterized by diffuse erythema and edema involving at least one third of skin of the affected breast. Overt cases are characterized by diffuse erythema, edema (*peau d'orange*), breast enlargement, or other skin involvement as well as skin color changes [2],[110], [111], however significant variation at presentation leads to ambiguity in those diagnosed with IBC. We examined whether a visible constellation of clinical breast signs deemed “classic” by a high-volume IBC clinic correlated with overall survival, and observed for the first time advanced stage and poorer outcome among the classic presenting patients compared to all others. Our study further demonstrates the extent of variation in presentation and warrants the need to further refine diagnostics for the ambiguous or less overt presenting cases.

The scoring criteria for classic IBC in this study were based on experience in our dedicated single institution IBC clinic and in part confirmed by a recent working group to refine diagnostic IBC symptoms. In an initiative to improve IBC patient clinical diagnosis and further outcome, several groups including Susan G. Komen, the Inflammatory Breast Cancer Research Foundation, and the Milburn Foundation convened patient advocates and breast cancer researchers, clinicians and experts to improve and progress IBC diagnostics beyond clinical subjectivity [34]. This was achieved by establishing detailed criteria and scoring systems to facilitate IBC diagnosis and subsequently patient care. The proposed scoring system based on the experience of the involved experts and literature review included variables such as timing of initial signs/symptoms to diagnosis, skin changes including any *peau d'orange* or skin edema/thickening involving over a third of the breast, breast swelling supplemented by skin discoloration (darkening, purplish or bruising appearance) and nipple abnormalities such

as nipple inversion or new nipple flattening or asymmetry. The detailed scoring system established through the Komen initiative accounted for the heterogeneity in characteristics commonly associated with IBC, thus broadening the scope of the IBC clinical subjectivity. Importantly, focusing on skin change as a classic criteria as opposed to skin erythema, would potentially reduce inaccurate exclusion of black women who may go underdiagnosed due to presentation bias attributed to skin change not being explicitly red [8], [12], [15],[112], [113]. In addition, this more intricate and detailed disease classification could help develop a staging system specific to IBC.

Though similarities may surface, there are clinical practices which distinguish skin changes seen with IBC from the skin changes associated with non-inflammatory breast tumors (T4a-c) [13], [114], [115]. Variability in features and characterizations observed in presentation among IBC patients were observed in our patient cohort. Only 24.8% had classic appearing IBC by these criteria, highlighting the majority of cases take some further diagnostic work to make the diagnosis. Interestingly, as has been described previously, many women don't describe erythema on presentation [3], [34]. Since erythema is a part of the AJCC staging for T4D, it could be argued these patients are misdiagnosed, however, in the presence of overt skin change such as diffuse peau d'orange, it is felt instead that the staging imperfectly describes some IBC patients.

Additionally, we examined the impact of clinical, epidemiologic and reproductive factors on the visual presentation scoring of classic among IBC patients. Reproductive factors were explored in more detail in a subset of patients that completed more extensive questionnaires. Interestingly, smoking was significantly increased among patients with classic presentation. Atkinson et al, previously reported in a single-institution case-control study, that epidemiological risk factors such as obesity and smoking were associated with IBC [32]. A

recent study evaluated the effect of demographic and lifestyle factors as well as the presence of crown-like structures in breast adipose tissue (CLS-B) on breast cancer outcome in African American versus white women [71]. CLS-Bs which are composed of adipocytes encircled by macrophages, are associated with obesity as higher BMIs result in increased adipose tissue in the breast, which recruit macrophages creating a pro-inflammatory microenvironment. This study concluded that current smoking was positively associated with the detection of CLS-B, and at a higher density in comparison to non-smoking individuals [71]. This association with CLS-B could explain how BMI and smoking induce changes in the breast microenvironment promoting a more classic IBC presentation.

IBC is highly lymphotactic, dilated dermal lymph vessels containing large tumor emboli are pathologic hallmarks histologically [87], [72], and are the underlying mechanism for the peau d'orange skin feature of IBC. In a comprehensive comparative study between IBC and non-IBC, peritumoral lymph vessels in tumor specimens of IBC patients had higher proliferating lymphatic endothelial cells compared to non-IBC tumors [116]. These distinguishable features are critical in differentiating IBC and non-IBC [117], [118]. Interestingly, lymphovascular skin invasion (LVSI) on pathology report from the tumor showed no correlation with classic presentation.

Some limitations to this study include the pros and cons of background of photo scorers, one non-IBC expert physician and one IBC research trainee without clinical experience. As non-experts, the review reflects results expected from non-experts which strengthens the utility of these findings beyond an expert clinic. Some nuances may be overlooked or incorrectly attributed by non-experts however. Discrepancy review highlighted the impact of uncommon clinical findings such non-healing biopsies, prior surgical scars, or changes related to prior breast therapy. In addition, based on a prior hypothesis, this analysis does not explore the

outcomes of patients with obvious skin findings and breast retraction which may represent a distinct biology and deserves further study. Although the study data was collected prospectively, this review was retrospective which has inherent biases that may not be accounted for. Another limitation was the non-representative racial distribution among the women in our patient cohort. Disparities in breast cancer screenings and treatment impact Black and Hispanic women. Black women are disproportionately impacted by IBC and are more likely to be diagnosed with triple negative-IBC and a worse outcome than any other racial group [6], [11], [17], [87], [119], [120]. Underrepresentation of black women in our cohort precludes analysis of classic presentation by race; no significant associations were observed in our analysis however this limitation makes it inconclusive.

In conclusion, we show a triad “classic” IBC breast signs is independently prognostic for overall survival. While classic IBC presentation is associated with worse overall survival, the majority of the IBC patients in our study did not fall into the “classic” group, and thus defining diagnostic criteria for those non-classic patients who risk misdiagnosis or not receiving required treatments is critical. Future molecular studies comparing IBC tissues by presentation may help to shed light on the underlying biological mechanisms for IBC presentation and potential targets.

Chapter 4: High fat diet but not weaning timing increases pre-tumor mammary gland lymphatic vessel pulsing and subsequent inflammatory breast cancer tumor growth in a pre-clinical model.

ABSTRACT

Background

IBC is an aggressive breast cancer that presents suddenly with breast swelling and redness due purportedly to abundant tumor emboli in the breast and breast skin lymphatics. An association between IBC risk and obesity as well as breastfeeding duration has been established, however the mechanistic effects of obesity and weaning status on the IBC tumor progression have not been explicitly studied. We sought to model the simultaneous effects of a diet and weaning on *in vivo* lymphatic function pre- and post-tumor initiation, IBC tumor growth, and mammary gland microenvironment. We hypothesized that weaning status and high fat diet would synergize to induce pro-lymphatic changes in the microenvironment before tumor initiation and subsequent enhanced IBC tumor growth.

Methods

In vivo near-infrared fluorescent (NIRF) imaging of a NIRF probe draining from bilaterally injected mammary glands was performed to assess lymphatic pulsing in mice. Lymphatic pulsing was compared among Balb/c SCID/Beige mice fed a high fat diet (HFD, 60 kCal%) versus low fat diet (LFD, 10 kCal%) (Experiment 1, N = 10) and mice fed HFD vs. LFD who were randomized to nursing or force weaning after each of two rounds of pregnancy (Experiment 2, N = 20). Consecutive NIRF lymphatic imaging was performed at weeks 8, 11 and 14 following diet initiation in experiment 1. In experiment 2, imaging was performed at 6-7 months (interrupted due to covid), at 14 months, and at 16 months after the initiation of SUM149 tumors. Tumors were assessed for tumor growth and skin invasion at the time of resection. Mammary gland tissues contralateral to the tumors were embedded at the time of sacrifice and stained using multi-plexed immunofluorescence for 12 markers of microenvironment and tumor markers. Algorithms to quantitate cells and structures were designed using the Leica Imagescope software and statistics were performed using prism and SPSS.

Results

In nulliparous mice, HFD increased lymphatic pulsing compared to LFD. Average ventral lymphatic contractile frequency at 8, 11 and 14 weeks after diet initiation were 5, 8.64, 15.9 pulses/4 mins vs 11.8, 18.5, 28.2 pulses/4 mins, ($P = 0.01, 0.05, \text{ and } 0.0005$ respectively). In multiparous mice, lymphatic pulsing pre-tumor in HFD force-weaned (HFFW) and HFD nurse-weaned (HFNW) animals was increased compared to LFFW and LFNW ($P < 0.001$ and $P = 0.003$ respectively). Lymphatic pulsing after tumor initiation (16 months after initiation of diet) was significantly increased compared to baseline in all groups and increased compared to LFD groups at the pre-tumor timepoint (all $P < 0.05$). HFD promoted tumor growth independent of nursing variables ($P = 0.02$) and lymphatic pulsing was associated with a trend for direct correlation to tumor growth ($P = 0.08$). Lymphatic pulsing was significantly associated with cells expressing lymphatic tracking ligand, CCL21 ($P = 0.05$). HFD significantly increased monocyte-derived cells including IBA-1+, CD163+ and CD11c+ cells ($P < 0.0001, P < 0.0001, P = 0.0005$) in the mammary gland. Further, while number of lymphatic vessels (PDPN+) were not different across groups ($P = \text{NS}$), lymphangiogenic PDPN-expressing macrophages (PDPN+/IBA-1+; PoEMs) cells were increased in ducts of HFD and forced weaned mice (all $P < 0.003$).

Conclusion

HFD increased changes in mammary gland lymphatic function prior to tumor initiation that correlate to increased SUM149 tumor growth and increased inflammatory cells in the mammary gland. Tumors increased lymphatic function to a similar extent. Increased CCL21+ cells, a ligand for lymphatic traffic homing, was correlated to pulsing, and the relationship between lymphatic pulsing, tumor growth and CCR7-CCL21 related tumor trafficking warrant further investigation.

INTRODUCTION

Inflammatory breast cancer (IBC) is an aggressive breast cancer that presents rapidly with breast swelling and redness or skin color changes purportedly due to abundant congested lymphatics in the breast and breast skin [34], [36]. These symptoms are attributed to IBC tumor emboli clogging dermal lymphatics around the breast, causing lymphovascular skin invasion (LVSI) [106, 107]. In many cases, metastatic spread has a diffuse lymphatic-based pattern, suggesting that the lymphatics attract and facilitate the spread of the tumor to, for example, the contralateral axillary and mediastinal nodes [4],[9], [121]. This highlights the importance of understanding lymphatic development and function in mediating the poor outcomes of this disease.

Emerging evidence suggests the microenvironment can induce and promote IBC symptoms and the diffuse IBC-like growth pattern [122],[123]. We previously reported that mesenchymal stromal cells signal through macrophages to promote skin invasion by IBC cells in the SUM149 *in vivo* model [123]. Individual breast cancer risk factors are well known to alter the mammary gland microenvironment [13], [63]. The factors in the breast microenvironment that contribute to LVSI have not been well-studied and established. However, Atkinson et al. reported in a single-institution case-control study that epidemiological risk factors specifically, obesity and never breast feeding were associated with IBC [13]. Genomic analysis demonstrated IBC tissues were enriched for gene signatures associated with abrupt weaning, suggesting this could contribute to the development of aggressive breast cancer [63]. Obesity and breast-feeding duration have been implicated in IBC risk [13], yet clearly these overlap with non-IBC, and correlation of the underlying microenvironment changes to IBC specific biology remains elusive. Thus, we propose to investigate the synergy of IBC risk factors obesity and weaning timing in creating a pro-IBC, lymphatic-rich mammary stroma, even before tumor initiation. Recognizing the critical role of lymphatic function in IBC and the lack

of data specifically examining function, we used NIRF of mammary-draining fluorescent dye to study the synergy of risk factors on function and subsequent tumor progression.

We hypothesize that obesity and force weaning after pregnancy synergistically promote pro-inflammatory microenvironments in the breast, increasing the density and function of the lymphatics of breast tissue, contributing to the IBC skin symptoms and spread caused by dense lymphatics clogged by tumor emboli (lympho-vascular space invasion). We report HFD is associated with increased mammary lymphatic pulsing, but fewer lymphatic vessels. Tumor initiation increases lymphatic pulsing to a similar degree as HFD. For the first-time, we report that high fat diet promotes IBC tumor growth in mice. The HFD significantly increased inflammation of specific mammary duct-infiltrating macrophages and dendritic cells. Lymphatic pulsing was correlated with CCL21, a ligand for CCR7 a leukocyte receptor, which mediates macrophages and dendritic cell trafficking to the lymphatics. Further, we find increased lymphangiogenic subset of macrophages, PDPN+ macrophages (PoEMs) in lymphatic vessels and mammary ducts of HFD and forced weaned mice, potentially highlighting a mechanism for IBC tumor growth and lymphovascular skin invasion, this warrants further study.

RESULTS

High fat diet significantly increased lymphatic pulsing in nulliparous and multiparous mice.

To initially investigate the effect of HFD versus control, LFD on lymphatic function from the mammary gland, we measured lymphatic pulsing in nulliparous mice started on diets at 3 weeks of age. *In vivo* NIRF lymphatic imaging of IgG dye drainage from the mammary gland was assessed from three lymphatics, the ventral, right, and left at three timepoints, 8, 11, and 14 weeks after initiation of diet (Figure 3). The average weight of the low fat and high fat mice were 21.3g and 26.8g, respectively ($P=0.005$). The HFD mice developed greasy coats over time, which impacted the intradermal IgG administration. *In vivo* NIRF imaging was performed on the dermal lymphatic vessels around the #4 mammary gland. Representative images of the ventral dermal lymphatic vessels in LFD and HFD mice were captured following the IgG subdermal injection (Figure 3A and 3B). At week 8 and 11, we conducted *in vivo* NIRF dermal lymphatic imaging on the ventral, right and left sides. At week 8, the lymphatic pulsing activity was significantly increased in the ventral and right dermal lymphatic vessels in the HFD mice (Figure 3C, $P=0.001$ and $P=0.01$, respectively). At week 11, the lymphatic pulsing activity was significantly increased in the right and left dermal lymphatic vessels in the HFD mice (Figure 3D, $P=0.01$ and $P=0.01$, respectively). At week 14, the mice did not display lymphatic pulsing during imaging on the left and right, due to lymphatic collapse, however ventral dermal lymphatic pulsing was measured and demonstrated a significant increase in lymphatic pulsing in the HFD mice (Figure 3E, $P<0.001$). The lymphatic pulsing activity increased in all the animals over time, however it was only statistically significant in HFD animals. Average ventral lymphatic contractile frequency for LFD and HFD at week 8, 11 and 14 weeks were 1.25, 2.16, 3.97 pulses/min vs 2.94, 4.63, 7.06 pulses/min (Figure 3F, $P=0.001$, 0.04, 0.006, respectively).

Figure 3: HFD increases mammary lymphatic pulsing compared to LFD in nulliparous mice.

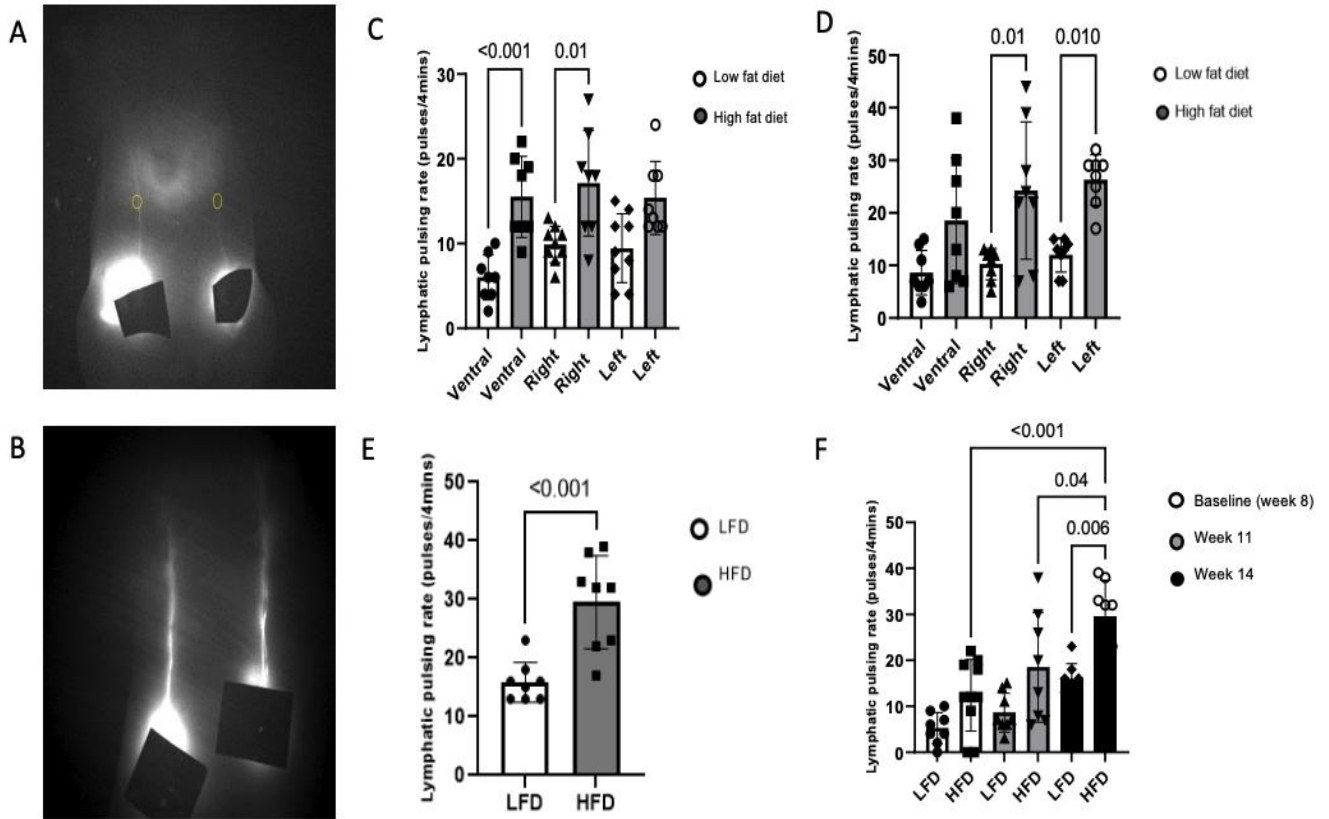


Figure 3. HFD increases mammary lymphatic pulsing compared to LFD in nulliparous mice. Representative LFD and HFD *in vivo* NIRF images of the ventral dermal lymphatic vessels above mammary gland #4 following ICG intradermal injections (Figure 3A, B). High fat diet fed mice increased lymphatic contractile activity using *In vivo* NIRF Imaging conducted in the ventral, right and left view of dermal lymphatic vessels following ICG intradermal injections at week 8 (Figure 3C, P = 0.0006 and P=0.0118, respectively) and 11 (Figure 3D, significant increases in the right and left lymphatic; P=0.0117 and P=0.0098, respectively). At week 14, the mice did not display lymphatic pulsing during imaging on the left and right, due to lymphatic collapse, however increased pulsing in the ventral lymphatic was significant (Figure 3E, P=0.0005). Lymphatic contractile activity increased in all animals over time, but was only statistically significant in HFD animals (Figure 3F, P=0.0001, 0.0410, 0.0057, respectively). Unpaired t-tests and one-way Anova's were used for statistical analysis, P<0.05 were significant.

To investigate the synergistic effects of HFD and weaning timing on dermal lymphatic pulsing activity, multiparous mice fed a specialized diet were either forced or nursed weaned (Figure 4). We hypothesized that the synergistic effects of obesity and weaning timing would increase lymphatic pulsing activity to facilitate increased lymphovascular skin invasion. Due to Covid interruptions the first lymphatic imaging session was at 6-7 months; limited access to the imaging facilities resulted in baseline imaging measurements spread over weeks, and delayed the subsequent imaging timepoint for the mice. Therefore, pre-tumor imaging was repeated at 14 months in one session as intended. Mice were maintained on the diets without interruption during this time. In multiparous mice, lymphatic pulsing pre-tumor in HFD force-weaned (HFFW) and HFD nurse-weaned (HFNW) animals was increased compared to LFFW and LFNW (Figure 4A, $P < 0.001$ and $P = 0.01$), weaning did not have an impact on the lymphatic pulsing activity in the mice (Figure 4A $P =$ Not significant, N.S.). The second pre-tumor imaging timepoint was 14 months. The lymphatic imaging demonstrated the persisting effects of a HFD on lymphatic pulsing activity, in the HFNW and HFFW mice (Figure 4A, $P = 0.003$ and $P < 0.001$).

Figure 4: HFD increases lymphatic pulsing from mammary gland draining lymphatics in multiparous mice similar to pulsing induced by tumor initiation.

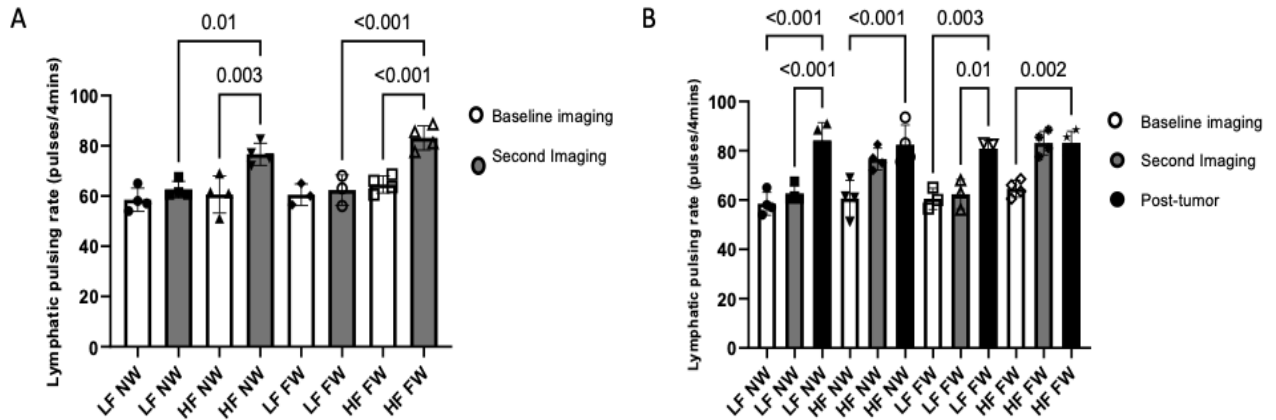


Figure 4. HFD increases lymphatic pulsing from mammary gland draining lymphatics in multiparous mice similar to pulsing induced by tumor initiation. In multiparous mice, lymphatic pulsing pre-tumor in HFD force-weaned (HFFW) and HFD nurse-weaned (HFNW) animals was increased compared to LFFW and LFNW, weaning did not have an impact on the lymphatic pulsing activity in the mice (Figure 4A, $P < 0.001$ and $P = 0.01$), The second pre-tumor imaging timepoint was 14 months, the lymphatic imaging demonstrated the persisting effects of a HFD on lymphatic pulsing activity, in the HFNW and HFFW mice (Figure 4A, $P = 0.003$ and $P < 0.001$). Tumor initiation significantly increased the lymphatic pulsing activity across all 4 mice groups independent of diet or weaning status (Figure 4B, LF NW $P < 0.001$, HF NW $P = 0.0002$, LF FW 0.0033 and HF FW $P = 0.0018$, respectively).

High fat diet significantly increased IBC tumor growth in multiparous mice.

We next sought to determine how risk factor-primed microenvironments would facilitate tumor growth and impact lymphatic activity and vasculature, following SUM149 tumor cells orthotopic inoculation into the #4 mammary gland fat pad of these mice. Mice were re-imaged at 16 months, 10 weeks after tumor initiation for post-tumor lymphatic imaging. Tumor initiation significantly increased the dermal lymphatic pulsing activity compared to the baseline pre-tumor pulsing across all 4 mice groups, independent of diet or weaning status (Figure 4B, LF NW $P < 0.001$, HF NW $P < 0.001$, LF FW $P = 0.003$ and HF FW $P = 0.002$, respectively). Kaplan Meier survival statistics were performed to assess tumorigenesis, demonstrating neither diet nor weaning status significantly altered tumor-free survival (Figure 5A, $P = \text{N.S.}$). In addition, skin invasion, which is defined by hair loss with bleeding or blisters on the skin, and a palpable tumor growing into the skin, was present in 13/14 animals that grew tumors, and thus was not significantly different across the groups (Figure 5B, 5C). HFD fed mice had increased tumor growth (Figure 5D, $P = 0.04$). However, weaning status did not impact IBC tumor growth (Figure 5E, $P = \text{N.S.}$). Lymphatic pulsing was correlated with tumor size at 42 days and CCL21, a ligand for leukocyte receptor, CCR7 which mediates leukocyte homing and trafficking towards lymphatics, using a chemotactic gradient. (Table 8, $P = 0.08$ and $P = 0.05$, respectively). In addition, we conducted CCR7 staining on tumors from these mice which were elevated in high fat and forced weaned mice. Further, CCR7 staining in tumors was strongly correlated with pre-tumor lymphatic pulsing (Supplemental Figure 1).

Figure 5: HFD promotes IBC tumor growth in scid/beige multiparous mice.

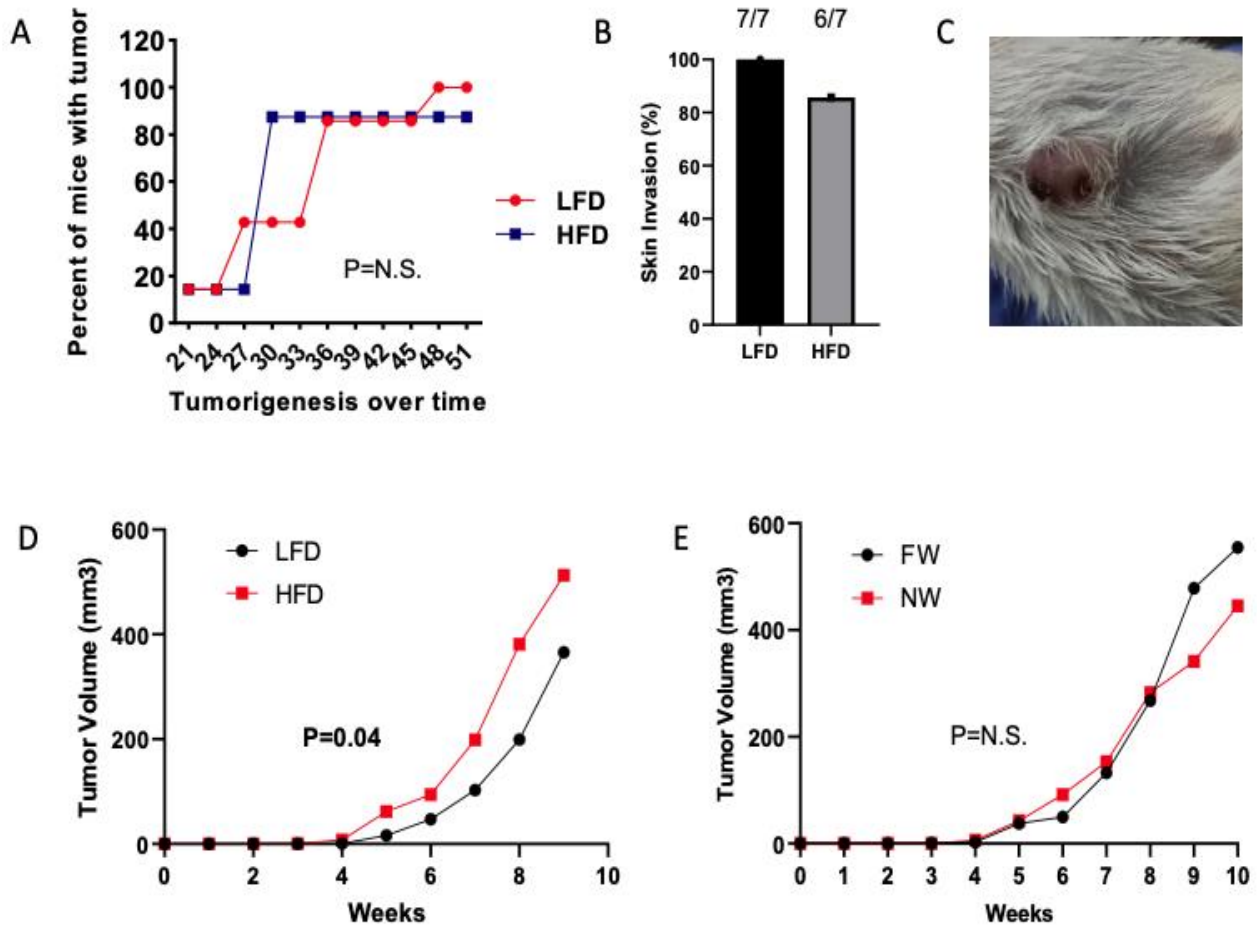


Figure 5. HFD promotes IBC tumor growth in scid/beige multiparous mice. Figure 5A, neither diet nor weaning status significantly altered tumor-free survival. Figure 5B, 5C, skin invasion was present in most animals in each group and not significantly different across groups. Figure 5D, 5E, demonstrates for the first time that HFD increases IBC tumor growth, in addition to the rate at which tumorigenesis occurs, independent of weaning status ($P=0.04$, $P=N.S.$, respectively).

Table 8. Correlation between lymphatic pulsing and tumor growth and lymphangiogenesis.

		CCL21	Lymphatic Pulsing
Tumor size	Pearson Correlation	0.16	0.5
	Significant (2-tailed)	0.61	0.08
	N	13	13
CCL21	Pearson Correlation	1	0.557*
	Significant (2-tailed)		0.05
	N	13	13
Lymphatic pulsing	Pearson Correlation	0.557*	1
	Significant (2-tailed)	0.05	
	N	13	13
CCR7	Pearson Correlation	0.708***	0.4
	Significant (2-tailed)	0.007	0.1
	N	13	13

High fat diet induced increase in lymphatic function is independent of lymphatic vessel count in mammary gland.

HFD significantly increased lymphatic pulsing activity, independent of weaning status, to a similar extent that tumor initiation did. To determine if this increase in lymphatic functionality was due to increased lymphatic vessel density, lymphatic vessels were individually annotated in the mammary glands from the multiparous mice cores for structural and functional analysis, using the algorithms created with the imagescope software. Tissue microarray multiplex immunofluorescence effectively stained for 12 markers across 2 panels including CD31, IBA-1, alpha-SMA, podoplanin, vimentin, CK19, CD163, CD11b, CCR7, CD11c and CCL21 on the tumor and mammary gland tissue (Figure 6, Supplemental Figure 1). Lymphatic endothelial marker podoplanin (PDPN) was used to identify lymphatics. There were no significant differences in PDPN-positive cells detected across all four treatment groups, and the HFD vs. LFD mice had significantly decreased PDPN+ lymphatic cells (Figure 7A, P=N.S., Figure 7B P=0.02). The average number of lymphatic vessels were identified by manual annotation in the mammary gland core sections across the treatment groups; LF NW, LF FW, HF NW and HF FW, were 18.3, 3.3, 7.7 and 8, respectively (Table 9, P=NS). HFD fed mice vs. LFD had significantly fewer PDPN+ lymphatic vessels (Figure 7B, P=0.02, representative images, Figure 7D, 7E). Thus, increased lymphatic function was associated with decreased detected vessels.

Figure 6: Tissue microarray multiplex immunofluorescence effectively stained for 12 markers across two panels on mammary gland tissue and tumors.

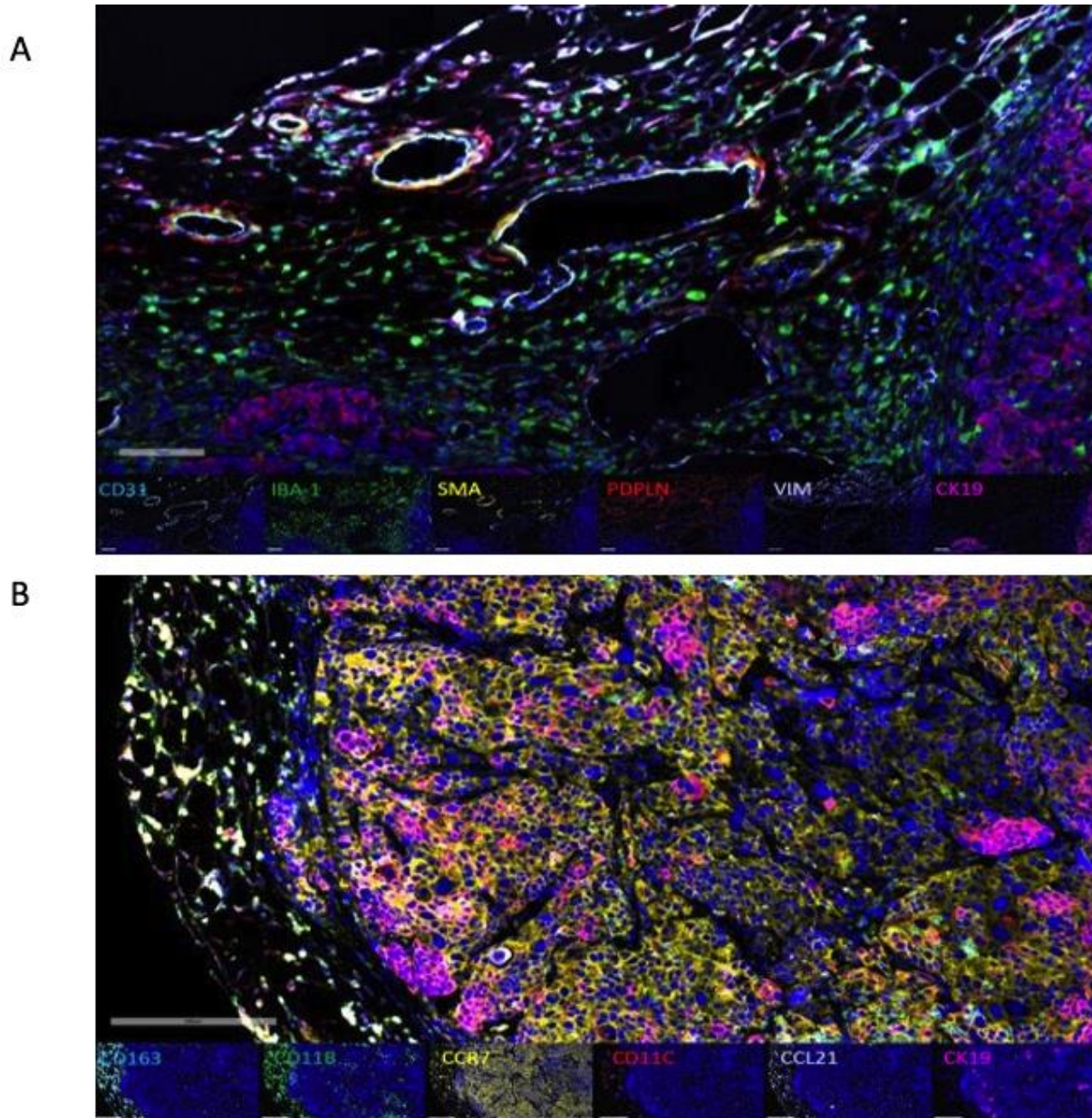
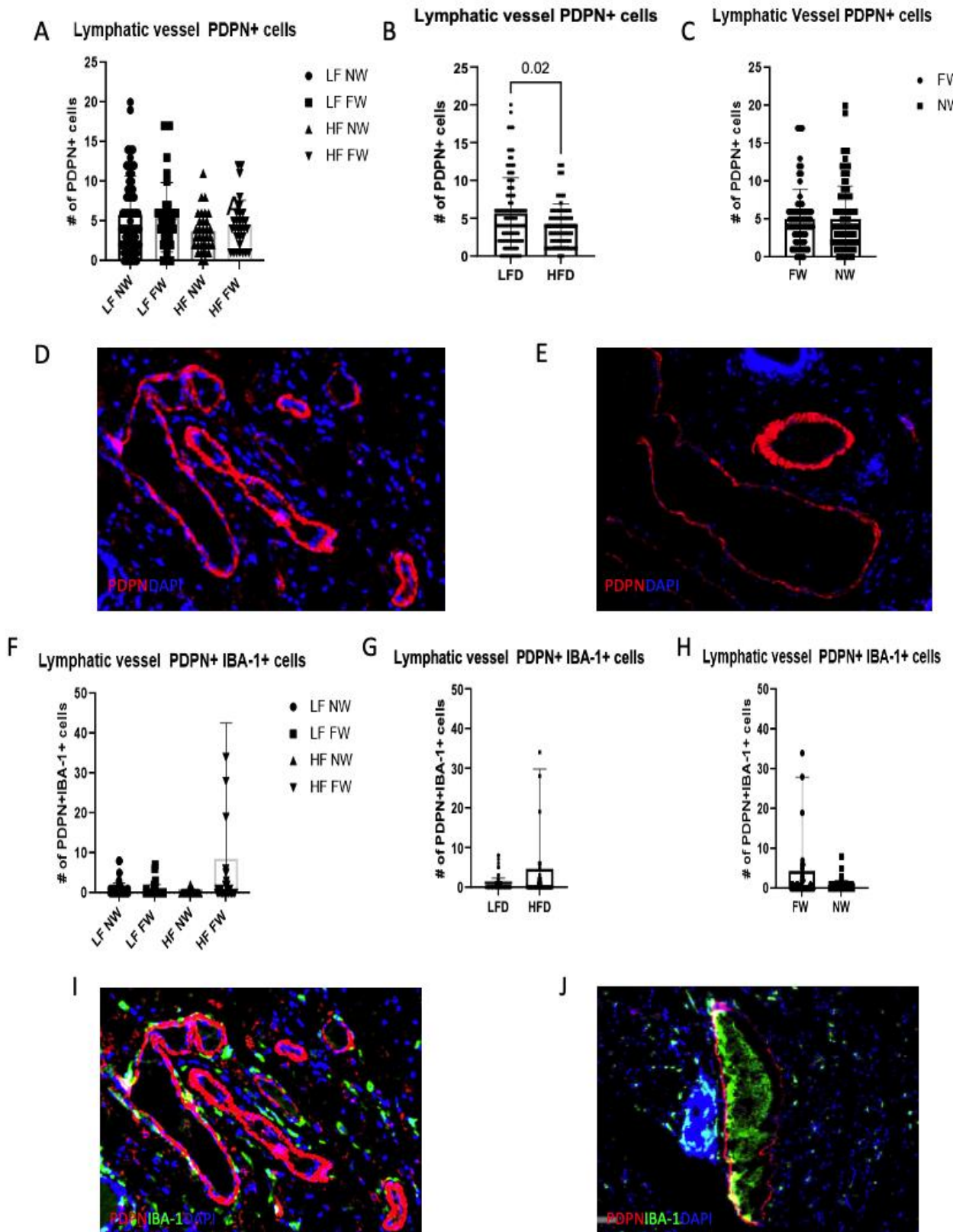


Figure 6: Tissue microarray multiplex immunofluorescence effectively stained for 12 markers across two panels on mammary gland tissue and tumors. Tumor stroma interface (20X) demonstrating panel A staining CD31 (teal), IBA-1 (green), Alpha-SMA (yellow), Podoplanin (red), Vimentin (white), CK19 (magenta) (A). Tumor section (20X) demonstrating panel B staining CD163 (teal), CD11b (green), CCR7 (yellow), CD11c (red), CCL21 (white) and CK19 (magenta) (B).

Table 9: Average number of lymphatic vessels in each mammary gland core quantified for each treatment group.

Treatment groups	Avg. #Lymphatic vessels	Avg. #Ducts
LF NW	18.3	15.7
LF FW	3.3	10
HF NW	7.7	31.7
HF FW	8	18.7
	P=0.46	P=0.38

Figure 7: HFD promotes lymphatic functionality independent of the number of lymphatic vessels



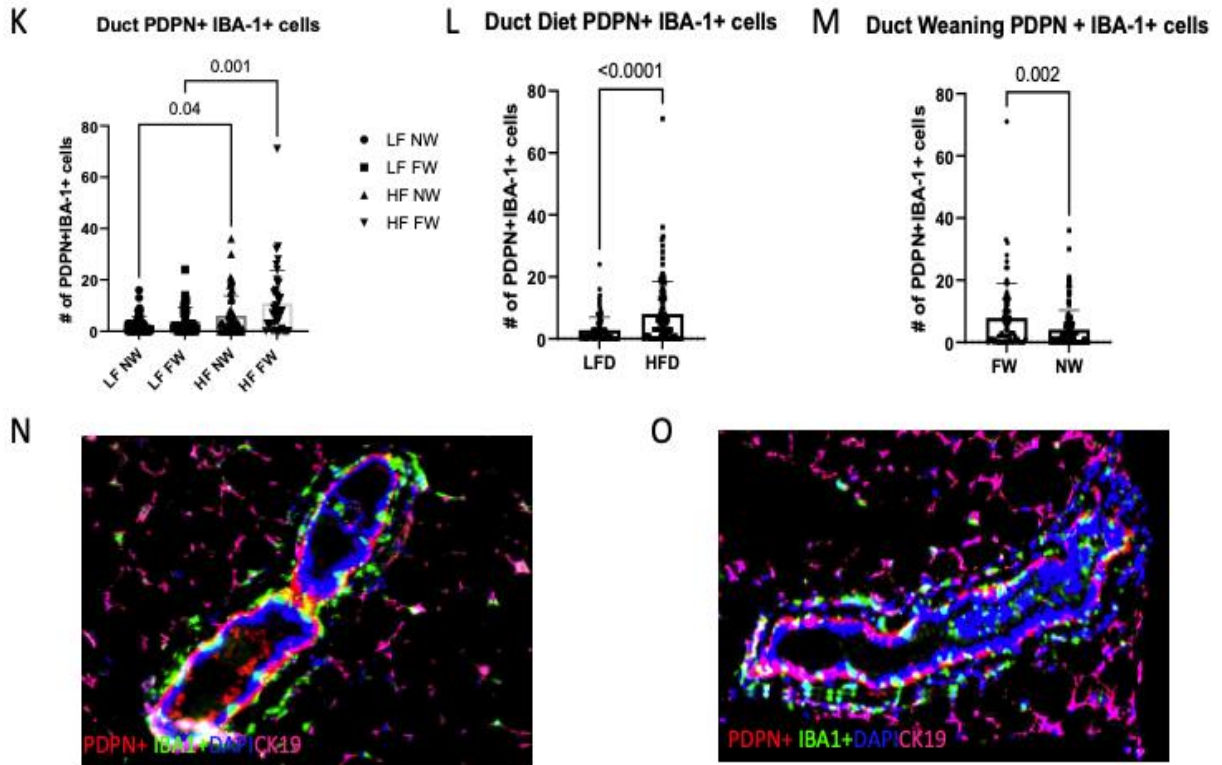


Figure 7. HFD promotes lymphatic functionality independent of the number of lymphatic vessels. The lymphatic vessels in HFD postpartum mice express tumor infiltrating immune cells that promote lymphangiogenesis and lymphoinvasion. There were no significant differences in PDPN-positive cells across all the treatment groups, LFD mice had significantly increased PDPN+ lymphatic cells (Figure 7A, $P=N.S.$, Figure 7B $P=0.0153$). The multiplex IF images show increased density of PDPN+ lymphatic vessels (red fluorophore) in the mammary gland sections in the low-fat diet mice, compared to the high-fat diet mice (Figure 7D, 7E). HFFW mice had the highest concentration of PDPN+IBA-1+ co-expressing cells in the lymphatic vessels (Figure 7F, $P=N.S.$). The HFD mice demonstrated increased PDPN+IBA-1+ lymphatic cells, similarly the FW mice had higher PDPN+IBA-1+ lymphatic cells compared to the NW mice (Figure 7G, 7H, $P=N.S.$). The lymphatic vessels in the HFFW versus LFFW mammary gland demonstrated noticeable infiltration of IBA-1+ macrophages (Figure 7I and 7J, $P=N.S.$). HFD and forced weaning synergistically increased PDPN-positive ductal macrophages (Figure 7K, $P<0.0001$, 7L $P<0.0001$, 7M $P=0.002$). This increased presence of PDPN+ macrophages in the FW duct was illustrated by the yellow fluorophore (representing combination of red PDPN, and green IBA-1 fluorophores) in the duct compared to the NW duct (Figure 7N, 7O).

Expression of mammary duct-infiltrating monocyte-derived species and lymphangiogenic PoEMs

Next, we sought to determine the mammary-duct infiltrating monocyte populations using manually annotated epithelial ductal structures. The HFFW mice had the highest concentration of PDPN+IBA-1+ (PoEMs) co-expressing cells in the lymphatic vessels (Figure 7F and 7G, P=NS), but was low overall and not statistically significant. Next, we explored the PDPN expressing ductal macrophages by quantifying the PDPN-positive ductal macrophages (PoEMs) populations. Similar to the lymphatic vessels, HFD and forced weaning increased ductal PoEMs (Figure 7L, $P<0.0001$ and Figure 7M $P=0.002$). This increased presence of PDPN+ macrophages in the FW duct was illustrated by the yellow fluorophore in the duct compared to the NW duct (Figure 7N, 7O). This significant increase in PDPN+ macrophage populations in the HFFW ducts could inform the changes diet and weaning induce in the breast microenvironment, facilitating LVSI in IBC patients. Further, ductal epithelial cells expressed significantly higher PDPN-positive cells in HFD mice (Figure 8B, $P=0.006$), in addition the FW mice expressed significantly higher ductal PDPN-positive cells (Figure 8C, $P<0.001$). Increased PDPN+ ductal cells were illustrated in the mammary ducts observed in the FW mice versus NW mice (Figure 8D, 8E). Additionally, alpha-SMA expressing ductal cells did not significantly vary across all the treatment groups, nor by diet (Figure 8F, 8G, $P=N.S.$). However, forced weaning did significantly increase the alpha-SMA-positive ductal cells (Figure 8H, $P=0.001$). We evaluated the lobular types in these mice based on criteria established by the Schedin group, with type 1, 2 and 3 defined as 11 to 15, >15 to 50, and >50-acini per lobule respectively, and type 4 defined as terminally differentiated milk-secreting lobule. Our results from assessing the lobular types using H&E slides from the multiparous mice were inconclusive.

Figure 8: High fat diet and forced weaning synergistically significantly increased PDPN-positive ductal cells.

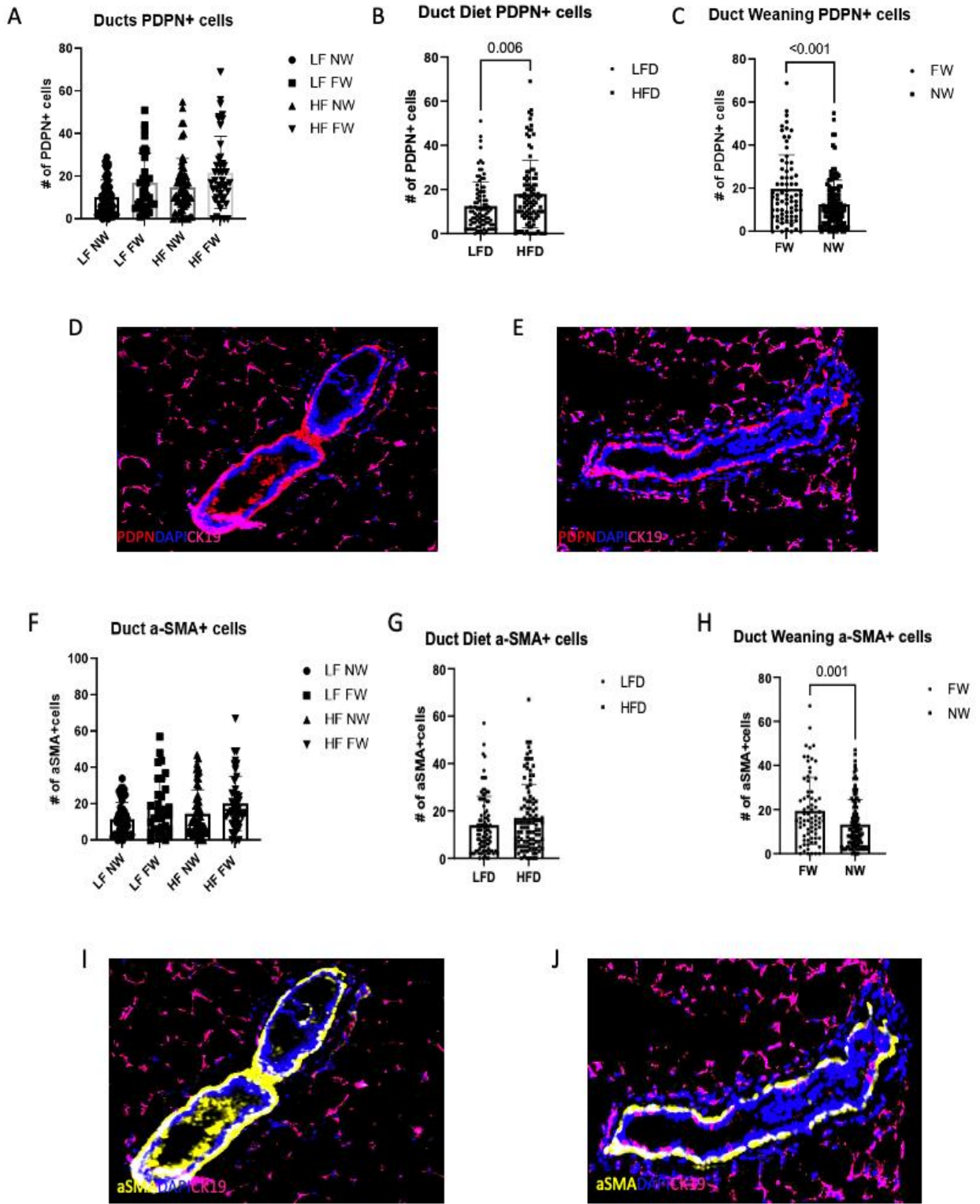
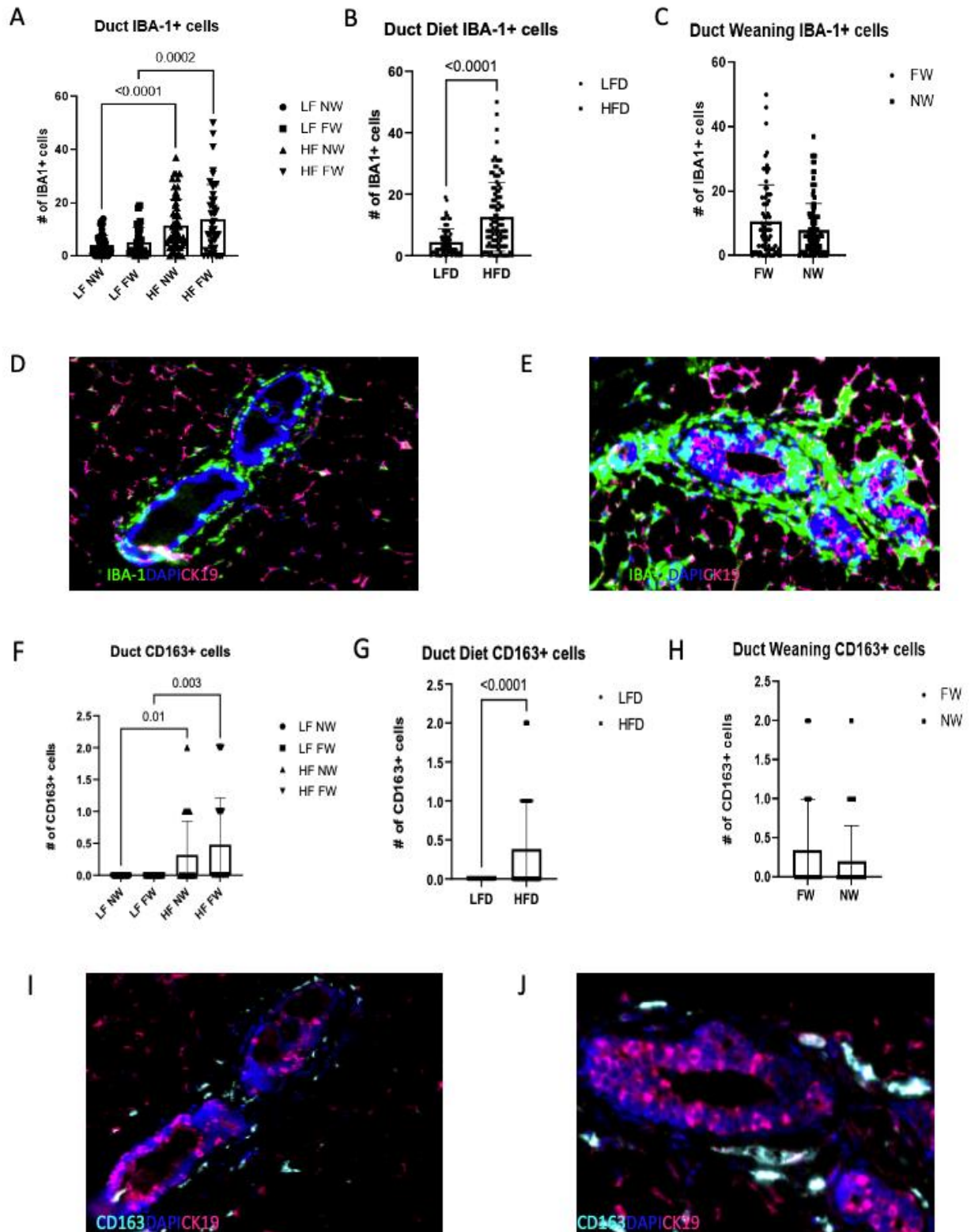


Figure 8. High fat diet and forced weaning synergistically significantly increased PDPN-positive ductal cells. The ductal cells expressed significantly higher PDPN-positive cells in HFD mice (Figure 8A, P=N.S., Figure 8B, P=0.0058), in addition the FW mice expressed significantly higher ductal PDPN-positive cells (Figure 8C, P=0.0004). Increased PDPN+ (red fluorophore) ductal cells were illustrated in the mammary ducts observed in the FW mice versus NW mice (Figure 8D, 8E). Alpha-SMA expressing ductal cells did not significantly vary across all the treatment groups, nor by diet (Figure 8F, 6G, P=N.S.). However, forced-weaning did significantly increase the alpha-SMA-positive ductal cells (Figure 8H, P=0.0015). Increased alpha-SMA+ (yellow fluorophore) ductal cells were illustrated in the mammary ducts observed in the FW mice versus NW mice (Figure 8I, 8J).

HFD also increased the ductal IBA-1 cell expression, independent of weaning status. (9A, P<0.0001 and P=0.0002, 9B, P<0.0001). These differences are illustrated in the postpartum mammary ducts from LFD vs. HFD mice. The positive IBA-1 ductal cells in and around the ductal epithelium, are higher in high fat ducts (9D, 9E). Additionally, although the CD163-positive ductal cell populations were generally low across all the mammary gland, the HFD mice had significantly higher CD163-positive ductal cells, independent of weaning status (9F, P=0.01, P=0.003, and 9G, P<0.0001 respectively). These differences are shown in the postpartum mammary ducts from LFD vs. HFD mice, HFD ducts demonstrated increased CD163-positive ductal cells in and around the ductal epithelium (Figure 9H, 9I). The ductal CD11c-positive cells were significantly higher in HFD mice (9L, P<0.001). Weaning status did not affect ductal CD11c-positive cells (Figure 9M, P=N.S.). The higher expression of ductal CD11c+ cells were demonstrated in the HFD ducts, compared to the LFD ducts (9N, 9O).

Figure 9: High fat diet significantly increased mammary ductal immune cell inflammation.



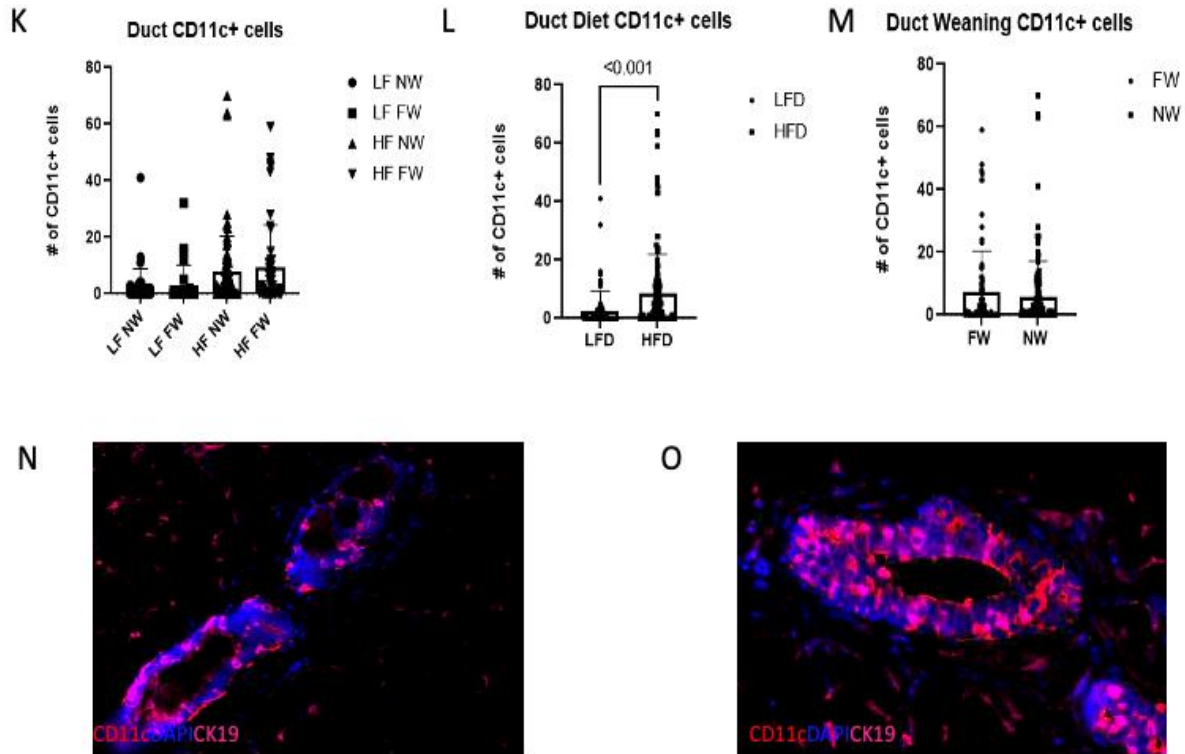
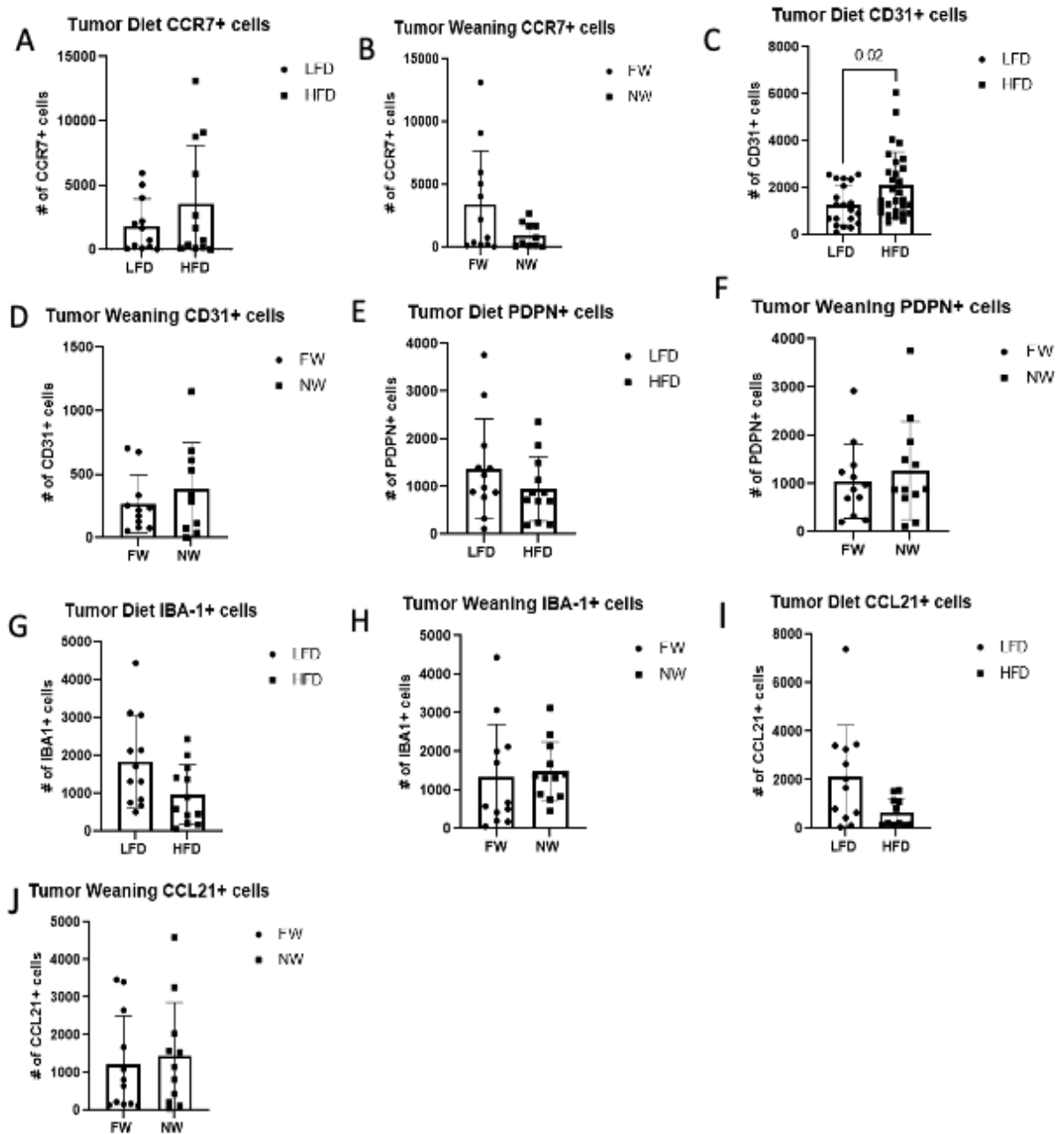
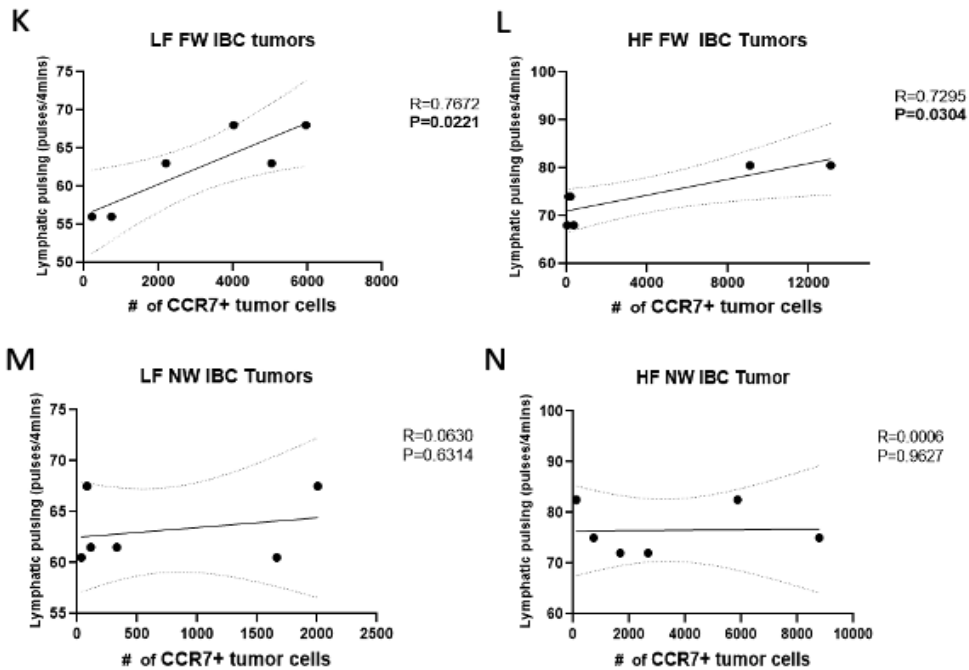


Figure 9. High fat diet significantly increased mammary ductal immune cell inflammation. HFD increased the ductal IBA-1 cell expression, independent of weaning status, this was demonstrated between the LFNW vs. HFNW mice, and the LFFW vs. HFFW mice. (Figure 9A, $P < 0.0001$ and $P = 0.0002$, Figure 9B, $P < 0.0001$ respectively). Weaning status did not influence the ductal IBA-1 cell populations (Figure 9C, $P = \text{N.S.}$). These differences are illustrated in the postpartum mammary ducts from LFD vs. HFD mice (Figure 9D, 9E). HFD mice had significantly higher CD163-positive ductal cells, across the NW and FW groups (9F, $P = 0.01$, $P = 0.003$, respectively). HFD significantly increased the ductal CD163 cell populations (Figure 9F, $P < 0.0001$), independent of weaning status (Figure 9G, $P = \text{N.S.}$). These differences are shown in the postpartum mammary ducts from LFD vs. HFD mice (Figure 9I, 9J). The ductal CD11c-positive cells were significantly higher in HFD mice (Figure 9K $P = \text{N.S.}$, Figure 9L, $P < 0.001$). Weaning status did not affect ductal CD11c-positive cells (Figure 9M, $P = \text{N.S.}$). The higher expression of ductal CD11c+ (red fluorophore) cells were demonstrated in the HFD ducts, compared to the LFD ducts (Figure 9N, 9O).

Supplemental Figure 1: Multiplex Immunofluorescence was conducted on IBC tumor sections from the multiparous mice.





Supplemental figure 1: Multiplex Immunofluorescence was conducted on IBC tumor sections from the multiparous mice. HFD increased the CCR7 expression in tumors, forced weaning also increased the CCR7+ tumors (A, B). HFD increased the CD31+ tumors (C). The LFD mice had a higher PDPN+ tumor cells (E), weaning did not impact the PDPN+ tumor cells (F). The LFD mice had higher IBA-1+ tumors cells (G), weaning did not impact the IBA-1+ tumor cells (H). The LFD mice had higher CCL21+ tumors cells (I), weaning did not impact the CCL21+ tumor cells (J). Correlations between CCR7+ tumor cells and pre-tumor lymphatic pulsing were assessed. The LFFW and HFFW IBC tumors demonstrated a strong association between the CCR7 tumor expression levels and the pre-tumor lymphatic pulsing rates in these mice (K, L).

DISCUSSION

HFD increased lymphatic function, assessed as pulsing post-mammary gland, in nulliparous and multi-parous mice prior to tumor initiation. Further, function trended towards a direct correlation with tumor growth. IBA-1 and CD163+ macrophages and CD11c+ dendritic cells in mammary gland ducts were also more prevalent in HFD animals. While weaning timing did not impact lymphatic pulsing or tumor growth in this model, this is the first study to model the combination of risk factors simultaneously as experienced by patients. HFD was also associated with increased lymphangiogenic PDPN+ macrophages in lymphatic vessels and mammary ducts of HFD as well as FW mice, highlighting a potential synergy in risk factors for further study. Lastly, prevalence of cells expressing CCL21, a ligand for lymphatic traffic homing, was directly correlated to pulsing, and may suggest a role for CCL21 in lymphatic function in addition to trafficking. This is the first report that high fat diet promotes xenograft growth of an IBC cell line. Interestingly, in these multiparous mice, all but one animal developed IBC-like skin invasion, potentially suggesting compared to nulliparous historical controls [9], that pregnancy induces a microenvironment that induces IBC-like skin invasion independent of weaning and diet. We suggest that further study of the role of inflammatory infiltrates and CCL21 in inducing lymphatic function and promoting CCR7-positive tumor growth are warranted.

C-C- chemokine receptor type 7 (CCR7), a member of a chemokine receptor family, expressed on mature leukocytes and T-cells, induces the leukocyte homing towards CCL21 expressing lymph nodes across a chemotaxis gradient [63], [124], [125], [126], [127]. CCR7 staining in the tumors from these mice was elevated in high fat and forced weaned mice. Further, CCR7 staining in tumors was strongly correlated with pre-tumor lymphatic pulsing (Supplemental Figure 1). Studies have shown that obesity promotes the accumulation of CCR7-positive macrophages and dendritic cells in adipose tissue in close proximity to lymph

nodes [128]. Melanoma studies have demonstrated that metastatic melanoma tumor cells express CCR7, which mediates chemotactic metastasis towards proximal lymphatics, resulting in lymphoinvasion [93], [129].

Other studies have reported the opposite phenomenon, where HFD or obesity cause lymphatic dysfunction characterized by the reduced ability transport lymph, leaky vessels, and change in the expression of lymphatic endothelial cell markers [130], [131]. Blum et al. explored the effects of a chronic high fat diet on lymphatic function and vasculature in three strains, including mice models for primary lymphedema, using *in vivo* NIRF lymphatic imaging. They demonstrated that across all groups, HFD was associated with impaired collecting lymphatic vessels, reduced lymphatic contractile activity, and even a reduced response to mechanostimulation. Further, the primary lymphedema mice model (K14-VEGF-C) had expanded dermal lymphatic vessels which decreased the spread of the lymphatic tracer in HFD mice [130]. Notably, in this study they quantified the lymphatic contractile activity in the collecting vessels in the limb, near the entrance to popliteal lymph node. Similarly, a separate study used obesity-resistant and obesity-prone mice strains, to assess how high fat diet-induced obesity effect lymphatic function. This study concluded that only obesity-prone mice, but not obesity-resistant mice on high fat diet had impaired lymphatic function, increased perilymphatic inflammation, and altered LEC gene expression [131]. There could be several reasons for the diverging results from the effects of obesity on lymphatic activity in mice models; including the amount of time the mice were given specialized diet prior to imaging, or the mice strain used, and more specifically if they were immunocompetent models. Additionally, it is critical to distinguish which vessels were being assessed. The effects of regional heterogeneity of lymphatic vessels on lymphatic contractile function have been published [132]. Studies have demonstrated using collecting lymphatic vessels from rats,

regional variations in lymphatic contractile responses to physical stimuli, and exposure to certain conditions and environments [133],[134].

Clinical studies in patients have also presented conflicting data, inferring obesity presents as a risk, however etiology in lymphatic disorders is not established. One study which sought to characterize obesity as a novel cause of lower-extremities lymphedema with obese patients (BMI>30 kg/m²), without any potential cause for lymphedema were evaluated with a lymphoscintigram [135]. They reported that patients with BMI>60 kg/m² had lower extremity lymphedema, whereas every patient with BMI<50 kg/m² had normal lymphatic function [135], [136]. Concurrently, a separate clinical study which evaluated patients with pitting odema, compared obese patients, non-obese and patients with idiopathic oedema using lymphoscintigraphy. They concluded that obese patients and those with idiopathic oedema had fewer and milder lymphoscintigraphic abnormalities, emphasizing that these structural lymphoscintigraphic abnormalities in clinical oedema are not caused by obesity [137].

Next, our study aimed to determine how risk-factor primed microenvironments would facilitate the tumor growth and lymphatic activity and vasculature following triple-negative parental IBC SUM149 tumor cells orthotopic inoculation into the #4 mammary gland fat pad. Lymphatic pulsing activity significantly increased following triple-negative IBC SUM149 tumor cells inoculation. Tumor initiation significantly increased the dermal lymphatic pulsing activity across all 4 mice groups independent of diet or weaning status. Agollah et al. 2014, demonstrated that immunocompromised mice imaged using *In vivo* near infra-red lymphatic imaging for up to 11 weeks prior to orthotopic SUM149 IBC tumor inoculation, and post-tumor inoculations. Mice with the IBC tumors demonstrated altered lymphatic drainage patterns resulting in the rerouting of lymphatic drainage, as a result of lymphatic obstruction during tumor growth [87].

Studies have established that not pregnancy, but the post-partum period in women increases the risk of developing breast cancer [67]. The breast undergoes dramatic remodeling following pregnancy and lactation during involution, the breast remodeling to its pre-pregnant state following weaning. During the process of involution, programmed cell death eliminates about 90% of the secretory mammary epithelium, produced for lactation, within the breast microenvironment. Changes in the breast occur including immune cell infiltration, stromal remodeling, M2 macrophages, fibroblast activation, fibrillar extracellular matrix deposition. The process of involution involves several tumor-promoting signals in the mammary epithelium and stroma [67], [138]. Studies have also shown that postweaning mammary glands have increased lymphangiogenesis [139]. Jindal et al. investigated these changes in the breast microenvironment using breast biopsies from healthy, young women collected prior to pregnancy, during lactation and postweaning. An increase in CD45+ immune cells in the breast lobules peaked at 0.5 months post-weaning and persisted for more than 12 months post-weaning. Further, they identified several lymphatic vessels with CK18+ epithelial cell debris, as CK18+ epithelial cells were not fully enclosed by the basal myoepithelial cells, during involution, allowing dying epithelial cells to escape the acinar structures and enter lymphatic vessels [70]. Additionally, they showed that lymphatic density and function peaked 1 month postweaning, and remained higher than pre-pregnancy levels up to 24 months postweaning. This suggests that changes that occur during pregnancy, and in preparation for lactation persist beyond involution, modifying the breast microenvironment eliciting pro-tumorigenic signals.

Normal adjacent tissue in IBC patients is enriched with mammary stem cell populations and macrophage infiltration. Thus, IBC normal tissue unique from normal non-IBC tissue, has an increased tumorigenic stem cell signature and a disease-specific tumor signature [140]. Macrophages are a dominant immune cell population in the mammary duct. A unique

population of tissue-resident ductal macrophages form a tight network with the epithelium, and thus constantly surveil the epithelium [138], [141]. Ductal macrophages proliferate during pregnancy to increase the epithelium for lactation, and facilitate phagocytosis of the milk producing cells following lactations [141]. These remodeling signals in ductal macrophage are like those seen mammary tumor macrophages. We investigated the macrophage populations in the post-partum mammary glands, we showed that HFD increased the IBA-1+ ductal cell populations, independent of weaning status (Figure 9). Similarly, the HFD increased the M2 macrophage, CD163+ cells, ductal cell populations, independent of weaning status. This is consistent with studies investigating post-lactational involution demonstrating an influx of macrophages, characterized by M2 macrophages in rodents and humans [138]. M2 macrophage populations increase during pregnancy and involution and return to nulliparous levels following full regression in the mammary glands. However, the persisting changes of M2 macrophages could contribute to a pro-tumorigenic microenvironment, promoting breast cancer in post-partum women [138]. Additionally, we have previously demonstrated in preclinical models that M2-educated mesenchymal stem cells promote IBC growth. Inhibiting macrophage recruitment *in vivo* inhibited the IBC tumor growth, tumor recurrence and skin invasion [122]. Although we assessed the long-term effects of weaning in postpartum mammary glands, it is critical to characterize how these persisting changes may contribute to a conducive microenvironment for IBC growth.

Skin symptoms are attributed to the IBC tumor emboli disseminating into the dermal lymphatics in the breast, with tumor emboli clogging the dermal lymphatics. Studies have determined that the presence of inflammatory breast carcinoma in the breast, induces the formation of new lymphatic vessels, promoting lymphangiogenesis [1]. Van der Auwera and colleagues compared the lymphangiogenic potential in IBC versus non-IBC, concluding increased proliferation of peripheral lymphatic endothelial cells around the tumors [71]. The

lymphatic system, is composed of an extensive network of lymphatic vessels, made up of lymph absorbing initial lymphatic capillaries, collecting lymphatic vessels which transport the lymph, and lymph nodes and lymphoid organs which are responsible for facilitating immune responses [77], [142]. Lymph propulsion requires a combination of extrinsic and intrinsic forces to move lymph against a hydrostatic pressure gradient. This requires action-potential stimulated, lymphatic contractile activity synchronized along the lymphangion, with functional intraluminal valves to prevent backflow [77], [142], [143]. In a study, assessing breast lymphatic mapping, they demonstrated that lymphatic collectors were identified in the subcutaneous tissue, and all superficial lymphatic vessels in their breast dissections entered the lymph node in the axilla [144]. Similarly, in a study using magnetic resonance lymphography, they demonstrated that following intradermal injections, the lymphatics in the fourth and fifth mammary glands drained into the inguinal and proper axillary nodes [145]. Additionally, our lymphatic pulsing imaging from the fourth mammary gland demonstrated lymph fluid being propelled towards the axilla lymph node.

Interestingly, we identified PDPN-expressing macrophages (PoEMs) in our postpartum mammary glands. These PoEMs can integrate into the lymphatic vasculature, promoting neo-lymphangiogenesis. Studies have shown that in breast cancer patients, the association of PoEMs with tumor lymphatic vessels correlates to increased lymph node and distant organ metastasis [146]. The Bieniasz-Krzywiec research group, published that among mammary tumor-infiltrating immune cells, the highest expression of PDPN was found in tumor associated macrophages (TAMs). When PDPN-expressing macrophages (PoEMs) are proximal to lymphatics, these PoEMs stimulate local matrix remodeling, and promote lymphatic vessel growth and lymphoinvasion [147]. Thus, we sought to determine whether the synergy between obesity and never-breastfeeding would result in IBC progression, and increased lymphangiogenesis and lymphoinvasion. Interestingly, our data showed HFD and

forced weaning increased PDPN+ macrophages in lymphatic vessels. Similarly, High fat diet and forced weaning significantly increased PoEMs in the ducts. Studies have shown that mammary lymphatic vessels are spatially closely associated with the epithelial ducts. The lymphatic vessel density increases during pregnancy with the extensive expansion of the epithelial tree. This correlation suggests the mammary epithelial elicits pro-lymphangiogenic signals [69]. The significantly increased PDPN+ macrophage in the high fat, forced weaned ducts could inform the changes diet and weaning induce in the breast microenvironment, facilitating LVSI in IBC patients. Despite the difference not being significant, which could be due to low experimental animals/groups resulting in less power for statistical significance, it is still critical to note that this trend of PoEMs, PDPN+ IBA-1+ cells in our mice models could inform the LVSI associated with IBC. Having more animals in each treatment group would have increased the statistical power and could have confirmed the trend of increased PDPN-expressing macrophages in high fat, forced weaned mice.

The quantification of PDPN-positive cells in the lymphatics of these mammary glands demonstrated that HFD promotes lymphatic functionality, independent of the number of lymphatic vessels. In fact, the LFD mice had significantly increased PDPN expressing cells in the mammary lymphatic vessels. This is consistent with the literature exploring the effects of both HFD and obesity on lymphatic pulsing activity, and lymphatic vessel density and vasculature. Studies have shown that HFD-induced obese mice have decreased lymphatic density, reduced lymphatic endothelial cell proliferation and reduced collecting vessel pumping capacity [148].

We also reported that the forced weaned ductal cells expressed significantly higher alpha-SMA, compared to the nursed weaned group. The mammary myoepithelial cells which are specialized smooth-muscle-like epithelial cells express alpha-SMA, which in response to oxytocin facilitates contractions of myoepithelial cells, facilitating milk ejection during lactation

[149]. The myoepithelial cell contractions reduce the alveolar lumen in the mammary glands. We evaluated the lobular types in these mice based on criteria established by the Schedin group [150], analysis of the lobular types using H&E slides from the multiparous mice were inconclusive. There is an increase in lobular composition and lobular complexity during pregnancy and lactation. However, lobular composition was not significantly different after a year and was indistinguishable after 18 months from the nulliparous group [150]. In a separate study, they highlight that mammary stromal remodeling in rodents is increasingly activated day 4-8 after weaning, in particular in forced-weaned mice they found that the mammary fibroblasts were more abundant [151]. Although we see the impact of weaning on the ductal alpha-SMA levels, we were not able to evaluate this impact on tumor growth. A limitation to our study was that we were not able to address the impact of alpha-SMA on tumor growth. This was partly due to immunocompromised mice model we used to assess the pregnancy and diet-induced changes in the mammary microenvironment, which remained immunosuppressive to the human IBC tumor initiated into the mice.

A limitation of this study was that the effects of weaning on the breast microenvironment were assessed several months after involution. This could suggest that we didn't capture the immediate changes in the microenvironment following involution, instead we assessed the persisting changes. However, these functional signals which persist months after involution could be facilitating IBC progression and lymphoinvasion. Elder et al. studied how immune cells in the mammary gland microenvironment promote lymphangiogenesis during post-partum mammary gland involution, and even breast cancer. They characterized that activated macrophages expressed lymphatic marker, (LYVE-1) during involution, and this peaked at day 6 of involution, at peak lymphatic density. In addition, PDPN-expressing macrophages were characterized, and promoted lymphangiogenesis [146]. Further, tumor cells inoculated into mammary glands at day 1 of involution, micrometastasized and were identified in the

axillary nodes at day 4 and day 6 of involution, suggesting early in an involuting mammary gland lymphatics can facilitate metastasis [146]. Additionally, there could be several reasons for the diverging results from the effects of obesity on lymphatic activity in mice models; including the amount of time the mice were given specialized diet prior to imaging, or the mice strain used and more specifically if they were immunocompetent models. It is critical to distinguish which vessels were being assessed.

In conclusion, we demonstrated for the first time that a high fat diet increased lymphatic function independent of weaning status in this model. Tumor initiation prompted further increased lymphatic pulsing activity beyond that observed after HFD across all groups. Further, we reported for the first time that HFD promoted SUM149 IBC tumor growth in immunocompromised mice. The increase in lymphatic contractile activity and functionality, was independent of lymphatic vessel density. However, we found that lymphatic pulsing was correlated to LEC marker CCL21, a ligand of a leukocyte trafficking receptor CCR7 found on macrophages and dendritic cells. We also demonstrated that a high fat diet promoted significant inflammation of specific mammary tumor-infiltrating immune cells such as macrophages, M2 macrophages and dendritic cells in the mammary ducts. In addition, PDPN+ macrophage (PoEMs) populations were elevated in the lymphatic vessels, and significantly increased in the high fat diet, forced weaned mammary glands. This suggests that the long term, persisting changes in the microenvironment from never-breast feeding and high fat diet synergistically promote IBC tumor growth, and lymphovascular skin invasion. Further, these persisting changes in the microenvironment, and their impact on the inflammatory infiltrates, and CCL21 in inducing lymphatic function and promoting tumor growth warrant further study.

Chapter 5: CCR7 is highly expressed in Inflammatory breast cancer, and breast cancer cell lines.

ABSTRACT

Background: Inflammatory breast cancer is an aggressive breast cancer characterized by florid congestion of lymphovascular spaces by tumor emboli. CCR7 is an immune cell receptor that mediates immune cell trafficking into lymphatics that can be expressed on tumor cells. An RNA-seq screen of tumor promoting mammary glands in mice identified CCR7 as an upregulated signal in mammary glands that promoted IBC-like skin invasion. We hypothesized this expression in pre-tumor glands may reflect a role for CCR7 based trafficking of tumor cells to lymphatics. Thus, we examined the expression of CCR7 in IBC and non-IBC cell lines and IBC patient tumors to determine the prevalence of this receptor in IBC tumor cells.

Methods: Tumor samples from the IBC consortium database were stratified as CCR7-high when expression in tumor was greater than or equal to the median, otherwise, the sample was classified as CCR7-low in the normal breast samples. Mann-Whitney tests were used when two groups were compared, and one-way analysis of variance was used for multiple experimental groups. Black lines in each group indicate median \pm SD, and p values of <0.05 were considered significant. Spearman rank correlation coefficient was used to measure the strength of the association between *CCR7*, and its ligand *CCL21* with lymphatic marker, *LYVE-1*. A P value of < 0.05 was considered significant. GRAPHPAD software (GraphPad Prism 8, La Jolla, CA, USA) was used. Descriptive statistics were examined for representation by receptor subtype. An IBC tissue microarray from post-chemotherapy mastectomy specimens of 39 patients, each with three replicates was subjected to immunohistochemical staining for CCR7 (Invitrogen, catalog number MA5-31992) performed using a Leica Bond RX autostainer with an incubation time of 60 minutes at 1:15,000 after 20 minutes of heat-induced antigen retrieval at pH 6.0. In 15 cases, there were no residual tumor cells observed in the cores. Staining was scored by an expert IBC pathologist for intensity and percent tumor stained. Protein lysates from IBC and non-IBC cell lines of multiple subtypes were subjected

to immunoblotting using anti-CCR7 (R&D systems). In addition, a panel of MCF7 cell lines including sublines resistant to standard therapies were assessed.

Results: In publicly available gene expression datasets, CCR7 expression is present in all subtypes, enriched in HER2+ and basal subtypes, and increased in IBC compared to non-IBC. Among 24 IBC patient cores with tumor in the tissue, 23 (96%) expressed CCR7 in tumor, 15 with complete membranous staining and 9 with incomplete membranous staining. In one case with tumor emboli in the core, the emboli were strongly CCR7 positive. Among the 23 positive cases, 21 were 3+ intensity while 2 were 2+. Nine CCR7+ cases were estrogen receptor (ER) ER+, 8 ER-, and 6 unknown. HER2 status is pending. CCR7 staining was strong in all lines examined including MCF7, SUM149, SUM190, MDA-IBC3, KLP4, MDA-231 and SUM159. MCF7 sublines resistant to tamoxifen, palbociclib, or abemaciclib had increased expression compared to MCF7 parental cells.

Conclusions: CCR7 gene expression is increased in IBC versus non-IBC cases, but is highly expressed in both groups. CCR7 expression is present across tumor subtypes in IBC cell lines and in both ER+ and ER- IBC patient tumors. Given developing novel pharmacologic targeting of CCR7, this target warrants further investigation in IBC and other breast cancers.

INTRODUCTION

Inflammatory breast cancer is a rare, but highly lethal form of breast cancer [10]. IBC rapidly progresses with unique clinical presentations, including erythema, breast swelling, nipple inversion, skin changes and peau d'orange [3]. These skin symptoms are attributed to IBC tumor emboli disseminating into the dermal lymphatics in the breast, with tumor emboli clogging the dermal lymphatics [1]. This phenomenon is called lympho-vascular space invasion (LVSI) and while present across all breast cancer subtypes in IBC and non-IBC, it is thought to be florid and as such complicit in the onset of IBC and propensity to metastasize. Given this key role of tumor cell trafficking to lymphatics in IBC, we identified CCR7 on a pilot comparative genomics screen for pre-tumor conditions that promoted IBC-like symptoms (Supplemental Table 1) as a gene of interest.

IBC is diagnosed at a later stage, partly due to limitations of mammography in detecting the scattered distribution of tumor throughout the breast [96]. Difficulty detecting tumor emboli, in combination with clinical features of IBC being mistaken for skin diseases such as mastitis, contribute to delayed diagnosis and treatment [9]. The recommended therapeutic guidelines for IBC patients encompass a trimodality approach entailing systemic therapy, surgery and radiation [4]. Clinical trials in IBC have explored neoadjuvant treatments with carboplatin and paclitaxel, in combination with antiangiogenic therapies [152]. Despite the advancements in clinical trials with immunotherapies, such as neoadjuvant pembrolizumab (PD-1 antagonist) in combination with chemotherapy in early-stage triple negative breast cancer [41], these advancements in IBC treatment have not been achieved. Studies have reported that PDL1 expression in IBC was higher than non-IBC, and even 38% overexpressed in IBC compared to normal breast samples [153]. Highlighting the potential for PD-1/PD-L1 therapies in IBC. Ongoing clinical trials are investigating the effects of neoadjuvant chemotherapy with PD-1 blockade (nivolumab) in IBC patients [154]. IBC tumors have a unique, heterogeneous

immune landscape, which is not well understood. Further impeding on the development of clinically available therapies [155]. Thus, it is important to identify therapeutic targets and options for IBC patients.

CCR7 is an immune cell receptor that mediates immune cell trafficking into lymphatics using chemotactic signals, that can be expressed on tumor cells [156], [157], [158]. CCR7 ligands, CCL19 and CCL21, signal through the CCR7 receptor found on immune cells [159]. Studies have highlighted that CCR7 contributes to lymph node metastasis, and have even found that CCR7 and VEGF-C (a lymphangiogenic marker) synergistically promote tumor spread into the lymphatics [159]. Multiple clinical studies have reported that CCR7 facilitates lymph node metastasis in breast cancer patients [96]. In a triple-negative (TN)-BC study, CCR7 knocked down in TNBC cell lines significantly reduced proliferation, migration and invasion. Similarly, the *in vivo* orthotopic models demonstrated reduced tumor metastasis [97]. Thus, CCR7 is an attractive candidate mediator of the IBC phenotype and LVSI in general.

Herein, we conducted immunohistochemistry staining on IBC patient tissue, mostly containing tumors to determine CCR7 expression levels. CCR7 tumor staining was assessed by an expert pathologist to determine staining positivity, and to evaluate whether the staining was stromal or tumor. Further, we analyzed both IBC and non-IBC patient data from the IBC consortium database to determine CCR7 and CCL21 expression across patient samples. Further, we sought to differentiate subtype-specific expression levels.

RESULTS

In a previous study conducted in the Woodard lab, similar to the multiparous study conducted in chapter 4, postpartum mice were put on a specialized diet to determine the role of a risk-factor primed microenvironment on tumor progression and skin invasion (Supplemental Table 1). RNA isolated from the tissue of high fat forced weaned (HFFW) animal and low-fat nursed (LFNW) animals were used to undergo RNA sequencing for molecular target discovery. In a comparative analysis, RNA sequencing data demonstrated in high fat, forced weaned mice an upregulation in an inflammatory response, specifically lymphocyte activation markers, adaptive immune responses, and hall mark inflammatory responses such as T cell activation. This included the lymphocyte homing chemokine receptor, CCR7 ($P < 0.0001$). The mice in this experiment had undergone two rounds of pregnancy and were put on a specialized diet after 8 months. Subsequently, after 1-month tumors were inoculated into 64 mice, only 31 grew palpable tumors. The tumors were resected to determine local recurrence of the tumor. Most of the mice in the HFFW group experienced skin invasion (65%, 11/17). This is when the tumor protrudes into the skin causing loss of hair, followed by the blistering and bleeding of the skin, $P = 0.08$.

Figure 10: CCR7 and CCL21 are highly expressed in IBC patient samples.

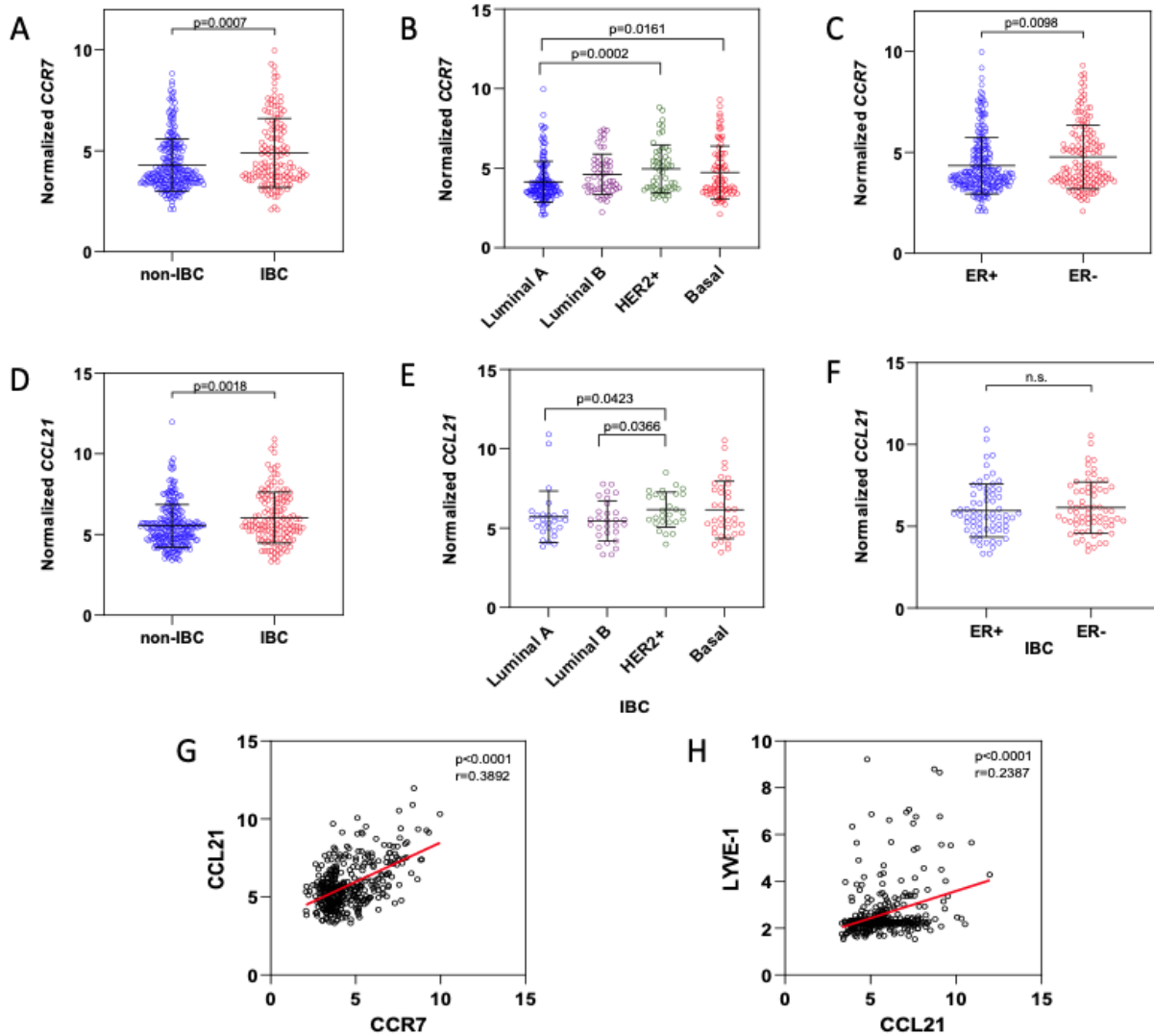


Figure 10: CCR7 and CCL21 are highly expressed in IBC patient samples. CCR7 levels were significantly higher in IBC patient samples compared to non-IBC (Figure 10A, $P=0.0007$), breast cancer subtype-specific expression reported CCR7 levels were higher in HER2+ and basal subtypes compared to the luminal subtypes (Figure 10B, $P=0.0161$ and $P=0.0002$, respectively). CCR7 levels compared based on ER positivity showed CCR7 levels were higher in ER- patients (Figure 10C). Similar analysis was performed for CCL21, revealing CCL21 levels were significantly higher in IBC patients compared to non-IBC ($P=0.0018$), and was not significantly different across IBC subtypes (Figure 10 D-F). CCR7 had strong association with its lymphatic ligand, CCL21 (Figure 10G, $P<0.0001$), and lymphangiogenic marker, LYVE-1 (Figure 10H, $P<0.0001$).

We sought to determine CCR7 expression in IBC patient samples, and differentiate subtype-specific expression levels. Comparative analyses using CCR7 levels in IBC vs. non-IBC patient samples, demonstrated that CCR7 levels were significantly higher in IBC patient samples compared to non-IBC (Figure 10A, $P=0.0007$). HER2+ and basal subtypes had higher levels of CCR7 compared to the luminal subtypes (Figure 10B, $P=0.0002$ and $P=0.0161$, respectively). When normalized for estrogen receptor status, the breast cancer samples with estrogen negative receptor status had significantly higher CCR7 expression (Figure 10C, $P=0.0098$). Similarly, we found that IBC patient samples had higher CCL21 expression, and the HER2+ subtypes had the higher CCL21 expression compared to the luminal subtypes (Figure 10D, $P=0.0018$ and 10E, $P=0.0423$ and $P=0.0366$, respectively). Next, we sought to determine the correlation between the CCR7 and ligand, CCL21 and lymphatic marker LYVE-1 expression using Spearman rank correlation coefficient analysis. CCR7 had strong association with its lymphatic ligand, CCL21, and lymphangiogenic marker, LYVE-1 in breast cancer patients (Figure 10G, $P<0.0001$, 10H, $P<0.0001$).

Immunohistological staining targeting CCR7 revealed 24 out of the 39 human IBC sections evaluated had tumors in them (Figure 11). Table 10, reveals the CCR7 positivity, membrane versus non-membranous staining patterns, ER status and the % of the tumor stained. 23 out of the 24 IBC tumor sections evaluated were positive for CCR7, 15 of which were completely membranous (Figure 11B), and 8 which were incompletely membranous (Figure 11C). An expert IBC pathologist determined 21 samples had 3+ staining, the highest intensity staining, compared to 2 samples with 2+ staining intensities. Further, the pathologist also determined the percentage of the tumor stained for CCR7. 14 of the samples were determined 100% stained for CCR7, 2 samples were determined 90% stained, 4 samples were 80% stained,

while 2 samples were 50% stained, and only 1 IBC tumor sample was determined 10% stained. CCR7 staining was identified and reported in ER- and ER+ cases (Table 10).

Table 10: CCR7 Pathology results and ER status for all tumor samples.

Pathology Data (N=24)	
CCR7 Positivity	
POS	23
NEG	1
Pattern	
Complete Membranous	15
Incomplete Membranous	8
Intensity	
2+	2
3+	21
% Tumor Stained	
100%	14
90%	2
80%	4
50%	2
10%	1
ER Status	
ER+	9
ER-	8
Unknown	6

Figure 11: Demonstration of pathologist categorizing and scoring CCR7 expression in IBC patient tumors.

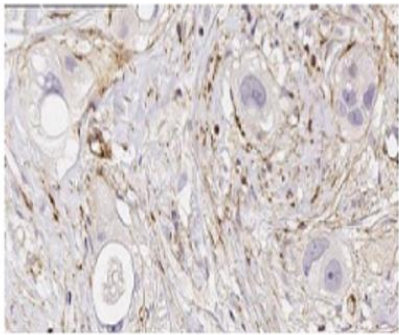


Figure 11A: Negative tumor. Tumor cells are present, but do not positively stain for CCR7.

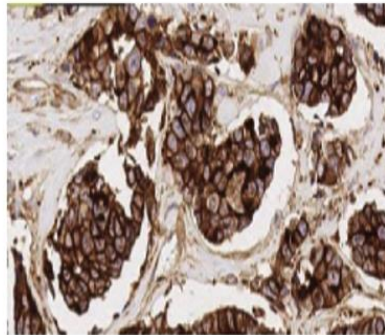


Figure 11B: Tumor cells are CCR7 positive with complete membranous pattern, 3+ intensity, and 100% stain.

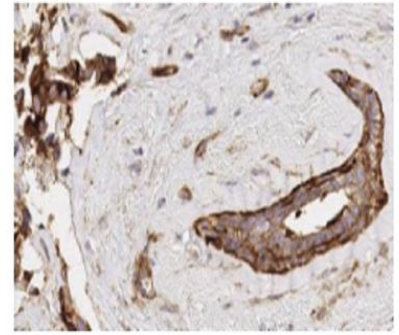


Figure 11C: Tumor cells are CCR7 positive with incomplete membranous pattern, 3+ intensity, and 100% stain.

Figure 12: In vitro analysis of CCR7 expression in IBC and non-IBC cell lines.

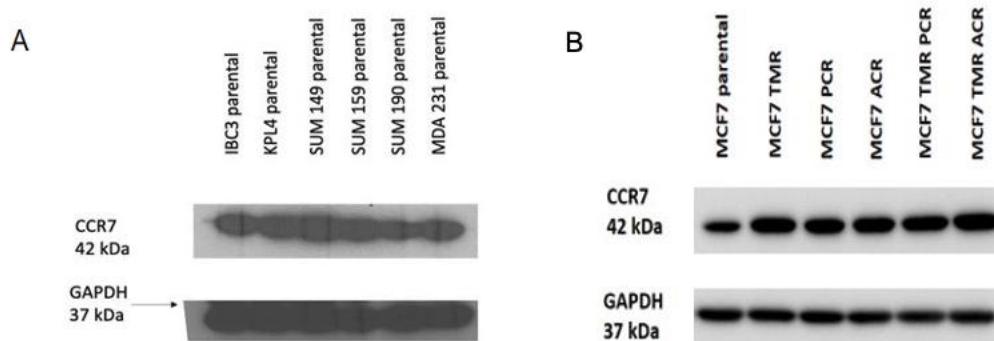


Figure 12: *In vitro* analysis of CCR7 expression in IBC and non-IBC cell lines. Protein lysates from both IBC and non-IBC cell lines expressed high levels of CCR7 *in vitro*. SUM149, SUM159, SUM190, KPL4, IBC3 and MDA-231 all express CCR7 (Figure 12A). MCF7 drug resistant cell lines have increased CCR7 expression compared to parental MCF7 (Figure 12B).

We examined CCR7 protein expression in IBC cell lines SUM149 (triple negative), SUM190 (HER2+), KPL4 (HER2+) and IBC3 (HER2+) and non-IBC MDA-231 (triple negative) and SUM159 (metaplastic triple negative). All of the cell lines we assessed highly expressed CCR7 (Figure 12A). Further, we assessed the CCR7 expression levels in MCF7 parental and drug resistant sub-cell lines (Figure 12B). MCF-7 therapy resistant cell lines including MCF7 TAM: tamoxifen-resistant, ACR: abemaciclib-resistant, PCR: palbociclib-resistant and TAM-ACR or TAM-PCR: double-resistant, respectively have increased CCR7 expression compared to parental MCF7 cells.

DISCUSSION

We report that CCR7 and its ligand CCL21 are expressed across breast cancer subtypes, however specifically enriched in IBC based on gene expression data. Immunohistochemical staining for CCR7 identified 23/24 IBC patients as CCR7 positive. Further, we report that CCR7 expression across a range of IBC and non-IBC cell lines, with increased expression in drug resistant sublines of MCF7 compared to parental MCF7. These studies demonstrate a strikingly consistent expression of CCR7 across breast cancer including aggressive subtypes. This work prompts interest in CCR7 as a potential antibody-directed conjugate target and further work is warranted to investigate the potential biologic significance of CCR7.

The CCR7 receptor, is a member of the C-C Chemokine receptor family. It is characterized as a G protein coupled receptor (GPCR), which mediates physiological responses to external stimuli. GPCRs are defined as integral membrane proteins made up of seven transmembrane consisting of alpha-helical segments with alternating intracellular and extracellular loop regions [160]. CCR7 is expressed on immune cells including B cells, T cells and mature dendritic cells. Preclinical studies have reported that CCR7-deficient mice demonstrate impaired T cell migration to lymphoid tissue, where dendritic cells failed to enter lymphatic vessels following inflammatory stimuli [161]. CCR7 has two ligands, CCL19 and CCL21, which is found on the surface of endothelial cells, and high endothelial venules. CCL21 has a uniquely long C-terminal which supports the regular binding to glycosaminoglycans. This localizes chemokines on cell surfaces facilitating cell signaling and trafficking direction [162]. This binding is critical for CCL21 presentation on the surface of endothelial cells [162]. The binding of CCR7 and CCL21, mediates immune cell trafficking towards the lymphoid organs [163].

In line with this, we demonstrated using *In vitro* models, that MCF-7 drug resistant cell lines expressed increased CCR7, including Tamoxifen-resistant cell lines. Tamoxifen is an

estrogen receptor-targeted therapy [164]. CCR7 expression was also demonstrated in MCF7 resistant cell lines to Abemaciclib and Palbociclib, which are cyclin-dependent kinase 4/6 (CDK 4/6) inhibitors used for advanced metastatic breast cancers both in HER2-positive and negative patients [165], [166]. CDK 4/6 inhibitors function by interrupting the intracellular and mitogenic hormone signals which promote tumor cell proliferation [167]. CDK 4/6 inhibitors are increasingly effective in combination with drugs that inhibit the downstream estrogen-dependent stimulation of cancer cells [168]. This highlights that CCR7 could be driving the biology in aggressive breast cancer, proving the therapeutic potential that targeting CCR7 presents for breast cancers.

Highly aggressive cancers are frequently characterized by tumor cell emboli within the lymphatic and blood vasculature (LVSI). IBC presentation of swelling and erythema have been attributed to the clogging the lymphatics in the breast and skin, thus we expected and found higher CCR7 in IBC cases. Approximately 40% of breast cancer patients are characterized by LVSI, making LVSI-related mechanisms highly pertinent for understanding breast cancer biology. In clinical studies, CCR7 has been determined as a biological marker to predict lymph node metastasis in breast cancer patients [169]. Further, cytoplasmic CCR7 staining in small breast cancer tumor biopsies were predictive of increased lymph node metastasis [170]. In a separate study, this group identified that CCR7 positive tumors in patients with axillary node positive, primary breast cancer had increased skin relapses [169]. The role of the CCR7/CCL21 axis in facilitating tumor-induced lymphangiogenesis in breast cancer has been established [171]. CCR7 mRNA expression from human breast cancer tissue have demonstrated positive correlations with the expression levels of lymphatic markers including LYVE-1, podoplanin, PROX-1 and VEGF-C [98]. These studies together with the broad expression of CCR7 we describe here, further support work exploring functional significance of CCR7 in aggressive breast cancers.

CCR7 may be important even in the absence of functional tumor driver activity, however. Antibody-drug conjugates (ADC) are an emerging important therapeutic in breast cancer. ADCs are mainly composed of a monoclonal antibody (mAbs) covalently bonded to a cytotoxic drug through a chemical linker, this optimizes a highly specific targetable efficiency with a functional killing effect [172]. Unfortunately, breast cancer patients with low levels of human epidermal growth factor 2 (HER2) amplification, have not benefitted from the overarching HER2 therapy such as trastuzumab [173]. A recent innovative phase II study demonstrated that Trastuzumab Deruxtecan, a new antibody-drug conjugate of humanized anti-HER2 monoclonal antibody, bonded to a topoisomerase I inhibitor significantly improved progression-free and overall survival in metastatic HER2-low breast cancer patients [173]. This type of strategy may be targeted to CCR7 if toxicity were manageable. Encouragingly, Catapult therapeutics reported a phase I study for CAP-100, a clinical anti-CCR7 antibody, for refractory chronic lymphocytic leukemia (CLL), thus toxicity will be determined in the near future [174]. If drug safety and efficacy profiles are approved, this could serve as a systemic therapeutic option in IBC clinics.

In conclusion, we demonstrated that CCR7 is highly expressed in IBC patient tumor samples, at significantly higher levels than non-IBC patients. Further, the HER-2 enriched, and basal IBC subtypes expressed the highest levels of CCR7. We also report that CCR7 was highly expressed *in vitro* in both IBC and non-IBC cell lines. Interestingly, CDK 4/6 inhibitor and estrogen receptor targeted therapy-resistant breast cancer cell lines demonstrate increased CCR7. Thus, we hypothesize CCR7 could be driving the tumor biology in aggressive breast cancers, but may present a potential therapeutic target for future studies regardless. Further, a limitation to our study examining the CCR7 expression in human IBC patient tumors, was that the IBC tumor subtype information was incomplete. IBC is enriched for the HER2+ and

triple-negative subtypes, which could account for the increased CCR7 gene expression in IBC vs non-IBC, and further multi-variable analysis is warranted to normalize for this.

Supplemental Table 1: Summary of the top genes that were upregulated in the HFFW mice compared to LFNW (P<0.001).

Summary of RNA seq. data from HFFW vs. LFNW			
Genes	Base Mean	log2 Fold change	p-Value (P<0.0001)
Ighv1-26	165.797204	22.25563045	0.000182978
Spata31d1b	39.4636733	8.424334005	0.000241624
Il12b	30.7713411	8.068198279	0.000886685
Insm1	29.4147357	7.997222111	0.000612921
Cd8a	27.9913383	7.922255857	0.000723384
Cd6	104.892631	7.378322096	5.08306E-06
Ccr7	291.915488	6.859435671	3.39246E-12
Ccl22	135.683209	6.755298559	1.40766E-07
Hspb7	59.3229159	6.550739505	0.000678533
Myoz2	58.9094566	6.540565624	0.000694307
Agbl1	52.7172517	6.378670751	0.000811456
Themis	122.32809	6.00937726	1.84537E-08
Slamf1	37.2576219	5.885766124	0.000927621
Dscam1l	79.6459264	5.390123547	1.78668E-06
Mmp25	191.796882	5.241329186	3.28762E-10
Marco	348.325955	5.193593494	5.14953E-14
Cacna1b	91.9109527	5.176006645	2.52299E-07
Cd3d	44.6376134	5.129416569	0.000242098
Slc4a8	524.891111	5.104599983	8.92405E-21
Pcdh15	178.819502	4.965311389	7.3126E-11
Slco5a1	209.746164	4.905047569	1.19947E-11
H2-M2	376.525775	4.814578991	4.77966E-13
Cd3g	109.437307	4.086124066	5.39172E-07
Cd3e	137.931993	3.928287358	5.31146E-08
Zap70	142.514625	3.873711303	4.48582E-08

Mreg	225.465639	3.858607279	1.35835E-09
Insrr	55.7292709	3.84251368	0.000233306
Cd163l1	537.706813	3.838252056	8.29936E-12
Ntrk1	55.1812203	3.828066416	0.000267151
Eomes	73.8840993	3.826527781	7.10322E-05
Cxcr2	35.5051312	3.772742296	0.002554572

Supplemental figure 1: Summary of the top genes that were upregulated in the HFFW mice compared to LFNW (P<0.001). The fold change in the gene expression levels comparing HFFW versus LFNW mice, demonstrated an upregulation in inflammatory response genes, increased T-cell and lymphocyte activation and differentiation, hallmark inflammatory responses and key markers in adaptive immune response. Additionally, the fold change also showed a downregulation in pubertal mammary gland development genes.

Chapter 6: Discussion

DISCUSSION

In this study, we sought to understand how changes in the breast microenvironment prior to tumor initiation facilitated IBC progression and signs of lymphovascular invasion. We showed that a triad of IBC clinical symptoms (derived clinically but attributed to clogged lymphatics), including swollen involved breast, nipple change and diffuse skin change, independently predicted overall survival (OS). Further, we found that the classic presentation was strongly associated with smoking, post-menopausal status and metastatic disease. Herein, we sought to determine the biological drivers and risk factors associated with IBC, contributing to a tumor-promoting microenvironment, and further lymphangiogenesis. We demonstrated for the first time using *in vivo* Near infra-red fluorescence (NIRF) imaging, that a HFD significantly increases the lymphatic pulsing activity in immunocompromised mice. We also report for the first time that IBC tumor drives lymphatic pulsing, and that a HFD promotes IBC tumor growth. We found that HFD increased mammary gland immune cell infiltration in the mammary ducts. We also identified that a HFD and forced weaning increased the unique macrophage populations in the lymphatic vessels and mammary glands of these mice. Interestingly, we found that CCR7+ IBC tumors correlated with the pre-tumor lymphatic pulsing rate. This finding is interesting as CCR7 is expressed across IBC patient tumors and IBC cell lines, proving its therapeutic potential.

As previously mentioned, there are no unique genomic drivers in IBC compared to non-IBC, which drive the aggressive phenotype of IBC [49], [38]. IBC is a rapidly progressing, aggressive breast cancer, with limited understanding of this disease and even fewer intervention or preventative care options. Therefore, identifying stromal changes in the breast microenvironment which contribute to IBC provide a pathway to improved treatment options and patient outcomes. It is essential to study how the “pre-tumor” biology following events such as pregnancy, inform IBC tumor occurrence and progression. In this study, we used

established IBC risk factors to model the effects of diet and weaning status in the microenvironment to determine changes that occur in the breast, promoting tumor growth and metastasis [12], [13], [18]. Although, we assessed the long-term persisting weaning impacts, studies have highlighted that dynamic events such as involution in the breast, functionally change the breast environment. These functional changes provide insight into *de novo* changes that occur throughout a woman's life, leading to an IBC diagnosis. Further, as this study highlighted, studying the risk factor-induced changes in the mammary gland's microenvironment led to the identification of CCR7 as a potential therapeutic molecular target.

This warrants the inquires around how to effectively study IBC, to improve the therapeutic options and outcomes for patients. In the simplest terms, we have to shift and expand our investigative paradigm to better understand this complex and highly heterogenous disease. This can be achieved through establishing this overlap between "pre-tumor" biology in a normal breast microenvironment and tumor occurrence (Figure 13). In this thesis, we discussed critical risk factors including reproductive traits and lifestyle factors which contribute to breast cancer. Several pre-clinical and clinical studies have examined how immune cells in the breast microenvironment such as macrophage and immune cell infiltration contribute to breast cancer. Studies in IBC and aggressive breast cancers have shown obesity recruits and activates macrophages via the CCL2/CXCL12 signaling pathway, facilitating CCL2 chemokine-induced macrophage expansion, supporting the growth of tumors enriched in macrophages [175], [176]. Further, a separate study investigated the link between higher frequencies of TNBC rates and obesity. Demonstrating that HFD fed mice experienced faster tumor growth and metastasis, with obesity stimulating hypoxia-promoting tumor progression. Immunological differences in the HFD mice revealed fewer M1 macrophages, and more tumor-associated neutrophils compared to the normal diet fed mice [177]. Risk factors such as pregnancy and involution elicit signals which change the biology in the breast. The

remodeling programs that are utilized following lactation in murine mammary glands, resemble wound-healing programs [178]. The weaning-induced mammary gland microenvironment is remodeled with activated fibrillar collagen, high matrix metalloproteinase activity, and the infiltration of immune cells such as macrophages and neutrophils [178]. Thus, these changes following pregnancy and lactation persist in the microenvironment even after the initial post-partum stages [70]. Elevated immune infiltration and lymphatic density persist months, and even years following pregnancy in the normal breast [70]. This highlights that further work is warranted to understand how these “pre-tumor” signals in the normal breast provide a conducive microenvironment for IBC initiation and lymphovascular invasion.

Figure 13: A summary of overlapping “pre-tumor” signals in the normal breast and the IBC tumor microenvironment.

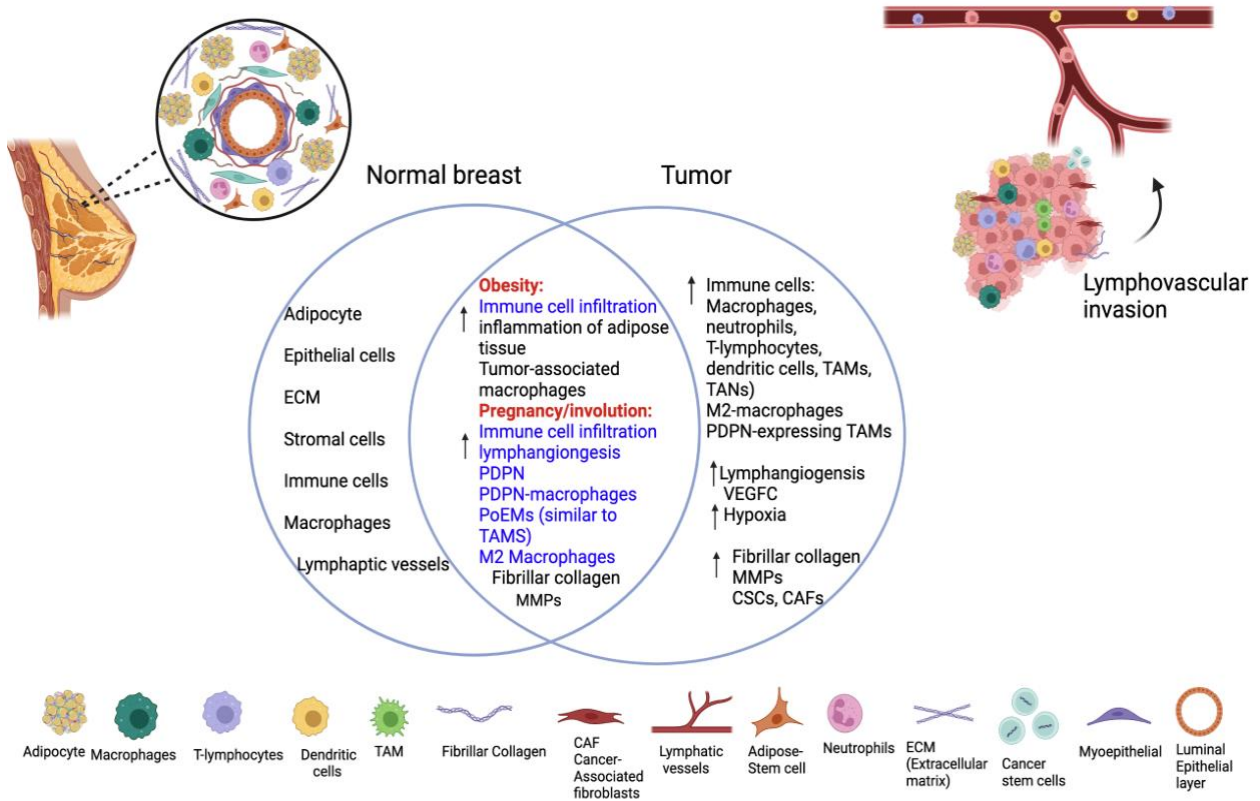


Figure 13: A summary of overlapping “pre-tumor” signals in the normal breast and the IBC tumor microenvironment. The IBC risk factors we studied, obesity and the role of pregnancy and involution, induce stromal changes (blue) which mimic a tumor-promoting microenvironment, demonstrating a conducive environment for IBC progression and further lymphovascular invasion.

In recent years, the increase in comprehensive gene analyses studies have facilitated the translating of the IBC genomic landscape into applicable molecular therapies. However, several factors have hindered illustrating the genomic landscape of IBC. A recent single sample gene enrichment analysis (ssGSEA) of IBC evaluated the epithelial-mesenchymal transition (EMT) phenotypes in IBC versus non-IBC samples. The results demonstrated a higher heterogeneity across the EMT spectrum in IBC, characterizing the unique microenvironment in IBC [179]. A separate study reported that IBC patients have a higher

frequency of circulating tumor cells clusters, possessing stem-like characteristics with increased metastatic capacity contributing to worse survival [179]. Further, a recent whole-exome sequencing study highlighted the somatic mutations and intra-tumoral heterogeneity in IBC samples versus normal breast samples. They identified *KMT2C*, a histone methyltransferase which contributes to oncogenic estrogen receptor signaling in breast cancer [180], [181], as the most frequently mutated gene [182]. Most critically, their analysis highlighted that even amongst the IBC samples, there were various sub-clonal structures and varying levels of intra-tumoral heterogeneity [182]. This looming reality of genomic heterogeneity among IBC tumors, underscores the difficulty of developing therapies for this rare disease, and emphasizes the urgency for improved therapeutic options.

Despite these limitations, researchers sought to establish the molecular hallmarks of IBC [49], [183], [184]. Various genomic studies have attempted to map out the molecular footprint of IBC to improve the therapeutic options for IBC patients. Comprehensive genome-wide gene expression profiling comparing IBC versus non-IBC identified differentially activated pathways in IBC including *HER2*, *MYC* and *VEGF*. This led to the rise of targeted therapies as using Anti-VEGFR and Anti-HER2 have further improved pCR to 35% [37]. However, the impact of Anti-HER2 targeted therapies only extends to 24% of IBC patients [24]. A clinical study assessing the use of Trastuzumab in HER2-positive IBC emphasized the obstacles in patient care, including Trastuzumab-induced cardiotoxicity characterized by cardiac dysfunction, and risk factors such as diabetes, hypertension and age associated with the therapy [185], [186]. Alternatively, IBC gene-expression profiling revealed the attenuation of TGF-beta and *P53* [49]. The TGF-beta signaling in tumor cells promotes single cell motility, facilitating invasion into the lymphatic vessels [187]. This finding could predict prognosis for IBC patients [10]. However, upon further examining, this finding was limited to the HER-2-positive subtype [1]. Additional studies have also highlighted clinically relevant genomic alterations in IBC,

including the amplification of *TP53*, *MYC* and *ER*. *MYC* amplification have been characterized in aggressive breast cancers. Pre-clinical studies have even demonstrated the therapeutic potential of CDK (Cyclin-dependent kinase) inhibitors in *MYC* overexpressing tumors [188]. Despite advancements in identifying molecular targets, the success in translating these findings into clinical settings for IBC patients has been sparse. Limitations in these treatments range from inconsistent patient responses in clinical trials, to treatment efficacy diminishing due to the tumor cells ability to suppress apoptotic signals, mitigating cell death [4], [67]. Overall, IBC is still not well understood, and increased research is required to advance preventative care and therapeutic options to save lives. There is a critical need and urgency to characterize this aggressive, and highly lethal disease to improve outcomes and overall survival for all patients.

In conclusion, the work of this dissertation highlighted the aggressiveness of IBC, and the significance of understanding this disease to provide improved treatment options. Thus, we emphasized the importance of studying the breast microenvironment as it can unveil unique functional and molecular signals, uncovering new markers and avenues for improved therapeutics and patient care. Most importantly, understanding how changes in the breast microenvironment elicit pre-tumor signals, can inform the trajectory of future research to improve interventions and prevention strategies, to ultimately reduce IBC incidence.

Bibliography

1. Woodward, W. A. (2015). Inflammatory breast cancer: unique biological and therapeutic considerations. *Lancet Oncol*, 16(15), e568-e576. [https://doi.org/10.1016/S1470-2045\(15\)00146-1](https://doi.org/10.1016/S1470-2045(15)00146-1)
2. Amin, M. B., Greene, F. L., Edge, S. B., Compton, C. C., Gershenwald, J. E., Brookland, R. K., Meyer, L., Gress, D. M., Byrd, D. R., & Winchester, D. P. (2017). The Eighth Edition AJCC Cancer Staging Manual: Continuing to build a bridge from a population-based to a more "personalized" approach to cancer staging. *CA Cancer J Clin*, 67(2), 93-99. <https://doi.org/10.3322/caac.21388>
3. Dawood, S., Merajver, S. D., Viens, P., Vermeulen, P. B., Swain, S. M., Buchholz, T. A., Dirix, L. Y., Levine, P. H., Lucci, A., Krishnamurthy, S., Robertson, F. M., Woodward, W. A., Yang, W. T., Ueno, N. T., & Cristofanilli, M. (2011). International expert panel on inflammatory breast cancer: consensus statement for standardized diagnosis and treatment. *Ann Oncol*, 22(3), 515-523. <https://doi.org/10.1093/annonc/mdq345>
4. Ueno, N. T., Espinosa Fernandez, J. R., Cristofanilli, M., Overmoyer, B., Rea, D., Berdichevski, F., El-Shinawi, M., Bellon, J., Le-Petross, H. T., Lucci, A., Babiera, G., DeSnyder, S. M., Teshome, M., Chang, E., Lim, B., Krishnamurthy, S., Stauder, M. C., Parmar, S., Mohamed, M. M., . . . Woodward, W. A. (2018). International Consensus on the Clinical Management of Inflammatory Breast Cancer from the Morgan Welch Inflammatory Breast Cancer Research Program 10th Anniversary Conference. *J Cancer*, 9(8), 1437-1447. <https://doi.org/10.7150/jca.23969>

5. Kamal, R. M., Hamed, S. T., & Salem, D. S. (2009). Classification of inflammatory breast disorders and step by step diagnosis. *Breast J*, 15(4), 367-380. <https://doi.org/10.1111/j.1524-4741.2009.00740.x>
6. Robertson, F. M., Bondy, M., Yang, W., Yamauchi, H., Wiggins, S., Kamrudin, S., Krishnamurthy, S., Le-Petross, H., Bidaut, L., Player, A. N., Barsky, S. H., Woodward, W. A., Buchholz, T., Lucci, A., Ueno, N. T., & Cristofanilli, M. (2010). Inflammatory breast cancer: the disease, the biology, the treatment. *CA Cancer J Clin*, 60(6), 351-375. <https://doi.org/10.3322/caac.20082>
7. Le, M. G., Arriagada, R., Contesso, G., Cammoun, M., Pfeiffer, F., Tabbane, F., Bahi, J., Dilaj, M., Spielmann, M., Travagli, J. P., Tursz, T., & Mourali, N. (2005). Dermal lymphatic emboli in inflammatory and noninflammatory breast cancer: a French-Tunisian joint study in 337 patients. *Clin Breast Cancer*, 6(5), 439-445. <https://doi.org/10.3816/CBC.2005.n.049>
8. Rosenbluth, J. M., & Overmoyer, B. A. (2019). Inflammatory Breast Cancer: a Separate Entity. *Curr Oncol Rep*, 21(10), 86. <https://doi.org/10.1007/s11912-019-0842-y>
9. Menta, A., Fouad, T. M., Lucci, A., Le-Petross, H., Stauder, M. C., Woodward, W. A., Ueno, N. T., & Lim, B. (2018). Inflammatory Breast Cancer: What to Know About This Unique, Aggressive Breast Cancer. *Surg Clin North Am*, 98(4), 787-800. <https://doi.org/10.1016/j.suc.2018.03.009>
10. Lim, B., Woodward, W. A., Wang, X., Reuben, J. M., & Ueno, N. T. (2018). Inflammatory breast cancer biology: the tumour microenvironment is key. *Nat Rev Cancer*, 18(8), 485-499. <https://doi.org/10.1038/s41568-018-0010-y>
11. Abraham, H. G., Xia, Y., Mukherjee, B., & Merajver, S. D. (2021). Incidence and survival of inflammatory breast cancer between 1973 and 2015 in the SEER database.

- Breast Cancer Res Treat*, 185(1), 229-238. <https://doi.org/10.1007/s10549-020-05938-2>
12. Schairer, C., Li, Y., Frawley, P., Graubard, B. I., Wellman, R. D., Buist, D. S., Kerlikowske, K., Onega, T. L., Anderson, W. F., & Miglioretti, D. L. (2013). Risk factors for inflammatory breast cancer and other invasive breast cancers. *J Natl Cancer Inst*, 105(18), 1373-1384. <https://doi.org/10.1093/jnci/djt206>
 13. Atkinson, R. L., El-Zein, R., Valero, V., Lucci, A., Bevers, T. B., Fouad, T., Liao, W., Ueno, N. T., Woodward, W. A., & Brewster, A. M. (2016). Epidemiological risk factors associated with inflammatory breast cancer subtypes. *Cancer Causes Control*, 27(3), 359-366. <https://doi.org/10.1007/s10552-015-0712-3>
 14. Hance, K. W., Anderson, W. F., Devesa, S. S., Young, H. A., & Levine, P. H. (2005). Trends in inflammatory breast carcinoma incidence and survival: the surveillance, epidemiology, and end results program at the National Cancer Institute. *J Natl Cancer Inst*, 97(13), 966-975. <https://doi.org/10.1093/jnci/dji172>
 15. Schairer, C., Hablas, A., Eldein, I. A. S., Gaafar, R., Rais, H., Mezlini, A., Ayed, F. B., Ayoub, W. B., Benider, A., Tahri, A., Khouchani, M., Aboulazm, D., Karkouri, M., Eissa, S., Pfeiffer, R. M., Gadalla, S. M., Swain, S. M., Merajver, S. D., Brown, L. M., & Soliman, A. S. (2019). Clinico-pathologic and mammographic characteristics of inflammatory and non-inflammatory breast cancer at six centers in North Africa. *Breast Cancer Res Treat*, 176(2), 407-417. <https://doi.org/10.1007/s10549-019-05237-5>
 16. Fouad, T. M., Ueno, N. T., Yu, R. K., Ensor, J. E., Alvarez, R. H., Krishnamurthy, S., Lucci, A., Reuben, J. M., Yang, W., Willey, J. S., Valero, V., Bondy, M. L., Cristofinalli, M., Shete, S., Woodward, W. A., & El-Zein, R. (2018). Distinct epidemiological profiles associated with inflammatory breast cancer (IBC): A comprehensive analysis of the IBC registry at The University of Texas MD Anderson Cancer Center. *PLoS One*, 13(9), e0204372. <https://doi.org/10.1371/journal.pone.0204372>

17. Mejri, N., El Benna, H., Rachdi, H., Labidi, S., Benna, M., Daoud, N., Hamdi, Y., Abdelhak, S., & Boussen, H. (2020). Reproductive Risk Factors of Inflammatory Breast Cancer according to Luminal, HER2-Overexpressing, and Triple-Negative Subtypes: A Case Comparison Study. *Oncol Res Treat*, 43(5), 204-210. <https://doi.org/10.1159/000506691>
18. Soliman, A. S., Kleer, C. G., Mrad, K., Karkouri, M., Omar, S., Khaled, H. M., Benider, A. L., Ayed, F. B., Eissa, S. S., Eissa, M. S., McSpadden, E. J., Lo, A. C., Toy, K., Kantor, E. D., Xiao, Q., Hampton, C., & Merajver, S. D. (2011). Inflammatory breast cancer in north Africa: comparison of clinical and molecular epidemiologic characteristics of patients from Egypt, Tunisia, and Morocco. *Breast Dis*, 33(4), 159-169. <https://doi.org/10.3233/BD-2012-000337>
19. Stecklein, S. R., Reddy, J. P., Wolfe, A. R., Lopez, M. S., Fouad, T. M., Debeb, B. G., Ueno, N. T., Brewster, A. M., & Woodward, W. A. (2017). Lack of Breastfeeding History in Parous Women with Inflammatory Breast Cancer Predicts Poor Disease-Free Survival. *J Cancer*, 8(10), 1726-1732. <https://doi.org/10.7150/jca.20095>
20. Schlichting, J. A., Soliman, A. S., Schairer, C., Schottenfeld, D., & Merajver, S. D. (2012). Inflammatory and non-inflammatory breast cancer survival by socioeconomic position in the Surveillance, Epidemiology, and End Results database, 1990-2008. *Breast Cancer Res Treat*, 134(3), 1257-1268. <https://doi.org/10.1007/s10549-012-2133-2>
21. Li, X., Sun, S., Li, N., Gao, J., Yu, J., Zhao, J., Li, M., & Zhao, Z. (2017). High Expression of CCR7 Predicts Lymph Node Metastasis and Good Prognosis in Triple Negative Breast Cancer. *Cell Physiol Biochem*, 43(2), 531-539. <https://doi.org/10.1159/000480526>

22. Yersal, O., & Barutca, S. (2014). Biological subtypes of breast cancer: Prognostic and therapeutic implications. *World J Clin Oncol*, 5(3), 412-424. <https://doi.org/10.5306/wjco.v5.i3.412>
23. Nadji, M., Gomez-Fernandez, C., Ganjei-Azar, P., & Morales, A. R. (2005). Immunohistochemistry of estrogen and progesterone receptors reconsidered: experience with 5,993 breast cancers. *Am J Clin Pathol*, 123(1), 21-27. <https://doi.org/10.1309/4wv79n2ghj3x1841>
24. Kertmen, N., Babacan, T., Keskin, O., Solak, M., Sarici, F., Akin, S., Arik, Z., Aslan, A., Ates, O., Aksoy, S., Ozisik, Y., & Altundag, K. (2015). Molecular subtypes in patients with inflammatory breast cancer; a single center experience. *J BUON*, 20(1), 35-39. <https://www.ncbi.nlm.nih.gov/pubmed/25778293>
25. Manfrin, E., Remo, A., Pancione, M., Cannizzaro, C., Falsirollo, F., Pollini, G. P., Pellini, F., Molino, A., Brunelli, M., Vendraminelli, R., Ceccarelli, M., Pagnotta, S. M., Simeone, I., & Bonetti, F. (2014). Comparison between invasive breast cancer with extensive peritumoral vascular invasion and inflammatory breast carcinoma: a clinicopathologic study of 161 cases. *Am J Clin Pathol*, 142(3), 299-306. <https://doi.org/10.1309/AJCPOXKX67KRAOVM>
26. Charpin, C., Bonnier, P., Khouzami, A., Vacheret, H., Andrac, L., Lavaut, M. N., Allasia, C., & Piana, L. (1992). Inflammatory breast carcinoma: an immunohistochemical study using monoclonal anti-pHER-2/neu, pS2, cathepsin, ER and PR. *Anticancer Res*, 12(3), 591-597. <https://www.ncbi.nlm.nih.gov/pubmed/1352440>
27. Watanabe, T., Honma, R., Kojima, M., Nomura, S., Furukawa, S., Soeda, S., Watanabe, S., & Fujimori, K. (2019). Prediction of lymphovascular space invasion in endometrial cancer using the 55-gene signature selected by DNA microarray analysis. *PLoS One*, 14(9), e0223178. <https://doi.org/10.1371/journal.pone.0223178>

28. Rakha, E. A., Martin, S., Lee, A. H., Morgan, D., Pharoah, P. D., Hodi, Z., Macmillan, D., & Ellis, I. O. (2012). The prognostic significance of lymphovascular invasion in invasive breast carcinoma. *Cancer*, 118(15), 3670-3680. <https://doi.org/10.1002/cncr.26711>
29. Fujii, T., Yajima, R., Tatsuki, H., Suto, T., Morita, H., Tsutsumi, S., & Kuwano, H. (2015). Significance of lymphatic invasion combined with size of primary tumor for predicting sentinel lymph node metastasis in patients with breast cancer. *Anticancer Res*, 35(6), 3581-3584. <https://www.ncbi.nlm.nih.gov/pubmed/26026130>
30. Zhong, Y. M., Tong, F., & Shen, J. (2022). Lympho-vascular invasion impacts the prognosis in breast-conserving surgery: a systematic review and meta-analysis. *BMC Cancer*, 22(1), 102. <https://doi.org/10.1186/s12885-022-09193-0>
31. Molckovsky, A., Fitzgerald, B., Freedman, O., Heisey, R., & Clemons, M. (2009). Approach to inflammatory breast cancer. *Can Fam Physician*, 55(1), 25-31. <https://www.ncbi.nlm.nih.gov/pubmed/19155362>
32. Le-Petross, H. T., Cristofanilli, M., Carkaci, S., Krishnamurthy, S., Jackson, E. F., Harrell, R. K., Reed, B. J., & Yang, W. T. (2011). MRI features of inflammatory breast cancer. *AJR Am J Roentgenol*, 197(4), W769-776. <https://doi.org/10.2214/AJR.10.6157>
33. Gunhan-Bilgen, I., Ustun, E. E., & Memis, A. (2002). Inflammatory breast carcinoma: mammographic, ultrasonographic, clinical, and pathologic findings in 142 cases. *Radiology*, 223(3), 829-838. <https://doi.org/10.1148/radiol.2233010198>
34. Jagsi, R., Mason, G., Overmoyer, B. A., Woodward, W. A., Badve, S., Schneider, R. J., Lang, J. E., Alpaugh, M., Williams, K. P., Vaught, D., Smith, A., Smith, K., Miller, K. D., & Susan, G. K.-I. I. B. C. C. i. p. w. t. M. F. (2022). Inflammatory breast cancer defined: proposed common diagnostic criteria to guide treatment and research. *Breast Cancer Res Treat*, 192(2), 235-243. <https://doi.org/10.1007/s10549-021-06434-x>

35. Fernandez, S. V., MacFarlane, A. W. t., Jillab, M., Arisi, M. F., Yearley, J., Annamalai, L., Gong, Y., Cai, K. Q., Alpaugh, R. K., Cristofanilli, M., & Campbell, K. S. (2020). Immune phenotype of patients with stage IV metastatic inflammatory breast cancer. *Breast Cancer Res*, 22(1), 134. <https://doi.org/10.1186/s13058-020-01371-x>
36. Balema, W., Liu, D., Shen, Y., El-Zein, R., Debeb, B. G., Kai, M., Overmoyer, B., Miller, K. D., Le-Petross, H. T., Ueno, N. T., & Woodward, W. A. (2021). Inflammatory breast cancer appearance at presentation is associated with overall survival. *Cancer Med*, 10(18), 6261-6272. <https://doi.org/10.1002/cam4.4170>
37. Chaititkun, S., Saleem, S., Lim, B., Valero, V., & Ueno, N. T. (2021). Update on systemic treatment for newly diagnosed inflammatory breast cancer. *J Adv Res*, 29, 1-12. <https://doi.org/10.1016/j.jare.2020.08.014>
38. Bertucci, F., Ueno, N. T., Finetti, P., Vermeulen, P., Lucci, A., Robertson, F. M., Marsan, M., Iwamoto, T., Krishnamurthy, S., Masuda, H., Van Dam, P., Woodward, W. A., Cristofanilli, M., Reuben, J. M., Dirix, L., Viens, P., Symmans, W. F., Birnbaum, D., & Van Laere, S. J. (2014). Gene expression profiles of inflammatory breast cancer: correlation with response to neoadjuvant chemotherapy and metastasis-free survival. *Ann Oncol*, 25(2), 358-365. <https://doi.org/10.1093/annonc/mdt496>
39. Cakar, B., Surmeli, Z., Oner, P. G., Yelim, E. S., Karabulut, B., & Uslu, R. (2018). The Impact of Subtype Distribution in Inflammatory Breast Cancer Outcome. *Eur J Breast Health*, 14(4), 211-217. <https://doi.org/10.5152/ejbh.2018.4170>
40. Dobiasova, B., & Mego, M. (2020). Biomarkers for Inflammatory Breast Cancer: Diagnostic and Therapeutic Utility. *Breast Cancer (Dove Med Press)*, 12, 153-163. <https://doi.org/10.2147/BCTT.S231502>

41. Schmid, P., Cortes, J., Dent, R., Puztai, L., McArthur, H., Kummel, S., Bergh, J., Denkert, C., Park, Y. H., Hui, R., Harbeck, N., Takahashi, M., Untch, M., Fasching, P. A., Cardoso, F., Andersen, J., Patt, D., Danso, M., Ferreira, M., . . . Investigators, K.-. (2022). Event-free Survival with Pembrolizumab in Early Triple-Negative Breast Cancer. *N Engl J Med*, 386(6), 556-567. <https://doi.org/10.1056/NEJMoa2112651>
42. Gianni, L., Pienkowski, T., Im, Y. H., Roman, L., Tseng, L. M., Liu, M. C., Lluch, A., Staroslawska, E., de la Haba-Rodriguez, J., Im, S. A., Pedrini, J. L., Poirier, B., Morandi, P., Semiglazov, V., Srimuninnimit, V., Bianchi, G., Szado, T., Ratnayake, J., Ross, G., & Valagussa, P. (2012). Efficacy and safety of neoadjuvant pertuzumab and trastuzumab in women with locally advanced, inflammatory, or early HER2-positive breast cancer (NeoSphere): a randomised multicentre, open-label, phase 2 trial. *Lancet Oncol*, 13(1), 25-32. [https://doi.org/10.1016/S1470-2045\(11\)70336-9](https://doi.org/10.1016/S1470-2045(11)70336-9)
43. Dawood, S., & Cristofanilli, M. (2015). IBC as a Rapidly Spreading Systemic Disease: Clinical and Targeted Approaches Using the Neoadjuvant Model. *J Natl Cancer Inst Monogr*, 2015(51), 56-59. <https://doi.org/10.1093/jncimonographs/lgv017>
44. Biswas, T., Jindal, C., Fitzgerald, T. L., & Efirid, J. T. (2019). Pathologic Complete Response (pCR) and Survival of Women with Inflammatory Breast Cancer (IBC): An Analysis Based on Biologic Subtypes and Demographic Characteristics. *Int J Environ Res Public Health*, 16(1). <https://doi.org/10.3390/ijerph16010124>
45. van Uden, D. J. P., van Maaren, M. C., Bult, P., Strobbe, L. J. A., van der Hoeven, J. J. M., Blanken-Peeters, C., Siesling, S., & de Wilt, J. H. W. (2019). Pathologic complete response and overall survival in breast cancer subtypes in stage III inflammatory breast cancer. *Breast Cancer Res Treat*, 176(1), 217-226. <https://doi.org/10.1007/s10549-019-05219-7>

46. Stauder, M. C., Caudle, A. S., Allen, P. K., Shaitelman, S. F., Smith, B. D., Hoffman, K. E., Buchholz, T. A., Chavez-Macgregor, M., Hunt, K. K., Meric-Bernstam, F., & Woodward, W. A. (2016). Outcomes of Post Mastectomy Radiation Therapy in Patients Receiving Axillary Lymph Node Dissection After Positive Sentinel Lymph Node Biopsy. *Int J Radiat Oncol Biol Phys*, 96(3), 637-644. <https://doi.org/10.1016/j.ijrobp.2016.07.003>
47. Corrigan, K. L., Woodward, W. A., & Stauder, M. C. (2021). How should radiation be done for inflammatory breast cancer patients?-a narrative review of modern literature. *Chin Clin Oncol*, 10(6), 60. <https://doi.org/10.21037/cco-21-153>
48. Tutt, A. N. J., Garber, J. E., Kaufman, B., Viale, G., Fumagalli, D., Rastogi, P., Gelber, R. D., de Azambuja, E., Fielding, A., Balmana, J., Domchek, S. M., Gelmon, K. A., Hollingsworth, S. J., Korde, L. A., Linderholm, B., Bandos, H., Senkus, E., Suga, J. M., Shao, Z., . . . Investigators. (2021). Adjuvant Olaparib for Patients with BRCA1- or BRCA2-Mutated Breast Cancer. *N Engl J Med*, 384(25), 2394-2405. <https://doi.org/10.1056/NEJMoa2105215>
49. Van Laere, S. J., Ueno, N. T., Finetti, P., Vermeulen, P., Lucci, A., Robertson, F. M., Marsan, M., Iwamoto, T., Krishnamurthy, S., Masuda, H., van Dam, P., Woodward, W. A., Viens, P., Cristofanilli, M., Birnbaum, D., Dirix, L., Reuben, J. M., & Bertucci, F. (2013). Uncovering the molecular secrets of inflammatory breast cancer biology: an integrated analysis of three distinct affymetrix gene expression datasets. *Clin Cancer Res*, 19(17), 4685-4696. <https://doi.org/10.1158/1078-0432.CCR-12-2549>
50. Zwick, R. K., Rudolph, M. C., Shook, B. A., Holtrup, B., Roth, E., Lei, V., Van Keymeulen, A., Seewaldt, V., Kwei, S., Wysolmerski, J., Rodeheffer, M. S., & Horsley, V. (2018). Adipocyte hypertrophy and lipid dynamics underlie mammary gland

- remodeling after lactation. *Nat Commun*, 9(1), 3592. <https://doi.org/10.1038/s41467-018-05911-0>
51. Quarrie, L. H., Addey, C. V., & Wilde, C. J. (1996). Programmed cell death during mammary tissue involution induced by weaning, litter removal, and milk stasis. *J Cell Physiol*, 168(3), 559-569. [https://doi.org/10.1002/\(SICI\)1097-4652\(199609\)168:3<559::AID-JCP8>3.0.CO;2-O](https://doi.org/10.1002/(SICI)1097-4652(199609)168:3<559::AID-JCP8>3.0.CO;2-O)
52. Alex, A., Bhandary, E., & McGuire, K. P. (2020). Anatomy and Physiology of the Breast during Pregnancy and Lactation. *Adv Exp Med Biol*, 1252, 3-7. https://doi.org/10.1007/978-3-030-41596-9_1
53. Jena, M. K., Jaswal, S., Kumar, S., & Mohanty, A. K. (2019). Molecular mechanism of mammary gland involution: An update. *Dev Biol*, 445(2), 145-155. <https://doi.org/10.1016/j.ydbio.2018.11.002>
54. Lyons, T. R., O'Brien, J., Borges, V. F., Conklin, M. W., Keely, P. J., Eliceiri, K. W., Marusyk, A., Tan, A. C., & Schedin, P. (2011). Postpartum mammary gland involution drives progression of ductal carcinoma in situ through collagen and COX-2. *Nat Med*, 17(9), 1109-1115. <https://doi.org/10.1038/nm.2416>
55. Tamburini, B. A. J., Elder, A. M., Finlon, J. M., Winter, A. B., Wessells, V. M., Borges, V. F., & Lyons, T. R. (2019). PD-1 Blockade During Post-partum Involution Reactivates the Anti-tumor Response and Reduces Lymphatic Vessel Density. *Front Immunol*, 10, 1313. <https://doi.org/10.3389/fimmu.2019.01313>
56. Anderson, S. M., Rudolph, M. C., McManaman, J. L., & Neville, M. C. (2007). Key stages in mammary gland development. Secretory activation in the mammary gland: it's not just about milk protein synthesis! *Breast Cancer Res*, 9(1), 204. <https://doi.org/10.1186/bcr1653>

57. Lefrere, H., Lenaerts, L., Borges, V. F., Schedin, P., Neven, P., & Amant, F. (2021). Postpartum breast cancer: mechanisms underlying its worse prognosis, treatment implications, and fertility preservation. *Int J Gynecol Cancer*, 31(3), 412-422. <https://doi.org/10.1136/ijgc-2020-002072>
58. Schedin, P., O'Brien, J., Rudolph, M., Stein, T., & Borges, V. (2007). Microenvironment of the involuting mammary gland mediates mammary cancer progression. *J Mammary Gland Biol Neoplasia*, 12(1), 71-82. <https://doi.org/10.1007/s10911-007-9039-3>
59. Stein, T., Salomonis, N., & Gusterson, B. A. (2007). Mammary gland involution as a multi-step process. *J Mammary Gland Biol Neoplasia*, 12(1), 25-35. <https://doi.org/10.1007/s10911-007-9035-7>
60. Stein, T., Morris, J. S., Davies, C. R., Weber-Hall, S. J., Duffy, M. A., Heath, V. J., Bell, A. K., Ferrier, R. K., Sandilands, G. P., & Gusterson, B. A. (2004). Involution of the mouse mammary gland is associated with an immune cascade and an acute-phase response, involving LBP, CD14 and STAT3. *Breast Cancer Res*, 6(2), R75-91. <https://doi.org/10.1186/bcr753>
61. Martinson, H. A., Jindal, S., Durand-Rougely, C., Borges, V. F., & Schedin, P. (2015). Wound healing-like immune program facilitates postpartum mammary gland involution and tumor progression. *Int J Cancer*, 136(8), 1803-1813. <https://doi.org/10.1002/ijc.29181>
62. Stein, T., Salomonis, N., Nuyten, D. S., van de Vijver, M. J., & Gusterson, B. A. (2009). A mouse mammary gland involution mRNA signature identifies biological pathways potentially associated with breast cancer metastasis. *J Mammary Gland Biol Neoplasia*, 14(2), 99-116. <https://doi.org/10.1007/s10911-009-9120-1>
63. Bambhroliya, A., Van Wyhe, R. D., Kumar, S., Debeb, B. G., Reddy, J. P., Van Laere, S., El-Zein, R., Rao, A., & Woodward, W. A. (2018). Gene set analysis of post-

- lactational mammary gland involution gene signatures in inflammatory and triple-negative breast cancer. *PLoS One*, 13(4), e0192689. <https://doi.org/10.1371/journal.pone.0192689>
64. Gupta, P. B., Proia, D., Cingoz, O., Weremowicz, J., Naber, S. P., Weinberg, R. A., & Kuperwasser, C. (2007). Systemic stromal effects of estrogen promote the growth of estrogen receptor-negative cancers. *Cancer Res*, 67(5), 2062-2071. <https://doi.org/10.1158/0008-5472.CAN-06-3895>
65. Radisky, D. C., & Hartmann, L. C. (2009). Mammary involution and breast cancer risk: transgenic models and clinical studies. *J Mammary Gland Biol Neoplasia*, 14(2), 181-191. <https://doi.org/10.1007/s10911-009-9123-y>
66. McCready, J., Arendt, L. M., Glover, E., Iyer, V., Briendel, J. L., Lyle, S. R., Naber, S. P., Jay, D. G., & Kuperwasser, C. (2014). Pregnancy-associated breast cancers are driven by differences in adipose stromal cells present during lactation. *Breast Cancer Res*, 16(1), R2. <https://doi.org/10.1186/bcr3594>
67. Wallace, T. R., Tarullo, S. E., Crump, L. S., & Lyons, T. R. (2019). Studies of postpartum mammary gland involution reveal novel pro-metastatic mechanisms. *J Cancer Metastasis Treat*, 5. <https://doi.org/10.20517/2394-4722.2019.01>
68. Basree, M. M., Shinde, N., Koivisto, C., Cuitino, M., Kladney, R., Zhang, J., Stephens, J., Palettas, M., Zhang, A., Kim, H. K., Acero-Bedoya, S., Trimboli, A., Stover, D. G., Ludwig, T., Ganju, R., Weng, D., Shields, P., Freudenheim, J., Leone, G. W., . . . Ramaswamy, B. (2019). Abrupt involution induces inflammation, estrogenic signaling, and hyperplasia linking lack of breastfeeding with increased risk of breast cancer. *Breast Cancer Res*, 21(1), 80. <https://doi.org/10.1186/s13058-019-1163-7>
69. Betterman, K. L., Paquet-Fifield, S., Asselin-Labat, M. L., Visvader, J. E., Butler, L. M., Stacker, S. A., Achen, M. G., & Harvey, N. L. (2012). Remodeling of the lymphatic

- vasculature during mouse mammary gland morphogenesis is mediated via epithelial-derived lymphangiogenic stimuli. *Am J Pathol*, 181(6), 2225-2238. <https://doi.org/10.1016/j.ajpath.2012.08.035>
70. Jindal, S., Narasimhan, J., Borges, V. F., & Schedin, P. (2020). Characterization of weaning-induced breast involution in women: implications for young women's breast cancer. *NPJ Breast Cancer*, 6, 55. <https://doi.org/10.1038/s41523-020-00196-3>
71. Van der Auwera, I., Van den Eynden, G. G., Colpaert, C. G., Van Laere, S. J., van Dam, P., Van Marck, E. A., Dirix, L. Y., & Vermeulen, P. B. (2005). Tumor lymphangiogenesis in inflammatory breast carcinoma: a histomorphometric study. *Clin Cancer Res*, 11(21), 7637-7642. <https://doi.org/10.1158/1078-0432.CCR-05-1142>
72. Van der Auwera, I., Van Laere, S. J., Van den Eynden, G. G., Benoy, I., van Dam, P., Colpaert, C. G., Fox, S. B., Turley, H., Harris, A. L., Van Marck, E. A., Vermeulen, P. B., & Dirix, L. Y. (2004). Increased angiogenesis and lymphangiogenesis in inflammatory versus noninflammatory breast cancer by real-time reverse transcriptase-PCR gene expression quantification. *Clin Cancer Res*, 10(23), 7965-7971. <https://doi.org/10.1158/1078-0432.CCR-04-0063>
73. Girard, J. P., Moussion, C., & Forster, R. (2012). HEVs, lymphatics and homeostatic immune cell trafficking in lymph nodes. *Nat Rev Immunol*, 12(11), 762-773. <https://doi.org/10.1038/nri3298>
74. Pepper, M. S., & Skobe, M. (2003). Lymphatic endothelium: morphological, molecular and functional properties. *J Cell Biol*, 163(2), 209-213. <https://doi.org/10.1083/jcb.200308082>
75. Butcher, E. C., & Picker, L. J. (1996). Lymphocyte homing and homeostasis. *Science*, 272(5258), 60-66. <https://doi.org/10.1126/science.272.5258.60>

76. Kataru, R. P., Baik, J. E., Park, H. J., Wiser, I., Rehal, S., Shin, J. Y., & Mehrara, B. J. (2019). Regulation of Immune Function by the Lymphatic System in Lymphedema. *Front Immunol*, *10*, 470. <https://doi.org/10.3389/fimmu.2019.00470>
77. Scallan, J. P., Zawieja, S. D., Castorena-Gonzalez, J. A., & Davis, M. J. (2016). Lymphatic pumping: mechanics, mechanisms and malfunction. *J Physiol*, *594*(20), 5749-5768. <https://doi.org/10.1113/JP272088>
78. Mukherjee, A., Hooks, J., Nepiyushchikh, Z., & Dixon, J. B. (2019). Entrainment of Lymphatic Contraction to Oscillatory Flow. *Sci Rep*, *9*(1), 5840. <https://doi.org/10.1038/s41598-019-42142-9>
79. Gashev, A. A., Wang, W., Laine, G. A., Stewart, R. H., & Zawieja, D. C. (2007). Characteristics of the active lymph pump in bovine prenodal mesenteric lymphatics. *Lymphat Res Biol*, *5*(2), 71-79. <https://doi.org/10.1089/lrb.2007.5202>
80. Vahtomeri, K., & Alitalo, K. (2020). Lymphatic Vessels in Tumor Dissemination versus Immunotherapy. *Cancer Res*, *80*(17), 3463-3465. <https://doi.org/10.1158/0008-5472.CAN-20-0156>
81. Nakajima, Y., Asano, K., Mukai, K., Urai, T., Okuwa, M., Sugama, J., & Nakatani, T. (2018). Near-Infrared Fluorescence Imaging Directly Visualizes Lymphatic Drainage Pathways and Connections between Superficial and Deep Lymphatic Systems in the Mouse Hindlimb. *Sci Rep*, *8*(1), 7078. <https://doi.org/10.1038/s41598-018-25383-y>
82. Rasmussen, J. C., Aldrich, M. B., Guilliod, R., Fife, C. E., O'Donnell, T. F., & Sevick-Muraca, E. M. (2015). Near-infrared fluorescence lymphatic imaging in a patient treated for venous occlusion. *J Vasc Surg Cases*, *1*(3), 201-204. <https://doi.org/10.1016/j.jvsc.2015.05.004>
83. Christensen, A., Juhl, K., Kiss, K., Lelkaitis, G., Charabi, B. W., Mortensen, J., Kjaer, A., & von Buchwald, C. (2019). Near-infrared fluorescence imaging improves the nodal

- yield in neck dissection in oral cavity cancer - A randomized study. *Eur J Surg Oncol*, 45(11), 2151-2158. <https://doi.org/10.1016/j.ejso.2019.06.039>
84. Arora, J., Sauer, S. J., Tarpley, M., Vermeulen, P., Rypens, C., Van Laere, S., Williams, K. P., Devi, G. R., & Dewhurst, M. W. (2017). Inflammatory breast cancer tumor emboli express high levels of anti-apoptotic proteins: use of a quantitative high content and high-throughput 3D IBC spheroid assay to identify targeting strategies. *Oncotarget*, 8(16), 25848-25863. <https://doi.org/10.18632/oncotarget.15667>
85. Kwon, S., Agollah, G. D., Wu, G., & Sevick-Muraca, E. M. (2014). Spatio-temporal changes of lymphatic contractility and drainage patterns following lymphadenectomy in mice. *PLoS One*, 9(8), e106034. <https://doi.org/10.1371/journal.pone.0106034>
86. Kwon, S., Agollah, G. D., Wu, G., Chan, W., & Sevick-Muraca, E. M. (2013). Direct visualization of changes of lymphatic function and drainage pathways in lymph node metastasis of B16F10 melanoma using near-infrared fluorescence imaging. *Biomed Opt Express*, 4(6), 967-977. <https://doi.org/10.1364/BOE.4.000967>
87. Agollah, G. D., Wu, G., Sevick-Muraca, E. M., & Kwon, S. (2014). In vivo lymphatic imaging of a human inflammatory breast cancer model. *J Cancer*, 5(9), 774-783. <https://doi.org/10.7150/jca.9835>
88. Saif, M. W. (2013). Anti-VEGF agents in metastatic colorectal cancer (mCRC): are they all alike? *Cancer Manag Res*, 5, 103-115. <https://doi.org/10.2147/CMAR.S45193>
89. Sasich, L. D., & Sukkari, S. R. (2012). The US FDAs withdrawal of the breast cancer indication for Avastin (bevacizumab). *Saudi Pharm J*, 20(4), 381-385. <https://doi.org/10.1016/j.jsps.2011.12.001>
90. Sun, Z., Lan, X., Xu, S., Li, S., & Xi, Y. (2020). Efficacy of bevacizumab combined with chemotherapy in the treatment of HER2-negative metastatic breast cancer: a network meta-analysis. *BMC Cancer*, 20(1), 180. <https://doi.org/10.1186/s12885-020-6674-1>

91. Leone, J. P., Emblem, K. E., Weitz, M., Gelman, R. S., Schneider, B. P., Freedman, R. A., Younger, J., Pinho, M. C., Sorensen, A. G., Gerstner, E. R., Harris, G., Krop, I. E., Morganstern, D., Sohl, J., Hu, J., Kasparian, E., Winer, E. P., & Lin, N. U. (2020). Phase II trial of carboplatin and bevacizumab in patients with breast cancer brain metastases. *Breast Cancer Res*, 22(1), 131. <https://doi.org/10.1186/s13058-020-01372-w>
92. Kobayashi, D., Endo, M., Ochi, H., Hojo, H., Miyasaka, M., & Hayasaka, H. (2017). Regulation of CCR7-dependent cell migration through CCR7 homodimer formation. *Sci Rep*, 7(1), 8536. <https://doi.org/10.1038/s41598-017-09113-4>
93. Takeuchi, H., Fujimoto, A., Tanaka, M., Yamano, T., Hsueh, E., & Hoon, D. S. (2004). CCL21 chemokine regulates chemokine receptor CCR7 bearing malignant melanoma cells. *Clin Cancer Res*, 10(7), 2351-2358. <https://doi.org/10.1158/1078-0432.ccr-03-0195>
94. Nandagopal, S., Wu, D., & Lin, F. (2011). Combinatorial guidance by CCR7 ligands for T lymphocytes migration in co-existing chemokine fields. *PLoS One*, 6(3), e18183. <https://doi.org/10.1371/journal.pone.0018183>
95. von Andrian, U. H., & Mempel, T. R. (2003). Homing and cellular traffic in lymph nodes. *Nat Rev Immunol*, 3(11), 867-878. <https://doi.org/10.1038/nri1222>
96. Li, X., Sun, S., Li, N., Gao, J., Yu, J., Zhao, J., Li, M., & Zhao, Z. (2017). High Expression of CCR7 Predicts Lymph Node Metastasis and Good Prognosis in Triple Negative Breast Cancer. *Cell Physiol Biochem*, 43(2), 531-539. <https://doi.org/10.1159/000480526>
97. Wu, J., Li, L., Liu, J., Wang, Y., Wang, Z., Wang, Y., Liu, W., Zhou, Z., Chen, C., Liu, R., & Yang, R. (2018). CC chemokine receptor 7 promotes triple-negative breast cancer growth and metastasis. *Acta Biochim Biophys Sin (Shanghai)*, 50(9), 835-842. <https://doi.org/10.1093/abbs/gmy077>

98. Tutunea-Fatan, E., Majumder, M., Xin, X., & Lala, P. K. (2015). The role of CCL21/CCR7 chemokine axis in breast cancer-induced lymphangiogenesis. *Mol Cancer*, 14, 35. <https://doi.org/10.1186/s12943-015-0306-4>
99. Cabioglu, N., Gong, Y., Islam, R., Broglio, K. R., Sneige, N., Sahin, A., Gonzalez-Angulo, A. M., Morandi, P., Bucana, C., Hortobagyi, G. N., & Cristofanilli, M. (2007). Expression of growth factor and chemokine receptors: new insights in the biology of inflammatory breast cancer. *Ann Oncol*, 18(6), 1021-1029. <https://doi.org/10.1093/annonc/mdm060>
100. Yang, W. T., Le-Petross, H. T., Macapinlac, H., Carkaci, S., Gonzalez-Angulo, A. M., Dawood, S., Resetkova, E., Hortobagyi, G. N., & Cristofanilli, M. (2008). Inflammatory breast cancer: PET/CT, MRI, mammography, and sonography findings. *Breast Cancer Res Treat*, 109(3), 417-426. <https://doi.org/10.1007/s10549-007-9671-z>
101. Le-Petross, C. H., Bidaut, L., & Yang, W. T. (2008). Evolving role of imaging modalities in inflammatory breast cancer. *Semin Oncol*, 35(1), 51-63. <https://doi.org/10.1053/j.seminoncol.2007.11.016>
102. Grueneisen, J., Nagarajah, J., Buchbender, C., Hoffmann, O., Schaarschmidt, B. M., Poeppel, T., Forsting, M., Quick, H. H., Umutlu, L., & Kinner, S. (2015). Positron Emission Tomography/Magnetic Resonance Imaging for Local Tumor Staging in Patients With Primary Breast Cancer: A Comparison With Positron Emission Tomography/Computed Tomography and Magnetic Resonance Imaging. *Invest Radiol*, 50(8), 505-513. <https://doi.org/10.1097/RLI.0000000000000197>
103. Al-Faham, Z., Al-Katib, S., Jaiyesimi, I., & Bhavnagri, S. (2015). Evaluation of a Case of Inflammatory Breast Cancer with 18F-FDG PET/CT. *J Nucl Med Technol*, 43(4), 289-291. <https://doi.org/10.2967/jnmt.114.148494>
104. Walker, G. V., Niikura, N., Yang, W., Rohren, E., Valero, V., Woodward, W. A., Alvarez, R. H., Lucci, A., Jr., Ueno, N. T., & Buchholz, T. A. (2012). Pretreatment

- staging positron emission tomography/computed tomography in patients with inflammatory breast cancer influences radiation treatment field designs. *Int J Radiat Oncol Biol Phys*, 83(5), 1381-1386. <https://doi.org/10.1016/j.ijrobp.2011.10.040>
105. Allison, K. H., Hammond, M. E. H., Dowsett, M., McKernin, S. E., Carey, L. A., Fitzgibbons, P. L., Hayes, D. F., Lakhani, S. R., Chavez-MacGregor, M., Perlmutter, J., Perou, C. M., Regan, M. M., Rimm, D. L., Symmans, W. F., Torlakovic, E. E., Varella, L., Viale, G., Weisberg, T. F., McShane, L. M., & Wolff, A. C. (2020). Estrogen and Progesterone Receptor Testing in Breast Cancer: ASCO/CAP Guideline Update. *J Clin Oncol*, 38(12), 1346-1366. <https://doi.org/10.1200/JCO.19.02309>
106. Bonnier, P., Charpin, C., Lejeune, C., Romain, S., Tubiana, N., Beedassy, B., Martin, P. M., Serment, H., & Piana, L. (1995). Inflammatory carcinomas of the breast: a clinical, pathological, or a clinical and pathological definition? *Int J Cancer*, 62(4), 382-385. <https://doi.org/10.1002/ijc.2910620404>
107. Mamouch, F., Berrada, N., Aoullay, Z., El Khanoussi, B., & Errihani, H. (2018). Inflammatory Breast Cancer: A Literature Review. *World J Oncol*, 9(5-6), 129-135. <https://doi.org/10.14740/wjon1161>
108. Koo, M. M., von Wagner, C., Abel, G. A., McPhail, S., Rubin, G. P., & Lyratzopoulos, G. (2017). Typical and atypical presenting symptoms of breast cancer and their associations with diagnostic intervals: Evidence from a national audit of cancer diagnosis. *Cancer Epidemiol*, 48, 140-146. <https://doi.org/10.1016/j.canep.2017.04.010>
109. Rea, D., Francis, A., Hanby, A. M., Speirs, V., Rakha, E., Shaaban, A., Chan, S., Vinnicombe, S., Ellis, I. O., Martin, S. G., Jones, L. J., Berditchevski, F., & group, U. K. I. B. C. W. (2015). Inflammatory breast cancer: time to standardise diagnosis

- assessment and management, and for the joining of forces to facilitate effective research. *Br J Cancer*, 112(9), 1613-1615. <https://doi.org/10.1038/bjc.2015.115>
110. Edge, S. B., & Compton, C. C. (2010). The American Joint Committee on Cancer: the 7th edition of the AJCC cancer staging manual and the future of TNM. *Ann Surg Oncol*, 17(6), 1471-1474. <https://doi.org/10.1245/s10434-010-0985-4>
 111. Guth, U., Jane Huang, D., Holzgreve, W., Wight, E., & Singer, G. (2007). T4 breast cancer under closer inspection: a case for revision of the TNM classification. *Breast*, 16(6), 625-636. <https://doi.org/10.1016/j.breast.2007.05.006>
 112. Devi, G. R., Hough, H., Barrett, N., Cristofanilli, M., Overmoyer, B., Spector, N., Ueno, N. T., Woodward, W., Kirkpatrick, J., Vincent, B., Williams, K. P., Finley, C., Duff, B., Worthy, V., McCall, S., Hollister, B. A., Palmer, G., Force, J., Westbrook, K., . . . Marcom, P. K. (2019). Perspectives on Inflammatory Breast Cancer (IBC) Research, Clinical Management and Community Engagement from the Duke IBC Consortium. *J Cancer*, 10(15), 3344-3351. <https://doi.org/10.7150/jca.31176>
 113. Wingo, P. A., Jamison, P. M., Young, J. L., & Gargiullo, P. (2004). Population-based statistics for women diagnosed with inflammatory breast cancer (United States). *Cancer Causes Control*, 15(3), 321-328. <https://doi.org/10.1023/B:CACO.0000024222.61114.18>
 114. Silverman, D., Ruth, K., Sigurdson, E. R., Egleston, B. L., Goldstein, L. J., Wong, Y. N., Boraas, M., & Bleicher, R. J. (2014). Skin involvement and breast cancer: are T4b lesions of all sizes created equal? *J Am Coll Surg*, 219(3), 534-544. <https://doi.org/10.1016/j.jamcollsurg.2014.04.003>
 115. Guth, U., Wight, E., Schotzau, A., Langer, I., Dieterich, H., Rochlitz, C., Herberich, L., Holzgreve, W., & Singer, G. (2006). A new approach in breast cancer with non-inflammatory skin involvement. *Acta Oncol*, 45(5), 576-583. <https://doi.org/10.1080/02841860600602953>

116. Cristofanilli, M., Valero, V., Buzdar, A. U., Kau, S. W., Broglio, K. R., Gonzalez-Angulo, A. M., Sneige, N., Islam, R., Ueno, N. T., Buchholz, T. A., Singletary, S. E., & Hortobagyi, G. N. (2007). Inflammatory breast cancer (IBC) and patterns of recurrence: understanding the biology of a unique disease. *Cancer*, *110*(7), 1436-1444. <https://doi.org/10.1002/cncr.22927>
117. Fouad, T. M., Kogawa, T., Liu, D. D., Shen, Y., Masuda, H., El-Zein, R., Woodward, W. A., Chavez-MacGregor, M., Alvarez, R. H., Arun, B., Lucci, A., Krishnamurthy, S., Babiera, G., Buchholz, T. A., Valero, V., & Ueno, N. T. (2015). Overall survival differences between patients with inflammatory and noninflammatory breast cancer presenting with distant metastasis at diagnosis. *Breast Cancer Res Treat*, *152*(2), 407-416. <https://doi.org/10.1007/s10549-015-3436-x>
118. Anderson, W. F., Schairer, C., Chen, B. E., Hance, K. W., & Levine, P. H. (2005). Epidemiology of inflammatory breast cancer (IBC). *Breast Dis*, *22*, 9-23. <https://doi.org/10.3233/bd-2006-22103>
119. Yamauchi, H., Woodward, W. A., Valero, V., Alvarez, R. H., Lucci, A., Buchholz, T. A., Iwamoto, T., Krishnamurthy, S., Yang, W., Reuben, J. M., Hortobagyi, G. N., & Ueno, N. T. (2012). Inflammatory breast cancer: what we know and what we need to learn. *Oncologist*, *17*(7), 891-899. <https://doi.org/10.1634/theoncologist.2012-0039>
120. Williams, F., & Thompson, E. (2017). Disparities in Breast Cancer Stage at Diagnosis: Importance of Race, Poverty, and Age. *J Health Dispar Res Pract*, *10*(3), 34-45. <https://www.ncbi.nlm.nih.gov/pubmed/30637180>
121. Takiar, V., Akay, C. L., Stauder, M. C., Tereffe, W., Alvarez, R. H., Hoffman, K. E., Perkins, G. H., Strom, E. A., Buchholz, T. A., Ueno, N. T., Babiera, G., & Woodward, W. A. (2014). Predictors of durable no evidence of disease status in de novo metastatic inflammatory breast cancer patients treated with neoadjuvant chemotherapy and post-mastectomy radiation. *Springerplus*, *3*, 166. <https://doi.org/10.1186/2193-1801-3-166>

122. Wolfe, A. R., Trenton, N. J., Debeb, B. G., Larson, R., Ruffell, B., Chu, K., Hittelman, W., Diehl, M., Reuben, J. M., Ueno, N. T., & Woodward, W. A. (2016). Mesenchymal stem cells and macrophages interact through IL-6 to promote inflammatory breast cancer in pre-clinical models. *Oncotarget*, 7(50), 82482-82492. <https://doi.org/10.18632/oncotarget.12694>
123. Lacerda, L., Debeb, B. G., Smith, D., Larson, R., Solley, T., Xu, W., Krishnamurthy, S., Gong, Y., Levy, L. B., Buchholz, T., Ueno, N. T., Klopp, A., & Woodward, W. A. (2015). Mesenchymal stem cells mediate the clinical phenotype of inflammatory breast cancer in a preclinical model. *Breast Cancer Res*, 17, 42. <https://doi.org/10.1186/s13058-015-0549-4>
124. Shi, M., Chen, D., Yang, D., & Liu, X. Y. (2015). CCL21-CCR7 promotes the lymph node metastasis of esophageal squamous cell carcinoma by up-regulating MUC1. *J Exp Clin Cancer Res*, 34, 149. <https://doi.org/10.1186/s13046-015-0268-9>
125. Hauser, M. A., & Legler, D. F. (2016). Common and biased signaling pathways of the chemokine receptor CCR7 elicited by its ligands CCL19 and CCL21 in leukocytes. *J Leukoc Biol*, 99(6), 869-882. <https://doi.org/10.1189/jlb.2MR0815-380R>
126. Comerford, I., Harata-Lee, Y., Bunting, M. D., Gregor, C., Kara, E. E., & McColl, S. R. (2013). A myriad of functions and complex regulation of the CCR7/CCL19/CCL21 chemokine axis in the adaptive immune system. *Cytokine Growth Factor Rev*, 24(3), 269-283. <https://doi.org/10.1016/j.cytogfr.2013.03.001>
127. Willmann, K., Legler, D. F., Loetscher, M., Roos, R. S., Delgado, M. B., Clark-Lewis, I., Baggiolini, M., & Moser, B. (1998). The chemokine SLC is expressed in T cell areas of lymph nodes and mucosal lymphoid tissues and attracts activated T cells via CCR7. *Eur J Immunol*, 28(6), 2025-2034. [https://doi.org/10.1002/\(SICI\)1521-4141\(199806\)28:06<2025::AID-IMMU2025>3.0.CO;2-C](https://doi.org/10.1002/(SICI)1521-4141(199806)28:06<2025::AID-IMMU2025>3.0.CO;2-C)

128. Hellmann, J., Sansbury, B. E., Holden, C. R., Tang, Y., Wong, B., Wysoczynski, M., Rodriguez, J., Bhatnagar, A., Hill, B. G., & Spite, M. (2016). CCR7 Maintains Nonresolving Lymph Node and Adipose Inflammation in Obesity. *Diabetes*, 65(8), 2268-2281. <https://doi.org/10.2337/db15-1689>
129. Emmett, M. S., Lanati, S., Dunn, D. B., Stone, O. A., & Bates, D. O. (2011). CCR7 mediates directed growth of melanomas towards lymphatics. *Microcirculation*, 18(3), 172-182. <https://doi.org/10.1111/j.1549-8719.2010.00074.x>
130. Blum, K. S., Karaman, S., Proulx, S. T., Ochsenbein, A. M., Luciani, P., Leroux, J. C., Wolfrum, C., & Detmar, M. (2014). Chronic high-fat diet impairs collecting lymphatic vessel function in mice. *PLoS One*, 9(4), e94713. <https://doi.org/10.1371/journal.pone.0094713>
131. Garcia Nores, G. D., Cuzzone, D. A., Albano, N. J., Hespe, G. E., Kataru, R. P., Torrissi, J. S., Gardenier, J. C., Savetsky, I. L., Aschen, S. Z., Nitti, M. D., & Mehrara, B. J. (2016). Obesity but not high-fat diet impairs lymphatic function. *Int J Obes (Lond)*, 40(10), 1582-1590. <https://doi.org/10.1038/ijo.2016.96>
132. Zawieja, D. C. (2009). Contractile physiology of lymphatics. *Lymphat Res Biol*, 7(2), 87-96. <https://doi.org/10.1089/lrb.2009.0007>
133. Gashev, A. A., Davis, M. J., Delp, M. D., & Zawieja, D. C. (2004). Regional variations of contractile activity in isolated rat lymphatics. *Microcirculation*, 11(6), 477-492. <https://doi.org/10.1080/10739680490476033>
134. Solari, E., Marcozzi, C., Negrini, D., & Moriondo, A. (2020). Lymphatic Vessels and Their Surroundings: How Local Physical Factors Affect Lymph Flow. *Biology (Basel)*, 9(12). <https://doi.org/10.3390/biology9120463>

135. Greene, A. K., Grant, F. D., Slavin, S. A., & Maclellan, R. A. (2015). Obesity-induced lymphedema: clinical and lymphoscintigraphic features. *Plast Reconstr Surg*, 135(6), 1715-1719. <https://doi.org/10.1097/PRS.0000000000001271>
136. Greene, A. K., Grant, F. D., & Slavin, S. A. (2012). Lower-extremity lymphedema and elevated body-mass index. *N Engl J Med*, 366(22), 2136-2137. <https://doi.org/10.1056/NEJMc1201684>
137. Vasileiou, A. M., Bull, R., Kitou, D., Alexiadou, K., Garvie, N. J., & Coppack, S. W. (2011). Oedema in obesity; role of structural lymphatic abnormalities. *Int J Obes (Lond)*, 35(9), 1247-1250. <https://doi.org/10.1038/ijo.2010.273>
138. O'Brien, J., Lyons, T., Monks, J., Lucia, M. S., Wilson, R. S., Hines, L., Man, Y. G., Borges, V., & Schedin, P. (2010). Alternatively activated macrophages and collagen remodeling characterize the postpartum involuting mammary gland across species. *Am J Pathol*, 176(3), 1241-1255. <https://doi.org/10.2353/ajpath.2010.090735>
139. Lyons, T. R., Borges, V. F., Betts, C. B., Guo, Q., Kapoor, P., Martinson, H. A., Jindal, S., & Schedin, P. (2014). Cyclooxygenase-2-dependent lymphangiogenesis promotes nodal metastasis of postpartum breast cancer. *J Clin Invest*, 124(9), 3901-3912. <https://doi.org/10.1172/JCI73777>
140. Reddy, J. P., Atkinson, R. L., Larson, R., Burks, J. K., Smith, D., Debeb, B. G., Ruffell, B., Creighton, C. J., Bambhroliya, A., Reuben, J. M., Van Laere, S. J., Krishnamurthy, S., Symmans, W. F., Brewster, A. M., & Woodward, W. A. (2018). Mammary stem cell and macrophage markers are enriched in normal tissue adjacent to inflammatory breast cancer. *Breast Cancer Res Treat*, 171(2), 283-293. <https://doi.org/10.1007/s10549-018-4835-6>

141. Hassel, C., Gausseres, B., Guzylack-Piriou, L., & Foucras, G. (2021). Ductal Macrophages Predominate in the Immune Landscape of the Lactating Mammary Gland. *Front Immunol*, 12, 754661. <https://doi.org/10.3389/fimmu.2021.754661>
142. Rasmussen, J. C., Aldrich, M. B., Fife, C. E., Herbst, K. L., & Sevick-Muraca, E. M. (2022). Lymphatic function and anatomy in early stages of lipedema. *Obesity (Silver Spring)*, 30(7), 1391-1400. <https://doi.org/10.1002/oby.23458>
143. Tan, I. C., Maus, E. A., Rasmussen, J. C., Marshall, M. V., Adams, K. E., Fife, C. E., Smith, L. A., Chan, W., & Sevick-Muraca, E. M. (2011). Assessment of lymphatic contractile function after manual lymphatic drainage using near-infrared fluorescence imaging. *Arch Phys Med Rehabil*, 92(5), 756-764 e751. <https://doi.org/10.1016/j.apmr.2010.12.027>
144. Suami, H., Pan, W. R., Mann, G. B., & Taylor, G. I. (2008). The lymphatic anatomy of the breast and its implications for sentinel lymph node biopsy: a human cadaver study. *Ann Surg Oncol*, 15(3), 863-871. <https://doi.org/10.1245/s10434-007-9709-9>
145. Sheng, F., Inoue, Y., Kiryu, S., Watanabe, M., & Ohtomo, K. (2011). Interstitial MR lymphography in mice with gadopentetate dimeglumine and gadoxetate disodium. *J Magn Reson Imaging*, 33(2), 490-497. <https://doi.org/10.1002/jmri.22422>
146. Elder, A. M., Stoller, A. R., Black, S. A., & Lyons, T. R. (2020). Macphatics and PoEMs in Postpartum Mammary Development and Tumor Progression. *J Mammary Gland Biol Neoplasia*, 25(2), 103-113. <https://doi.org/10.1007/s10911-020-09451-6>
147. Bieniasz-Krzywiec, P., Martin-Perez, R., Ehling, M., Garcia-Caballero, M., Pinioti, S., Pretto, S., Kroes, R., Aldeni, C., Di Matteo, M., Prenen, H., Tribulatti, M. V., Campetella, O., Smeets, A., Noel, A., Floris, G., Van Ginderachter, J. A., & Mazzone, M. (2019). Podoplanin-Expressing Macrophages Promote Lymphangiogenesis and Lymphoinvasion in Breast Cancer. *Cell Metab*, 30(5), 917-936 e910. <https://doi.org/10.1016/j.cmet.2019.07.015>

148. Kataru, R. P., Park, H. J., Baik, J. E., Li, C., Shin, J., & Mehrara, B. J. (2020). Regulation of Lymphatic Function in Obesity. *Front Physiol*, *11*, 459. <https://doi.org/10.3389/fphys.2020.00459>
149. Haaksma, C. J., Schwartz, R. J., & Tomasek, J. J. (2011). Myoepithelial cell contraction and milk ejection are impaired in mammary glands of mice lacking smooth muscle alpha-actin. *Biol Reprod*, *85*(1), 13-21. <https://doi.org/10.1095/biolreprod.110.090639>
150. Jindal, S., Gao, D., Bell, P., Albrektsen, G., Edgerton, S. M., Ambrosone, C. B., Thor, A. D., Borges, V. F., & Schedin, P. (2014). Postpartum breast involution reveals regression of secretory lobules mediated by tissue-remodeling. *Breast Cancer Res*, *16*(2), R31. <https://doi.org/10.1186/bcr3633>
151. Guo, Q., Minnier, J., Burchard, J., Chiotti, K., Spellman, P., & Schedin, P. (2017). Physiologically activated mammary fibroblasts promote postpartum mammary cancer. *JCI Insight*, *2*(6), e89206. <https://doi.org/10.1172/jci.insight.89206>
152. Palazzo, A., Dellapasqua, S., Munzone, E., Bagnardi, V., Mazza, M., Canello, G., Ghisini, R., Iorfida, M., Montagna, E., Goldhirsch, A., & Colleoni, M. (2018). Phase II Trial of Bevacizumab Plus Weekly Paclitaxel, Carboplatin, and Metronomic Cyclophosphamide With or Without Trastuzumab and Endocrine Therapy as Preoperative Treatment of Inflammatory Breast Cancer. *Clin Breast Cancer*, *18*(4), 328-335. <https://doi.org/10.1016/j.clbc.2018.01.010>
153. Bertucci, F., Finetti, P., Birnbaum, D., & Mamessier, E. (2016). The PD1/PDL1 axis, a promising therapeutic target in aggressive breast cancers. *Oncoimmunology*, *5*(3), e1085148. <https://doi.org/10.1080/2162402X.2015.1085148>
154. Kwa, M. J., Novik, Y., Speyer, J., Snuderl, M., Cotzia, P., Miller, K., Newton, E., Oratz, R., Meyers, M., Schnabel, R., Axelrod, D., Joseph, KA., Hiotis, K., Troxel, A., McCoy, S., Schneider, R.,

& Adams, S. (2022). Nivolumab with chemotherapy as neoadjuvant treatment for inflammatory breast cancer. *Journal of Clinical Oncology* **40**(16_suppl): e12633-e12633.

155. Nguyen, D. M., Sam, K., Tsimelzon, A., Li, X., Wong, H., Mohsin, S., Clark, G. M., Hilsenbeck, S. G., Elledge, R. M., Allred, D. C., O'Connell, P., & Chang, J. C. (2006). Molecular heterogeneity of inflammatory breast cancer: a hyperproliferative phenotype. *Clin Cancer Res*, *12*(17), 5047-5054. <https://doi.org/10.1158/1078-0432.CCR-05-2248>
156. Forster, R., Schubel, A., Breitfeld, D., Kremmer, E., Renner-Muller, I., Wolf, E., & Lipp, M. (1999). CCR7 coordinates the primary immune response by establishing functional microenvironments in secondary lymphoid organs. *Cell*, *99*(1), 23-33. [https://doi.org/10.1016/s0092-8674\(00\)80059-8](https://doi.org/10.1016/s0092-8674(00)80059-8)
157. Braun, A., Worbs, T., Moschovakis, G. L., Halle, S., Hoffmann, K., Bolter, J., Munk, A., & Forster, R. (2011). Afferent lymph-derived T cells and DCs use different chemokine receptor CCR7-dependent routes for entry into the lymph node and intranodal migration. *Nat Immunol*, *12*(9), 879-887. <https://doi.org/10.1038/ni.2085>
158. Bromley, S. K., Thomas, S. Y., & Luster, A. D. (2005). Chemokine receptor CCR7 guides T cell exit from peripheral tissues and entry into afferent lymphatics. *Nat Immunol*, *6*(9), 895-901. <https://doi.org/10.1038/ni1240>
159. Issa, A., Le, T. X., Shoushtari, A. N., Shields, J. D., & Swartz, M. A. (2009). Vascular endothelial growth factor-C and C-C chemokine receptor 7 in tumor cell-lymphatic cross-talk promote invasive phenotype. *Cancer Res*, *69*(1), 349-357. <https://doi.org/10.1158/0008-5472.CAN-08-1875>

160. Rosenbaum, D. M., Rasmussen, S. G., & Kobilka, B. K. (2009). The structure and function of G-protein-coupled receptors. *Nature*, *459*(7245), 356-363. <https://doi.org/10.1038/nature08144>
161. Forster, R., Davalos-Misslitz, A. C., & Rot, A. (2008). CCR7 and its ligands: balancing immunity and tolerance. *Nat Rev Immunol*, *8*(5), 362-371. <https://doi.org/10.1038/nri2297>
162. Jorgensen, A. S., Brandum, E. P., Mikkelsen, J. M., Orfin, K. A., Boilesen, D. R., Egerod, K. L., Moussouras, N. A., Vilhardt, F., Kalinski, P., Basse, P., Chen, Y. H., Yang, Z., Dwinell, M. B., Volkman, B. F., Veldkamp, C. T., Holst, P. J., Lahl, K., Goth, C. K., Rosenkilde, M. M., & Hjorto, G. M. (2021). The C-terminal peptide of CCL21 drastically augments CCL21 activity through the dendritic cell lymph node homing receptor CCR7 by interaction with the receptor N-terminus. *Cell Mol Life Sci*, *78*(21-22), 6963-6978. <https://doi.org/10.1007/s00018-021-03930-7>
163. Worbs, T., Mempel, T. R., Bolter, J., von Andrian, U. H., & Forster, R. (2007). CCR7 ligands stimulate the intranodal motility of T lymphocytes in vivo. *J Exp Med*, *204*(3), 489-495. <https://doi.org/10.1084/jem.20061706>
164. Rivera-Guevara, C., & Camacho, J. (2011). Tamoxifen and its new derivatives in cancer research. *Recent Pat Anticancer Drug Discov*, *6*(2), 237-245. <https://doi.org/10.2174/157489211795328486>
165. Finn, R. S., Aleshin, A., & Slamon, D. J. (2016). Targeting the cyclin-dependent kinases (CDK) 4/6 in estrogen receptor-positive breast cancers. *Breast Cancer Res*, *18*(1), 17. <https://doi.org/10.1186/s13058-015-0661-5>
166. Ma, C. X., Gao, F., Luo, J., Northfelt, D. W., Goetz, M., Forero, A., Hoog, J., Naughton, M., Ademuyiwa, F., Suresh, R., Anderson, K. S., Margenthaler, J., Aft, R., Hobday, T., Moynihan, T., Gillanders, W., Cyr, A., Eberlein, T. J., Hieken, T., . . . Ellis, M. J. (2017). NeoPalAna: Neoadjuvant Palbociclib, a Cyclin-Dependent Kinase 4/6 Inhibitor, and

- Anastrozole for Clinical Stage 2 or 3 Estrogen Receptor-Positive Breast Cancer. *Clin Cancer Res*, 23(15), 4055-4065. <https://doi.org/10.1158/1078-0432.CCR-16-3206>
167. Scott, S. C., Lee, S. S., & Abraham, J. (2017). Mechanisms of therapeutic CDK4/6 inhibition in breast cancer. *Semin Oncol*, 44(6), 385-394. <https://doi.org/10.1053/j.seminoncol.2018.01.006>
168. Braal, C. L., Jongbloed, E. M., Wilting, S. M., Mathijssen, R. H. J., Koolen, S. L. W., & Jager, A. (2021). Inhibiting CDK4/6 in Breast Cancer with Palbociclib, Ribociclib, and Abemaciclib: Similarities and Differences. *Drugs*, 81(3), 317-331. <https://doi.org/10.1007/s40265-020-01461-2>
169. Cabioglu, N., Sahin, A., Doucet, M., Yavuz, E., Igci, A., E, O. Y., Aktas, E., Bilgic, S., Kiran, B., Deniz, G., & Price, J. E. (2005). Chemokine receptor CXCR4 expression in breast cancer as a potential predictive marker of isolated tumor cells in bone marrow. *Clin Exp Metastasis*, 22(1), 39-46. <https://doi.org/10.1007/s10585-005-3222-y>
170. Cabioglu, N., Yazici, M. S., Arun, B., Broglio, K. R., Hortobagyi, G. N., Price, J. E., & Sahin, A. (2005). CCR7 and CXCR4 as novel biomarkers predicting axillary lymph node metastasis in T1 breast cancer. *Clin Cancer Res*, 11(16), 5686-5693. <https://doi.org/10.1158/1078-0432.CCR-05-0014>
171. Rizeq, B., & Malki, M. I. (2020). The Role of CCL21/CCR7 Chemokine Axis in Breast Cancer Progression. *Cancers (Basel)*, 12(4). <https://doi.org/10.3390/cancers12041036>
172. Fu, Z., Li, S., Han, S., Shi, C., & Zhang, Y. (2022). Antibody drug conjugate: the "biological missile" for targeted cancer therapy. *Signal Transduct Target Ther*, 7(1), 93. <https://doi.org/10.1038/s41392-022-00947-7>
173. Modi, S., Saura, C., Yamashita, T., Park, Y. H., Kim, S. B., Tamura, K., Andre, F., Iwata, H., Ito, Y., Tsurutani, J., Sohn, J., Denduluri, N., Perrin, C., Aogi, K., Tokunaga,

- E., Im, S. A., Lee, K. S., Hurvitz, S. A., Cortes, J., . . . Investigators, D. E.-B. (2020). Trastuzumab Deruxtecan in Previously Treated HER2-Positive Breast Cancer. *N Engl J Med*, 382(7), 610-621. <https://doi.org/10.1056/NEJMoa1914510>
174. Cuesta, C., Munoz-Callega, C., Loscertales, J., Terron, F., & Mol, W. (2019). CAP-100: First-in-class antibody for CCR7+ hematological malignancies. *Journal of Clinical Oncology*, 37(15_suppl), e19008-e19008. https://doi.org/10.1200/JCO.2019.37.15_suppl.e19008
175. Arendt, L. M., McCreedy, J., Keller, P. J., Baker, D. D., Naber, S. P., Seewaldt, V., & Kuperwasser, C. (2013). Obesity promotes breast cancer by CCL2-mediated macrophage recruitment and angiogenesis. *Cancer Res*, 73(19), 6080-6093. <https://doi.org/10.1158/0008-5472.CAN-13-0926>
176. Rogic, A., Pant, I., Grumolato, L., Fernandez-Rodriguez, R., Edwards, A., Das, S., Sun, A., Yao, S., Qiao, R., Jaffer, S., Sachidanandam, R., Akturk, G., Karlic, R., Skobe, M., & Aaronson, S. A. (2021). High endogenous CCL2 expression promotes the aggressive phenotype of human inflammatory breast cancer. *Nat Commun*, 12(1), 6889. <https://doi.org/10.1038/s41467-021-27108-8>
177. Bousquenaud, M., Fico, F., Solinas, G., Ruegg, C., & Santamaria-Martinez, A. (2018). Obesity promotes the expansion of metastasis-initiating cells in breast cancer. *Breast Cancer Res*, 20(1), 104. <https://doi.org/10.1186/s13058-018-1029-4>
178. McDaniel, S. M., Rumer, K. K., Biroc, S. L., Metz, R. P., Singh, M., Porter, W., & Schedin, P. (2006). Remodeling of the mammary microenvironment after lactation promotes breast tumor cell metastasis. *Am J Pathol*, 168(2), 608-620. <https://doi.org/10.2353/ajpath.2006.050677>
179. Chakraborty, P., George, J. T., Woodward, W. A., Levine, H., & Jolly, M. K. (2021). Gene expression profiles of inflammatory breast cancer reveal high heterogeneity

- across the epithelial-hybrid-mesenchymal spectrum. *Transl Oncol*, 14(4), 101026.
<https://doi.org/10.1016/j.tranon.2021.101026>
180. Gala, K., Li, Q., Sinha, A., Razavi, P., Dorso, M., Sanchez-Vega, F., Chung, Y. R., Hendrickson, R., Hsieh, J. J., Berger, M., Schultz, N., Pastore, A., Abdel-Wahab, O., & Chandarlapaty, S. (2018). KMT2C mediates the estrogen dependence of breast cancer through regulation of ERalpha enhancer function. *Oncogene*, 37(34), 4692-4710. <https://doi.org/10.1038/s41388-018-0273-5>
181. Toska, E., Osmanbeyoglu, H. U., Castel, P., Chan, C., Hendrickson, R. C., Elkabets, M., Dickler, M. N., Scaltriti, M., Leslie, C. S., Armstrong, S. A., & Baselga, J. (2017). PI3K pathway regulates ER-dependent transcription in breast cancer through the epigenetic regulator KMT2D. *Science*, 355(6331), 1324-1330.
<https://doi.org/10.1126/science.aah6893>
182. Luo, R., Chong, W., Wei, Q., Zhang, Z., Wang, C., Ye, Z., Abu-Khalaf, M. M., Silver, D. P., Stapp, R. T., Jiang, W., Myers, R. E., Li, B., Cristofanilli, M., & Yang, H. (2021). Whole-exome sequencing identifies somatic mutations and intratumor heterogeneity in inflammatory breast cancer. *NPJ Breast Cancer*, 7(1), 72.
<https://doi.org/10.1038/s41523-021-00278-w>
183. Bertucci, F., Finetti, P., Birnbaum, D., & Viens, P. (2010). Gene expression profiling of inflammatory breast cancer. *Cancer*, 116(11 Suppl), 2783-2793.
<https://doi.org/10.1002/cncr.25165>
184. Bekhouche, I., Finetti, P., Adelaide, J., Ferrari, A., Tarpin, C., Charafe-Jauffret, E., Charpin, C., Houvenaeghel, G., Jacquemier, J., Bidaut, G., Birnbaum, D., Viens, P., Chaffanet, M., & Bertucci, F. (2011). High-resolution comparative genomic hybridization of inflammatory breast cancer and identification of candidate genes. *PLoS One*, 6(2), e16950. <https://doi.org/10.1371/journal.pone.0016950>

185. Magalhaes, D., Rangel, I., & Mesquita, A. (2022). HER2-Positive Inflammatory Breast Cancer Challenges of Clinical Practices. *Cureus*, 14(3), e22925. <https://doi.org/10.7759/cureus.22925>
186. Jawa, Z., Perez, R. M., Garlie, L., Singh, M., Qamar, R., Khandheria, B. K., Jahangir, A., & Shi, Y. (2016). Risk factors of trastuzumab-induced cardiotoxicity in breast cancer: A meta-analysis. *Medicine (Baltimore)*, 95(44), e5195. <https://doi.org/10.1097/MD.00000000000005195>
187. Giampieri, S., Manning, C., Hooper, S., Jones, L., Hill, C. S., & Sahai, E. (2009). Localized and reversible TGFbeta signalling switches breast cancer cells from cohesive to single cell motility. *Nat Cell Biol*, 11(11), 1287-1296. <https://doi.org/10.1038/ncb1973>
188. Horiuchi, D., Kusdra, L., Huskey, N. E., Chandriani, S., Lenburg, M. E., Gonzalez-Angulo, A. M., Creasman, K. J., Bazarov, A. V., Smyth, J. W., Davis, S. E., Yaswen, P., Mills, G. B., Esserman, L. J., & Goga, A. (2012). MYC pathway activation in triple-negative breast cancer is synthetic lethal with CDK inhibition. *J Exp Med*, 209(4), 679-696. <https://doi.org/10.1084/jem.20111512>

Vita

Wintana Addisalem Balema was born in Italy, the daughter of Tsehay Mituku and Dr. AddisAlem Balema Ph.D. Wintana was raised in Beijing, China and Addis Ababa, Ethiopia, before leaving to the US for college in 2013. After graduating from Mount Holyoke College with a B.A. in biological sciences, and with honors in Biochemistry in May 2017, she pursued her graduate studies. In August 2017, she matriculated into her PhD program at the University of Texas MD Anderson Cancer Center UTHHealth Graduate School of Biomedical Sciences.